UNCLASSIFIED

AD NUMBER

ADC034021

CLASSIFICATION CHANGES

TO: unclassified

FROM: confidential

LIMITATION CHANGES

TO:

Approved for public release, distribution unlimited

FROM:

Distribution limited to U.S. Gov't. agencies and their Contractors; Specific authority; 12 Apr 84. Other requests must be referred to the Commanding Officer, NORDA, Attn: Code 125L. NSTL Station, MS 39529.

AUTHORITY

ONR ltr., Ser 93/160, 10 Mar 1999; SAME

THIS PAGE IS UNCLASSIFIED

AD-E001572

CONFIDENTIAL

(3)

NORDA Report 36
Book 1 of 3

ADC034021

The Acoustic Model Evaluation Committee (AMEC) Reports

Volume III

Evaluation of the RAYMODE X Propagation Loss Model (U)

Prepared by

Richard B. Lauer, NORDA
Numerical Modeling Division

Including

The Physics of RAYMODE X (U)
by Ray Deavenport, NUSC
New London, Connecticut

September 1982

Distribution limited to U.S. Government agencies only. Other requests for this document must be referred to the Commanding Officer, Naval Ocean Research and Development Activity, NSTL Station, Mississippi 39529

T&E 12 APR 1984

Classified by OPNAVINST 5513.5 (3)

Declassify on:
Originating Agency's Determination Required

Naval Ocean Research and Development Activity
NSTL Station, Mississippi 39529

84 04 06 510

CONFIDENTIAL

Foreword (U)

(U) The Acoustic Model Evaluation Committee (AMEC) has been chartered to serve as an advisory group to the Director, Naval Oceanography Division (OP-952), on matters dealing with model evaluation. In fulfillment of it's charter, AMEC will produce a series of reports detailing the results of model evaluations. Volume I described the evaluation methodology selected and the manner in which it has been implemented. Volume IA describes experimental propagation loss data sets suitable for the evaluation of models in a range dependent environment. Volume II presented the results of evaluating the FACT PL9D propagation loss model. This report, Volume III, presents the results of evaluating the RAYMODE X propagation loss model.

G. T. Phelps

G. T. Phelps, Captain, USN
Commanding Officer
NORDA

Executive Summary (U)

(U) The Acoustic Model Evaluation Committee (AMEC) has applied the methodology described in Volume I of this series of reports to evaluate the RAYMODE X propagation loss model. The accuracy of RAYMODE X has been assessed by quantitative comparisons with eight set of experimental data covering a broad spectrum of environmental acoustic scenarios. The physics of RAYMODE X has been examined by R. Deavenport of the Naval Underwater Systems Center, New London Laboratory. RAYMODE X typically has run times between 5 and 30 seconds on the UNIVAC 1108 computer. The model is poorly documented with the exception of a well-written user's guyide; this extends to a severe lack of comment cards within the computer code. The program could clearly benefit from an improved surface duct module; no other serious deficiencies in the physics of RAYMODE X have been noted. Various versions of RAYMODE exist in fleet operations. These versions do not contain identical physics, are written in different computer languages, and are fun on hardware utilizing different word lengths. Consistency of results from these versions has not been demonstrated. It is recommended that a program of configuration management be aplied to all RAYMODE versions. RAYMODE X has many useful features including eigenray information, independence of initial range and range increment for propagation loss calculations, provision for vertical beampatterns and the ability to input an external bottom loss table. This evaluation was completed in September 1980.

Preface (U)

(U) This report was prepared under the joint sponsorship of the Naval Sea Systems Command, Program Manager, P. R. Tiedeman (SEA 63D3), PE 63708N; the Surveillance Environmental Acoustic Support Project, Program Manager, Dr. Robert A. Gardner (NORDA Code 520), PE 63795N; the Tactical ASW Environmental Acoustic Support Project, Program Manager, E. D. Chaika (NORDA Code 530), PE 63795N; via the auspices of OP-952D (Capt. J. Harlett).

Acknowledgments (U)

(U) The author wishes to acknowledge the valuable contributions of Dr. F. R. DiNapoli of the Naval Underwater Systems Center, New London, Conn., while he was chairman of the Panel on Sonar System Models (POSSM) for his support of the development of the model evaluation methodology adopted by AMEC on an interim basis. The stimulating discussions with Dr. A. L. Anderson, formerly of the Naval Ocean Research and Development Activity, resulted in many refinements of the model evaluation methodology and the concept of having a portable test package for model evaluation. This volume and its successors, giving the results of specific model evaluations, would not have been possible without the support and direction given by Mr. R. Winokur during his tenure in OP-095E and 952D. Dr. M. C. Karamargin of the Naval Underwater Systems Center, New London, is well deserving of praise for editing and organizing a vast amount of environmental and acoustic data, running the acoustic models, and producing all the figures and quantitative accuracy assessment results by the "difference technique." Dr. G. Liebiger and Ms. D. Yarger of NUSC, New London, were most generous in supplying much information for this report, substantial portions of which are unpublished elsewhere. Finally, my thanks to the members of AMEC for valuable insight and for recommendations that have substantially increased the quality and the practicality of the model evaluation effort.

Contents (U)

Contents (U)

THIS PAGE

INTENTIONALLY

LEFT BLANK

The Acoustic Model Evaluation Committee (AMEC) Reports
Volume III, Evaluation of the RAYMODE X Propagation Loss Model (U)

1.0 (U) Introduction

(U) This volume is third in a series of Acoustic Model Evaluation Committee (AMEC) reports. Volume I deals in detail with the model evaluation methodology and its implementation in fulfillment of AMEC's charter. This volume details the application of that methodology for the evaluation of the RAYMODE X model as run on the UNIVAC 1108 computer at the Naval Underwater Systems Center, New London Laboratory. The RAYMODE X evaluation was completed on 30 September 1980. No modifications of RAYMODE X were required in order to perform the accuracy assessment portion of the evaluation; of importance in this regard, the RAYMODE X model has the capability of accepting an external bottom loss table input and provision for writing propagation loss versus range results to an external file.

(U) The model evaluation methodology is described in Section 1.1 of this volume and in greater detail in Volume I of this series. The primary areas in which we seek to provide model evaluation information are (1) model description, (2) physics and mathematics, (3) run time, (4) core storage, (5) complexity of program execution, (6) ease of effecting program alterations, (7) ease of implementation (on a different computer), (8) cognizant individual(s) or organizational element(s), (9) byproducts, (10) special features, (11) references, and (12) accuracy assessment.

(U) RAYMODE X is a computer program for the prediction of transmission loss versus range in an environment which can be characterized by a flat bottom and a single sound speed profile. This model is in extensive fleet usage, supporting the Optimum Mode Selection systems for TRIDENT, the BQQ-5, and the BQQ-6 in the submarine fleet and is the transmission loss module in the Sonar In Situ Mode Assessment System (SIMAS) used in the surface fleet. RAYMODE X has been distributed to other naval activities and Navy contractors.

(U) Four classes of models are described by Hersey (1977): Research Model, Candidate Model, Navy Evaluated Model, and Navy Operational Model. With the publication of this report, RAYMODE X has fulfilled the requirements for status as a Navy Evaluated Model. The RAYMODE model (in a variety of versions) has been a Navy Operational Model for many years.

(U) As we shall see below, RAYMODE X typically has run times ranging from 5 to 30 seconds on the UNIVAC 1108 with the EXEC VIII operating system. The core required by RAYMODE X as dimensioned for 400 points and 50 modes and ray paths is 17319 decimal words (exclusive of plot routines). These run times and core requirements allow RAYMODE to be implemented in desktop calculators (HP 9845 and Tektronix 4051) and to meet operational requirements for run time. As of the termination of this evaluation on 30 September 1980, RAYMODE documentation, both internal and external to the computer code, was lacking with the exception of a user's guide (Yarger, 1976) and a technical memorandum by Leibiger (1971) that presented the essence of the RAYMODE method but did not tie in to the computer code. The theory of RAYMODE is further described by DiNapoli and Deavenport (1980).

(U) The version of RAYMODE herein evaluated is RAYMODE X as resident and run on the UNIVAC 1108 computer. Other RAYMODE versions were not tested but are described in section 10. References to these versions are provided as available.

1.1 (U) The AMEC Methodology

(U) Volume I of this series of reports presents the AMEC model evaluation methodology in detail. The following list is a synopsis of this methodology; the items are taken from an information request form sent to those persons responsible (usually the developer) for a model which is to undergo evaluation and, taken together with the physics review and accuracy assessment, constitute the evaluation.

(U) Range Independent Propagation Loss Information requested for AMEC:

1. (U) Model Description

- Purpose(s) of the model.
- List of input variables and their units (inputs obtained from associated data bases, internal routines, functions or tables should be so identified).
- List of output options. Examples of tabular and graphical results.
- A list of systems (e.g., sonar prediction, engagement model, etc.) supported by the model, including the role of the model in the system and the stated purpose of the systems.
- Limitations designed into the model, through inherent limits of the physics, mathematics, environmental description, computer implementation, etc. These limitations, taken together, define the model's domain of applicability and include frequency, bandwidth, range, etc. Also included are limitations involving choice of computer, graphics, and telemetry links. Please outline the extent to which the limitations result from design decisions based upon the basic purpose of the model development effort and/or tradeoffs required by time (run time or product delivery), cost, and computer assets.
- A list of extant model versions. Note differences between versions including computer, changes in inputs and outputs, assignments of default values, graphics, program language, use of overlays, etc.

2. (U) Run Time

- Provide run time as function of computer, number of points and input/output selections, and model version. Divide run time into computation time and time required for printing and plotting. Describe tradeoffs between accuracy and run time as affected by input options.

3. (U) Core Storage

- Provide information on core storage requirements on a version basis. Identify techniques used to reduce core requirements including use of overlays, memory mapping, disk memory swap and the use of techniques such as interpolation in place of calculation.

4. (U) Complexity of Execution

- Provide a program listing.
- Define all input and output parameters under user control.
- What default values or conditions are assigned with the program?
- Identify restrictions on parameter values.
- Identify unusual parameters and provide guidance for their selection.
- Does a user's guide exist? If so, please give reference.

5. (U) Ease of Effecting Program Alterations

- Supply a program flow chart.
- A list of program variables and their definition.
- Extent to which a model is tied into a specific computer executive system or special equipments or programs, library routines, etc.

6. (U) Ease of Implementation on a Different Computer

- List of computers (and executive systems) on which model is presently running.
- List of military and civilian activities using the model.

• Computer language(s) used by the model (all versions).
• Special codes (e.g., plotting routines, library functions).
• To what extent is the program dependent on a given computer executive system?
• Identify test cases to assure proper running on a new computer (including scenarios treated); are all subroutines and lines of code exercised.
• A list of all errors returned and the situations which cause them.

7. (U) Cognizant Individual(s) and/or Organizational Elements, Names and Addresses of Those Reponsible for

• Theory upon which model is based.
• Model development.
• Computer implementation.
• Model maintenance and configuration management.

8. (U) References

(U) A list of references, including those which discuss theories upon which model is based, and numerical methods employed. References worthy of special mention are (a) a user's guide; and (b) a response to SECNAVINST 3560.1, Tactical Digital Systems Documentation Standards of 8 August 1974, or to DOD Standard 7935.1-S, Automated Data Systems Documentation Standards of 13 September 1977, or to other Navy or DOD documentation requirements.

9. (U) By-Products

• A list of output by-products (e.g., eigenray information, arrival angle vs. range, ray diagram).
• A list of by-products not available externally but which are internally calculated.

10. (U) Special Features

• A list of special features (e.g., provision for beampatterns, multi-frequency results through interpolation, etc.).

(U) The review of the physics and mathematics and computer implementation of a given model is undertaken by an independent expert in the appropriate field of modeling. In particular, the physics and mathematics are examined to define the model's domain of applicability through assumptions, approximations and the assignment of "nominal values" to various parameters.

(U) The reporting of the model's physics includes the basic foundations and approach and any unusual techniques and, especially, any extensions to theory and/or unique capabilities otherwise unavailable. Examination of the model's physics and mathematics is to include consideration of environmental inputs, including theories and the appropriateness of data base selection. The computer implementation is examined to assure that the calculations required by the theory are correctly performed. The efficiency or other aspects of the program code are not addressed here.

(U) Two accuracy assessment procedures are employed in AMEC evaluation. Both yield quantitative results and involve comparison of model outputs with experimental data or the output of a reference model. The steps of the first procedure, called the Difference technique, follow: (1) Smooth the reference data set (only if CW or exhibiting large fluctuations) and the output of the model (only if coherent phase addition was used) by applying a 2 km moving window. (2) Subtract the model output from the reference data set (after appropriate smoothing). (3) If possible, divide the difference curve into range intervals corresponding to direct path, bottom interaction and convergence zone modes. If not possible, either (a) do not subdivide into range intervals; (b) use quasiarbitrary intervals, which may be tactically useful; or (c) subdivide on the basis of any features evident in the measured data. (4) In each range interval calculate the mean μ and the standard deviation σ of the differences. (5) Analyze results, attempting to identify

causes of discrepancies. The above steps are supported by figures as follows: measured data, smoothed measured data, model output, smoothed model output, and difference between smoothed curves. These curves are drawn to the same scale and may be overlaid on a light table, facilitating eyeball comparison and diagnosis. As useful as this technique is in identifying significant differences and facilitating diagnosis, it has a number of shortcomings: (a) misleading in convergence zones where range errors are as significant as errors in level; (b) it is conceivable that large errors occur at dB levels of no consequence for operational systems; and (c) the difference approach leads to answers which are not particularly useful to fleet purposes, especially in the context of specific sonar systems. These shortcomings are eliminated in the second accuracy assessment technique, called the FOM (Figure of Merit) technique. In this technique the data is once again smoothed as in step (1) above. FOM are then selected in 5 dB steps. For each FOM, detection range information is tabulated: range of continuous coverage, ranges of convergence zone starts and ends, and in range intervals over which detection coverage is zonal in nature--the percentage of the interval over which detection can be made. This FOM vs. detection range analysis is performed for model and reference data set, the results compared and reasons sought for significant disparities.

(U) Taken together, the two accuracy assessment techniques, the Difference and FOM techniques, lead to results useful to scientific analysis and for system performance estimation.

2.0 (U) RAYMODE X Description

(U) RAYMODE X is the most recent in an evolutionary chain of RAYMODE models and is the basic version. The term, RAYMODE, indicates a method of calculating propagation loss that utilizes both ray and normal mode theories. In addition to the calculation of propagation loss versus range, RAYMODE also calculates arrival angle versus range and travel time versus range for the various rays and groups by index: surface duct (J=1), convergence zone (J=2), and bottom bounce (J=3) paths.

(U) The model is dimensioned to give a maximum of 400 range points at which propagation loss is calculated (using either coherent or incoherent phase addition). These range points are equally spaced between user-specified minimum and maximum ranges. Beam patterns may be input for both source and receiver. Although RAYMODE has an internal subroutine from which bottom loss versus grazing angle is specified given a bottom type (1 to 9), a bottom loss versus grazing angle table may be input from an external source. The bottom loss curves were obtained from Marine Geophysical Survey) (MGS) data (Podezwa, 1975). RAYMODE contains a subroutine for the calculation of surface loss (Beckman and Spizzichino, 1963). As run at NUSC, RAYMODE contains graphics routines utilizing Integrated Graphics System (IGS) software and the Information International FR80 hardware.

(U) A list of physical variables used in the RAYMODE program is given in Table 2-1. The Fortran label (or variable is given in the left-hand column and the definition in the right-hand column.

(U) In addition to a sound speed versus depth or temperature versus depth plus a constant salinity value, the program can access historical sound speed data fields. Adjacent equal sound speeds or temperatures are modified to avoid a zero gradient condition.

(U) Systems supported by the versions of the RAYMODE model (not RAYMODE X as it exits on the UNIVAC 1108) are:

- Optimum Mode Selection (OMS) for TRIDENT
- Improved Sonar Processing Equipment (ISPE) -- sonar suite replacement on SSBNs

Table 2-1. (U) Physical variables used in the RAYMODE program

ABS:	Absolute value function in Univac Library; takes real argument, gives real result.
ACOS:	Arccos function in Univac Library, $-1. \leq$ argument $\leq 1.$, result in radians.
ALOG:	Natural log function in Univac Library.
ALOG10:	Log_{10} in Univac Library.
AMAX1:	Univac function to select maximum of 2 real numbers.
AMIN1:	Univac function to select minimum of 2 real numbers.
AMPTUD:	Subroutine.
ANGLE:	$\pm$ Maximum sonar angle in degrees or velocity terms (input--see Yarger (1976)).
ANGLN:	$\pm$ Minimum sonar angle in degrees.
ANGLX:	$\pm$ Maximum sonar angle in degrees.
ANGLO:	$\pm$ Minimum sonar angle in degrees or velocity terms (input--see Yarger (1976)).
AR:	Internally computed range value in yards.
BEAM:	Subroutine.
BIGM:	Largest mode trapped.
BL:	Array of bottom loss values in dB (may be input--see Yarger (1976)).
BPI:	Large integral multiple of 2π for use in SQUD subroutine.
C:	Array of profile velocities (input--see Yarger (1976)).
CA:	Intermediate wave number.
CADEL:	Difference between wave numbers.
CAMAX:	Maximum wave number trapped by an angular interval.
CAMAXJ:	Array to save CAMAX values to provide plot routines.
CAMIN:	Minimum wave number trapped by an angular interval.
CAMINJ:	Array to save CAMIN values to provide plot routines.
CAMU:	Wave number associated with receiver depth.
CAN:	Wave number associated with bottom depth.

CANU:	Wave number associated with source depth.
CAONE:	Wave number associated with surface depth.
CAX:	Wave number associated with maximum sonar angle.
CAY:	Wave number values defined at points along a path.
CAO:	Wave number associated with velocity C_O.
CMAX:	Maximum velocity trapped by an angular interval.
CMIN:	Minimum velocity trapped by an angular interval.
CNU:	Slightly adjusted velocity to search for phase changes.
COS:	Univac Library function for trigonometric cosine; argument in radians.
CP:	Array of adjusted profile velocities in yards used internally.
CO:	Maximum velocity between source and receiver, slightly shifted.
D:	Term containing surface, bottom, and beam losses for bottom bounce.
DC:	Range derivative array associated with cycle range at each point along a ray.
DD:	Range derivative array associated with range adjustment to cycle range for receiver depth.
DEG:	Constant number of degrees per radian.
DELIM:	Imaginary part of complex propagation loss contribution.
DELRE:	Real part of complex propagation loss contribution.
DELTAR:	Range increment (input--see Yarger (1976)).
DJ:	Array of terms containing amplitude, surface and bottom losses for bottom bounce.
DJCUT:	Cutoff to determine if losses are so high as to be impractical to compute.
DL:	Array of losses in dB for source deviation loss table (input--see Yarger (1976)).
DLJ:	Computed beam loss.
DL2	Array of losses in dB for receiver deviation loss table (input--see Yarger (1976)).

UNCLASSIFIED

DS:	Range derivative array associated with range adjustment to cycle range for source depth.
DTAPLT:	Subroutine.
EMDEL:	Difference between mode numbers.
ENL14:	Factor determining spacing between wave number points along a path.
EXITG:	IGS subroutine to terminate plotter.
EXP:	Univac Library for to power.
F:	Frequency in Hz (input--see Yarger (1976)).
FIRST:	Subroutine to initialize time clock to 0.
FLOAT:	Univac Library function to convert integer to real variable.
G:	Gradient.
GETPRO:	Subroutine.
HALFPI:	$\pi/2$.
HC:	Phase array associated with cycle range points along a path.
HD:	Phase array for receiver depth adjustment associated with cycle range points along a path.
HDP:	Point linearly interpolated from HD array.
HDR:	Header array in format 12A6 (input--see Yarger (1976)).
HS:	Phase array for source depth adjustment associated with cycle range points along a path.
HSP:	Point linearly interpolated from HS array.
IDL:	Number of points in source beam pattern (input--see Yarger (1976)).
IFIX:	Univac Library function to convert real numbers to integer, i.e., truncated.
IFLAG:	Flag set by subroutine LINTRP indicated point to be interpolated already existed.
IJDL:	Indicator if >o that either source or receiver (or both) beam patterns exist.
INPUTS:	Name of NAMELIST inputs set.
INT:	Univac Library function to convert real argument to integer.

UNCLASSIFIED

IOCEAN: Ocean code (input--see Yarger (1976)).

IPRINT: Print option (input--see Yarger (1976)).

IPROFL: Profile code (input--see Yarger (1976)).

IQ: Cycle number index.

IQMAX: Maximum cycle number.

IQMIN: Minimum cycle number.

IQO: Cycle number internal value.

IR: Range index.

ISEASN: Season code (input--see Yarger (1976)).

ITAB: Number of points in bottom loss table (maybe input--see Yarger (1976)).

J: Index of angular interval trapped by profile.

JDL: Number of points in receiver beam pattern.

K: Generally used to index points along a path or wave numbers.

KEEPMU: Save receiver index MU as input.

KEEPNU: Save source index NU as input.

L: Path index.

LAMDA: Number of cycles for non-bottom bounce (input--see Yarger (1976)).

LAMDAB: Number of cycles for bottom bounce (input--see Yarger (1976)).

LAMDAJ: Array to save number of cycles for each angular interval to pass to ray and travel time plot routines.

LAMMIN: Minimum cycle (input--see Yarger (1976)).

LEROY: Subroutine.

LINTRP: Subroutine.

M: Mode index.

MAX: Univac Library function to pick maximum of 2 integers.

MAXJ: Parameter to show maximum number of allowable angular intervals for dimensions.

UNCLASSIFIED

MAXK:	Parameter to show maximum number of points along a path for dimensions.
MAXM:	Parameter to show maximum number of modes trapped for dimensions.
MAXMOD:	Maximum mode number (input--see Yarger (1976)).
MAXN:	Parameter to show maximum number of allowable points in profile and input tables.
MAXR:	Parameter to show maximum number of ranges allowed for dimensions.
MBIGST:	Biggest mode.
METRIC:	Metric input/output option (input--see Yarger (1976)).
MGSBL:	Subroutine.
MGSOP:	MGS bottom loss province (input--see Yarger (1976)).
MINMOD:	Minimum mode number (input--see Yarger (1976)).
MJ:	Number of modes between biggest and smallest.
MM1:	Number of bottom bounce J index.
MODESG:	IGS subroutine to initialize plotter.
MS:	Number of points in surface loss table.
MSMLST:	Smallest mode number.
MU:	Receiver index on profile (may be input--see Yarger (1976)).
MO:	Mode cutoff (input--see Yarger (1976)).
N:	Number of points in input profile (input--see Yarger (1976)).
NEGB:	Indicator to sense numbers beyond certain limits for mode summation.
NKEXP:	Exponent to determine spacing of wave numbers along a path (non-bottom).
NL:	Number of points along a path.
NLP:	Adjusted number of points along a path.
NLPJ:	Array to save NLP per angular interval to pass to ray and travel time routines.
NMODE:	Number of modes.
NP:	Adjusted number of points in velocity profile.

NR:	Number of ranges.
NU:	Index of source depth of profile (may be input--see Yarger (1976)).
NXPO:	Exponent to determine spacing of wave numbers along a path.
OMEGA:	2π frequency.
ONE3RD:	1/3.
PHI:	Total phase change.
PHI1:	Upper phase change.
PHI2:	Lower phase change.
PI:	π = 3.1415926535.
PL:	Array to accumulate real vs. range part of property loss calculation for coherent phase.
PLIM:	Array to accumulate real vs. image part of property loss calculation for coherent phase.
PLOTCZ:	Plot option (input--see Yarger (1976)).
PLOTOP:	Plot option (input--see Yarger (1976)).
PLOTPL:	Plot option (input--see Yarger (1976)).
PLOTT:	Plot option (input--see Yarger (1976)).
PLPLOT:	Subroutine.
PLRMS:	Random phase propagation loss vs. range.
PLO:	Minimum dB for scale of property loss plot.
PROFIL:	Subroutine.
P1:	Sign of receiver depth range adjustment.
P2:	Sign of source depth range adjustment.
Q:	Cycle variable:
QOMU:	Receiver term for amplitude calculation.
QOMUP:	Receiver term for amplitude calculation.
QONU:	Source term for amplitude calculation.
QONUP:	Source term for amplitude calculation.

UNCLASSIFIED

R:	Minimum range (input--see Yarger (1976)).
RANGE:	Range array in yards.
RAPLOT:	Subroutine.
RAYBLK:	Common block for plot routines.
RC:	Array of cycle ranges for wave numbers along a path.
RCMAX:	Maximum RC value for a single J index, all 4 paths.
RCMIN:	Minimum RC value for a single J index, all 4 paths.
RD:	Array of range adjustments to cycle range for receiver depth.
RDP:	Linearly interpolated RD value.
REK:	Real part of a complex term for each mode.
RESS:	Surface losses in dB.
RMAX:	Maximum range (input--see Yarger (1976)).
RS:	Array of range adjustments to cycle range for source depth.
RSP:	Linearly interpolated RS value.
RSS:	Subroutine.
R1:	Surface loss values.
R1J:	Linear interpolated R1 at a particular wave number.
R2:	Bottom loss array dependent on wave number.
SALNTY:	Salinity in 0/00 for XBT conversion (input--see Yarger (1976)).
SETSMG:	IGS subroutine to set.
SIN:	Univac trigonometric function for sine; argument in radians.
SMLM:	Smallest mode trapped.
SQRT:	Univac $\sqrt{\ }$ function.
SQUD:	Subroutine.
TESTB:	Used to determine range cutoffs for "RAYMODE Method".
TESTQ:	Used to determine range cutoffs for "RAYMODE Method".
TESTQP:	Used to determine range cutoffs for "RAYMODE Method".

UNCLASSIFIED

THEDA:	Array of angles for source deviation pattern (input--see Yarger (1976)).
THEDA2:	Array of angles for receiver deviation pattern (input--see Yarger (1976)).
THETA:	Bottom loss angles in degrees for bottom loss table (may be input--see Yarger (1976)).
THETAS:	Surface loss angles in degrees for surface loss table (may be input--see Yarger (1976)).
THREEH:	Subroutine.
TTPLOT:	Subroutine.
TWOPI:	2π in radians.
WS:	Wind speed (input--see Yarger (1976)).
XIM:	See XRE below except for imaginary part.
XRE:	Term containing real part of complex expression for property loss done by mode summation.
Z:	Profile depth array (input--see Yarger (1976)).
ZB:	Bottom depth (input--see Yarger (1976)).
ZP:	Depth array in yards of adjusted velocity profile used internally.
ZR:	Receiver depth (input--see Yarger (1976)).
ZRP:	Receiver depth in feet or meters to put in plot key.
ZS:	Source depth (input--see Yarger (1976)).
ZSP:	Source depth in feet or meters to put in plot key.

UNCLASSIFIED

- Submarine Systems Effectiveness and Assessment (SUBSEA)
- Submarine Active Detection Systems (SADS)
- BQQ-5 Sonar OMS
- BQQ-6 Sonar OMS
- Sonar In Situ Mode Assessment System (SIMAS)
- Fleet Mission Library

(U) The RAYMODE X program consists of fifteen subroutines as follows:

I.	RAMODX	Propagation Loss Model Main Program
II.	LEROY	Temperature to Velocity Conversion
III.	RSS	Surface Loss Computation
IV.	MGSBL	MGS Bottom Loss Computation
V.	THREEH	Ray Computations
VI.	GETPRO	Historical Velocity Profile Retrieval
VII.	PROFIL	Profile Manipulation
VIII.	LINTRP	Linear Interpolation
IX.	BEAM	Deviation Loss Computation
X.	AMPTUD	Amplitude Calculation
XI.	SQUD	Reduction of Trig Function Argument
XII.	DTAPLT	Plot SVP and Input Loss Tables
XIII.	RAPLOT	Plot Source and/or Receiver versus Range
XIV.	TTPLOT	Plot Travel Time versus Range
XV.	PLPLOT	Plot Random and/or Coherent Propagation Loss versus Range

(U) In the user's guide of Yarger (1976) an * marks RAMODX lines of code and plotting subroutines DTAPLT, RAPLOT, TTPLOT, and PLPLOT to be removed when the IGS graph plotting capability is not available.

(U) The RAYMODE model has error stops generally whenever inputs go beyond the allowable range as given in Table 7-1 or exceed dimension parameters established in the program. If an error exists on the HVP (Historical Velocity Profile) tape input, an error message will print the NTRAN status. Certain error conditions are automatically corrected by the program, for example, a zero profile gradient or illegal MGS province.

(U) In addition to accepting a user-specified sound speed profile, RAYMODE X at NUSC/NL can access historical velocity profile (HVP) data. The historical velocity profile data on magnetic tape is taken from NUSC Technical Documents 5271, 5447, 5555, and 6035 by E. Podeszwa that contain Sound Speed Profiles for the North Pacific Ocean, North Atlantic Ocean, Indian Ocean, and Norwegian Sea, respectively.

(U) A chart to illustrate the path and cycle structure as well as signs of ray angles in RAYMODE is given in Figure 2-1.

3.0 (U) The Physics of the RAYMODE X Model by R. Deavenport

3.1 (U) Introduction

(U) RAYMODE X is a computer program developed by G. A. Leibiger at the New London Laboratory of the Naval Underwater Systems Center. RAYMODE X calculates the acoustic pressure field P(r,z) at range (r) and depth (z) due to a point harmonic source, or angular frequency ω, located at ($r=o$, $z=z_s$) in a piecewise-layered medium (see Fig. 3-1). Transmission loss is then calculated both coherently and incoherently. Details regarding actual running of the computer program can be found in Yarger (1976).

Resolution* of sign of source and receiver angles in RAYMODE:

General range $\bar{R} = qR_c + R_s + R_d$ or $qR_c + P_2R_s + P_1Pd$ where q = cycle
R_c = cycle range
R_s = source term
R_d = receiver term

Path L	P_2	P_1	Equation $\bar{R}$	Source Angle	Receiver Angle
1	−	+	$qR_c - R_s + R_d$	+ down	− up
2	+	+	$qR_c - R_s + R_d$	− up	− up
3	−	−	$qR_c - R_s + R_d$	+ down	+ down
4	+	−	$qR_c - R_s + R_d$	− up	+ down

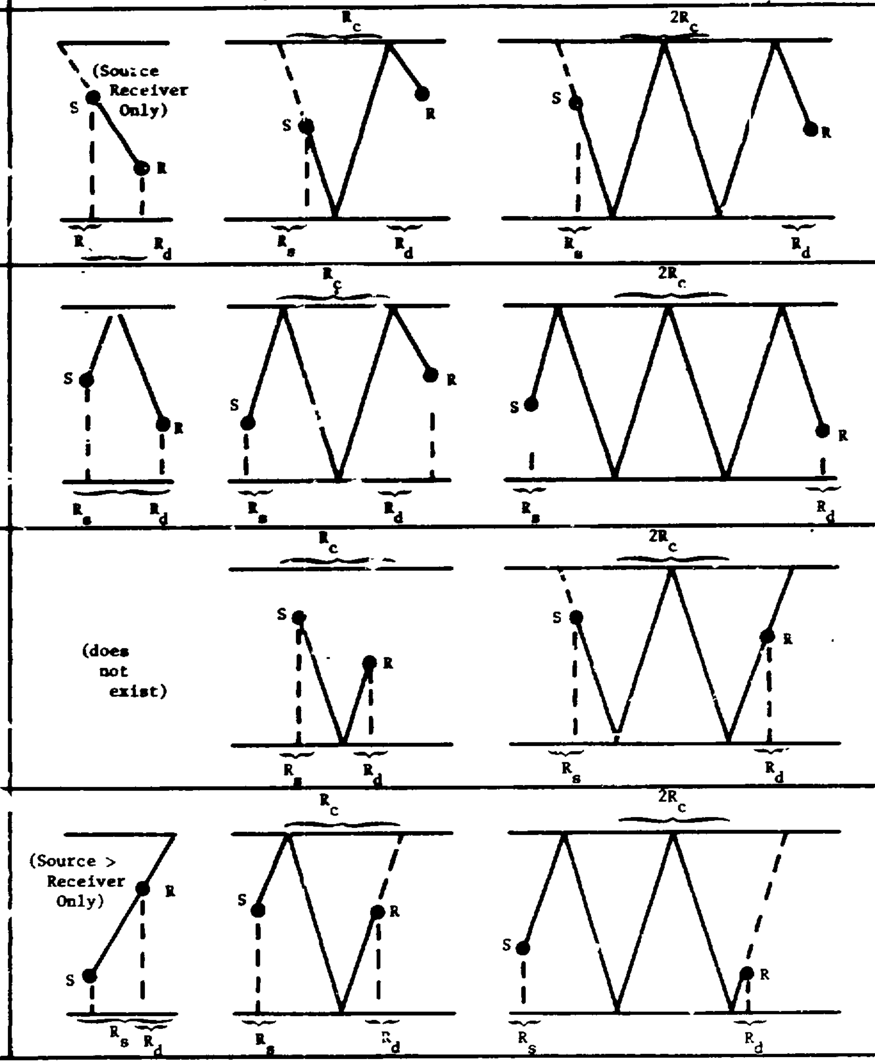

Cumulative upper phase change: $q\phi_1 + .s(P_1+P_2)$;
Cumulative lower phase change: $q\phi_2$

UNCLASSIFIED

Figure 2-1. (U) Path and Cycle Structure Chart

*Sign of angle is opposite sign of range term -- for both source and receiver.

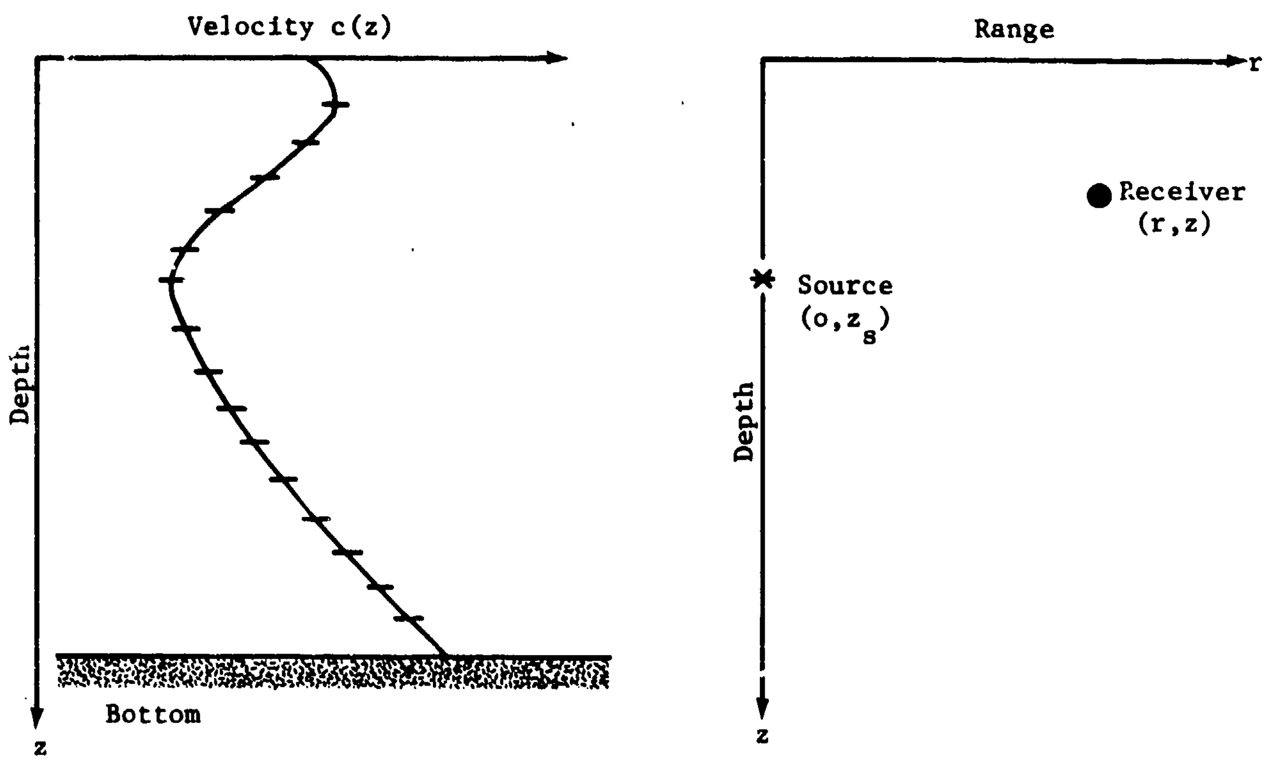

UNCLASSIFIED

Figure 3-1. (U) Diagram of Velocity Depth Profile Showing Location of Source and Receiver

(U) The philosophy adopted by Leibiger is to utilize the simpler tools of ray theory while retaining the more exact formulation of normal mode theory. Two benefits are thus realized: (1) it is possible to interpret mode theory expressions in a manner similar to ray theory, and (2) the use of ray theory simplifies some of the computational aspects of normal mode theory, allowing for considerable savings in computer execution time.

(U) The basic idea of RAYMODE is to partition the wavenumber integral solution for the acoustic field into expressions which individually have meaning in terms of conventional ray theory. This is accomplished by using the velocity-depth profile to divide the wavenumber domain into regions corresponding to surface duct (SD), convergence zone (CZ), and bottom bounce (BB) propagation paths. Each wavenumber integral is then expanded into four parts corresponding to the four rays associated with the upgoing/downgoing eigenrays at the source/receiver. These upgoing/downgoing ray integrals are then numerically evaluated by either normal mode theory or via a multipath expansion. Therefore, each propagation path consists of four parts and the total field is the result of summing all paths (i.e., SD + CZ + BB).

(U) This synopsis attempts to present the theory and approximations leading up to the equations which are ultimately used in the RAYMODE X program.

3.2 (U) Theory

Integral Solution (U)

(U) The acoustic pressure P(r,z) is found by applying the Fourier-Bessel transform to the Helmholtz wave equation in cylindrical coordinates (r, θ , z),

$$\frac{1}{r} \frac{\partial}{\partial r} \left(r \frac{\partial P}{\partial r}\right) + \frac{\partial^2 P}{\partial z^2} + \frac{\omega^2}{c^2(z)} P = \frac{-i\omega}{2\pi r} \delta(r)\delta(z-z_s) \qquad (3\text{-}1)$$

where azimuthal symmetry is assumed and c(z) is the sound speed as a function of depth. In addition, a time factor of exp ($i \omega t$) has been used. The Fourier-Bessel solution of (3-1) is given by

$$P(r,z,z_s) = \frac{i\omega}{4\pi} \int_{-\infty}^{\infty} G(z,z_s;\xi)\, H_0^2(\xi r)\xi d\xi \qquad (3\text{-}2)$$

where H_0^2 is the Hankel function of order zero and G is the depth dependent Green's function. In general G is a very complicated expression for a piecewise continuous medium. However, if it is assumed that sound speed profile discontinuities do not backscatter appreciable energy, then the Green's function can be written as

$$G(z,z_s;\xi) = \frac{[g(z_s) + R_u^k f(z_s)][f(z) + R_d^N g(z)]}{2ie^{i\phi_k^{z_N}}[1-R_u^k R_d^N e^{-2i\phi_k^{z_N}}]},\quad z,z_s \in \left[z_k,z_N\right],\ z > z_s \qquad (3\text{-}3)$$

and f and g are linearly independent traveling wave solutions of the separated wave equation in the depth variable z,

$$\left(\frac{d^2}{dz^2} + q(z)\right)\begin{Bmatrix} f(z) \\ g(z) \end{Bmatrix} = 0 \qquad (3\text{-}4)$$

where

$$q(z) = \left(\frac{\omega^2}{c^2(z)} - \xi^2\right)$$

and the wave phase $\phi_K^{z_N}$ is defined by

$$\phi_K^{z_N} = \int_{z_K}^{z_N} \left(\frac{\omega^2}{c^2(z)} - \xi^2\right)^{1/2} dz \qquad (3\text{-}5)$$

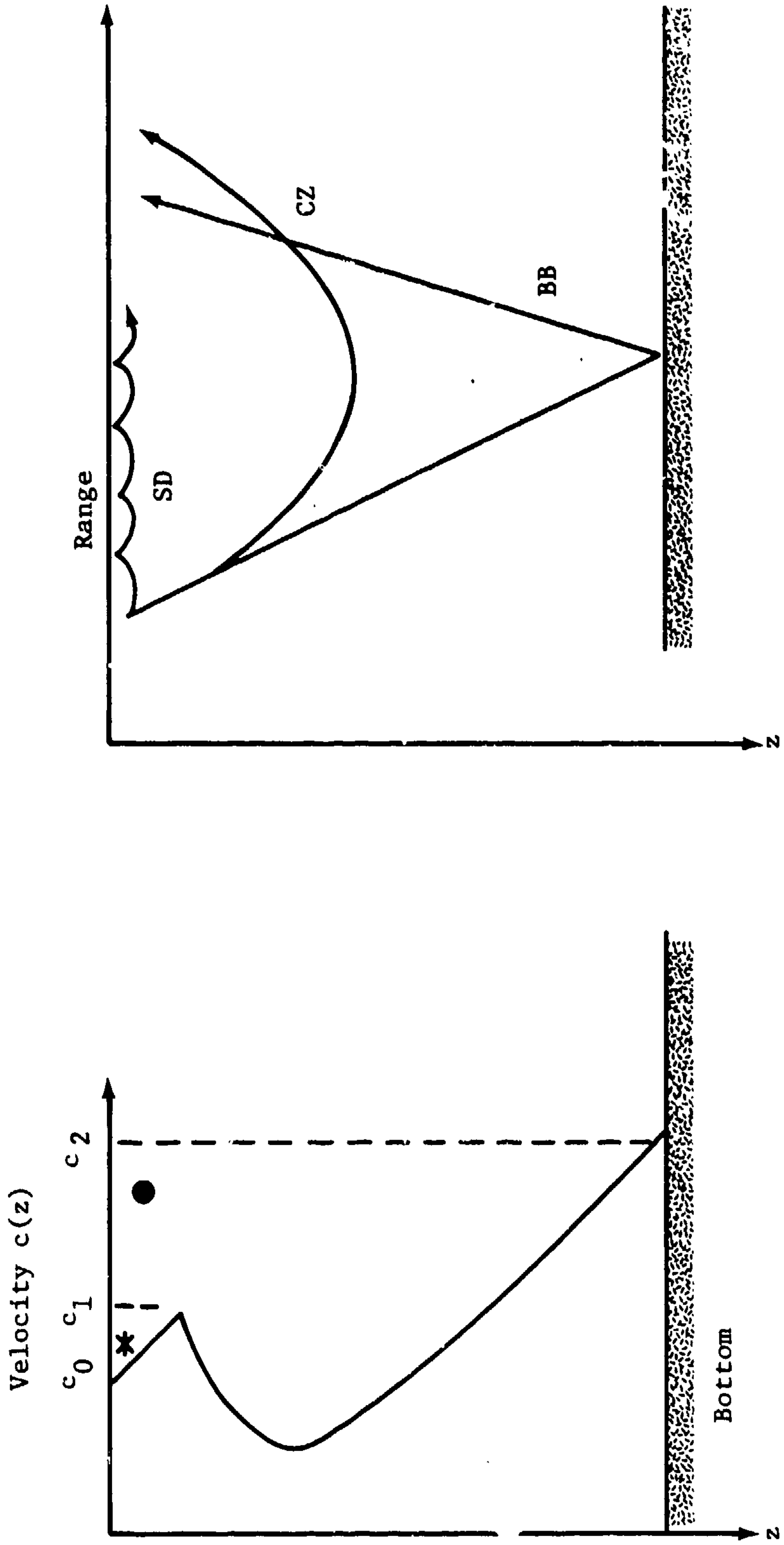

UNCLASSIFIED

Figure 3-2. (U) Velocity Depth Profile and Associated Ray Paths

(U) The depth z_k is the phase reference depth for the wave functions in z_s, and is either the ocean surface or an upper turning point depth corresponding to a downward refracted wave. Likewise, z_N is the phase reference depth for the wave functions in z and is either the bottom of a surface duct, the ocean bottom depth or a lower turning point depth corresponding to an upward refracted wave. The superscripts K and N on the reflection coefficients R_u^K and R_d^N, refer to the above reference depths, z_k and z_N, respectively. Thus, R_u^K is evaluated at z_k and R_d^N is evaluated at z_N. The subscripts u and d on the reflection coefficients R_u^K and R_d^N refer to the direction (up or down) of propagation of the wave functions that are reflected at z_k and z_N. Thus $R_u^K f(z)$ represents the reflected wave of the upward traveling wave $g(z)$. Likewise $R_d^N g(z)$ is the reflected wave of the downward traveling wave $f(z)$. The reflection coefficients must therefore be chosen such that the boundary conditions at z_k and z_N are satisfied.

Depth Dependent Solutions for a Segmented Velocity Profile (U)

(U) The RAYMODE method assumes that the sound speed profile $c(z)$ can be approximated by segments such that $q(z)$ is a linear function of z in each segment (layer). Therefore, within each layer segment, independent traveling wave solutions of (3-4) are exactly given by Hankel functions of order 1/3 and may be written in WKB form as

$$f(z) = V(z) \exp\left\{-i\int_{z_k}^{z} q^{1/2}(z)dz\right\} \qquad (3\text{-}6)$$

$$g(z) = V^*(z) \exp\left\{i\int_{z_k}^{z} q^{1/2}(z)dz\right\} \qquad (3\text{-}7)$$

where the amplitude $V(z)$ and its complex conjugate $V^*(z)$ are given in Appendix 3A. It is important to note that the profile is partitioned so that there is, at most, only one turning point (i.e., depth for which $q(z)=0$) within any layer, so that $V(z)$ is bounded near to and at the turning point.

Continuity Conditions and Reflection Coefficients (U)

(U) Due to the layering of the profile, the solutions $f(z)$ and $g(z)$, and their derivatives, should be continuous across all interfaces. This matching of the solutions (for exponential layers) is done exactly in the Fast Field Program (FFP). However, in RAYMODE X this matching is only done for the interface at the bottom of a surface duct, where R_d^N is replaced by a reflection coefficient obtained from the continuity conditions for a bilinear profile. Everywhere else Leibiger makes the approximation that a wave is totally transmitted across all interfaces until either a layer is reached where a turning point exists or the wave interacts with either the ocean surface or bottom. At a turning point the reflection coefficient is assigned unit magnitude and a $\pi/2$ phase shift. At the ocean surface a plane wave reflection coefficient is assumed with a $-\pi$ phase shift and a magnitude obtained from a semiempirical formula based on the works of Beckman and Spizzichino (1963) and Marsh and Schulkin (1962). Surface loss (i.e., $-20 \log_{10}|R|$) obtained from this magnitude consists of two parts: a high frequency loss, SL_1, and a low frequency loss, SL_2. The surface loss SL_1 is given by

$$SL_1 = -20 \operatorname{Log}_{10} (1-V3)^{1/2} \qquad (3\text{-}8)$$

where

$$V3 = \text{maximum of} \begin{cases} \sin\theta - \dfrac{\exp\left(\frac{a\theta^2}{4}\right)}{(\pi a)^{1/2}} \dfrac{\sin\theta}{\theta} \\[2ex] \dfrac{\sin\theta}{2} \end{cases} \qquad (3\text{-}9)$$

and $a = [2(.003 + 2.6 \times 10^{-3}\ WS)]^{-1}$, WS is the windspeed in knots; θ is the grazing angle in radians. If V3 is

larger than .99, then V3 is set equal to .99. The loss SL_2 is given by

$$SL_2 = -20 \log_{10} \left\{ .3 + \frac{.7}{(1 + .01\,(2 \cdot f \cdot WS \cdot 10^{-5})^2} \right\} \quad (3\text{-}10)$$

where f is the frequency in Hz. Details regarding the derivation of (3-8), (3-9) and (3-10) are given in Appendix IIIB. (A user of RAYMODE X can also specify his own surface loss.)

(U) At the ocean bottom the phase of the reflection coefficient is assumed zero and the magnitude is obtained from a set of modified MGS curves or by directly entering one's own bottom loss table. If nothing is specified, zero dB loss is assumed.

(U) Due to the fact that the MGS curves were originally meant for frequencies greater than 1000 Hz (specifically 3500 Hz), the RAYMODE X program modifies these curves for frequencies less than 1000 Hz. In particular for 100 Hz and below, a single curve derived by Christensen, et al. (1973) is used for all MGS provinces. This curve yields bottom loss BL_1 (θ) as a function of grazing angle (θ) in degress and is given by

$$BL_1(\theta) = -3.11 + .404\theta - 4.98 \times 10^{-3}\theta^2 + 2.89 \times 10^{-5}\theta^3 - 9.0 \times 10^{-3}\theta^4 \quad (3\text{-}11)$$

(U) For frequencies between 100 Hz and 1000 Hz bottom loss BL_2 (θ) as a function of frequency (f), province ($\hat{P}$) and grazing angle is found by interpolating between the 100 Hz curve and the MGS curve for the particular province.

(U) Explicitly, BL_2 (θ) is given by

$$BL_2(\theta) = BL_1(\theta) + [BL_3(\theta,\hat{P}) - BL_1(\theta)] \times \log_{10}(.01f) \quad (3\text{-}12)$$

where BL_3 (θ,P) represents the appropriate MGS curve as a function of grazing angle θ and province $\hat{P}$.

(U) The above assumptions regarding the reflection coefficients are equivalent to approximating solutions of equation (3-4) over $[z_k, z_N]$ by generalized WKB solutions which are valid at turning points.

Integration Limits (U)

(U) For computational purposes the integration limits on equation (3-2) are approximated and the integration performed piecewise. For example, for the profile given by Figure 3-2, with source and receiver both in the surface duct, the integration limits are partitioned so as to correspond to ray angles appropriate for surface duct (SD) paths, convergence zone (CZ) paths and bottom bounce (BB) paths. Thus,

$$\int_{-\infty}^{\infty} = \int_{\xi_3}^{\xi_0} - \underbrace{\int_{\xi_1}^{\xi_0}}_{(SD)} + \underbrace{\int_{\xi_2}^{\xi_1}}_{(CZ)} + \underbrace{\int_{\xi_3}^{\xi_2}}_{(BB)} \quad (3\text{-}13)$$

or

$$P = P_{SD} + P_{CZ} + P_{BB}$$

where $\xi_i = {}^{\omega}/c_i$ (i=0,1,2) and the velocitites C_0, C_1 and C_2 are defined by the profile in Fig. 3-2. ξ_3 is defined by the largest source (grazing) angle θ_s to be considered by using the relation,

$$\xi_3 = \left(\frac{\omega}{C_{Source}}\right) \cos\theta_s \quad (3\text{-}14)$$

(U) In general the limits of integration are approximated as follows: start with the Min $\{c_0, c_{source}, c_{receiver}\} \equiv c_{Min}$ and search for the next velocity maximum c_1; this defines the first set of limits, (ξ_1, ξ_{Max}), where $\xi_{Max} = {}^{\omega}/c_{Min}$. From c_1 to the next velocity maximum c_2 yields the second integration interval (ξ2, ξ1). This process is continued until the last velocity maximum is reached, which is usually the water velocity c_B at the ocean bottom.

The final set of integration limits are then (ξ_{final}, ξ_B) where final is determined by equation (3-14) when the largest desired source angle is specified.

(U) From the above description of the integration limits it is important to note that, for surface duct situations, complex source angles are included in the integration, thus allowing for leakage (diffraction) effects.

Upgoing and Downgoing Paths (U)

(U) Each of the ξ-partitioned integrals for the pressure P is now rewritten as the sum of four integrals

$$(P_{BB} = P_{BB_1} + P_{BB_2} + P_{BB_3} + P_{BB_4})$$

obtained when the numerator of the Green's function (3-3) is expanded in (3-2). These four integrals can be identified with the four ray paths associated with the upgoing/downgoing eigenrays at the source and receiver, for that particular ξ -partition. For example, when the ξ -partition is for bottom bounce paths, the four integrals correspond to the paths shown in Fig. 3-3. The easiest way to see this association is to use first order WKB forms for the solutions f and g, and then integrate each integral by stationary phase. The stationary phase points are simply the target (eigen-) rays for the four upgoing/downgoing rays at the source/receiver combination. This is interesting, but only gives a way to obtain ray theory from a wave theory. Leibiger has generalized the above picture by using generalized WKB forms for f(z) and g(z) and the integrating the above ray path integrals very accurately.

Numerical Evaluation of Integrals (U)

(U) Each of the four integrals is evaluated by either normal mode theory (when the number of modes within the ξ-partition is small) or via a multipath expansion. Leibiger has found that when the number of modes exceed ten it is computationally expedient to calculate the field integrals by the multipath expansion method. This allows for a considerable savings in computer execution time since the multipath expansion method effectively sums the higher order modes in one fast integration. In both instances the integrals (for same ξ-partition, ξ_A, ξ_B), to be evaluated are of the form,

$$P_{(\ )_1} \approx \int_{\xi_A}^{\xi_B} \frac{A(z,z_s;\xi)\, e^{-i\,(\phi_k^{z} - \phi_k^{z_s} + \xi r)}}{(1 - R_u^k R_d^N e^{-2i\phi_K^{z_N}})} ,$$

$$A(z,z_s;\xi) = -i\left(\frac{e^{i\pi/2}\xi}{2\pi r}\right)^{1/2} V^*(z_s)\, V(z) \qquad (3\text{-}15)$$

where for illustrative purposes only $P_{(\ )_1}$ of the above four integrals is considered. Also the first term in the asymptotic expansion of $H_0^{(2)}(\xi r)$ is assumed.

Normal Mode Evaluation (U)

(U) When normal mode theory is utilized, the singularities ξ_m associated with the modes are assumed to be simple poles obtained by solving the equation

$$W(\xi_m) = \left(1 - R_u^k R_d^N e^{-2i\phi_k^{z_N}}\right) = 0 \qquad (3\text{-}16)$$

(U) The normal mode residue associated with (3-15) then becomes

$$P_{(\ )_1} = 2\pi i \sum_m \frac{A(z,z_s;\xi_m)}{\left.\frac{\partial W}{\partial \xi}\right|_{\xi_m}} e^{-i(\phi_k^{z} - \phi_k^{z_s} + \xi_m r)} \qquad (3\text{-}17)$$

Details regarding the numerical determination of the complex eigenvalues ξ_m and specific evaluation of the normalization term $\left.\frac{\partial W}{\partial \xi}\right|_{\xi m}$ can be found in Appendix 3C.

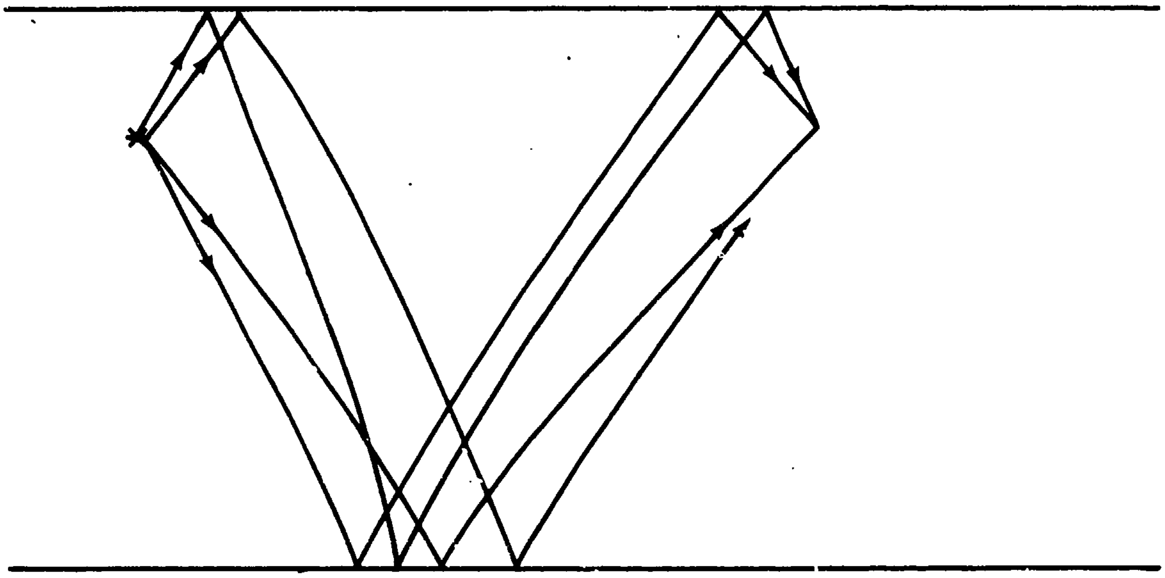

UNCLASSIFIED

Figure 3-3. (U) Upgoing and Downgoing Bottom Bounce Paths--for One Cycle

Multipath Expansion (U)

(U) For the multipath approach, the denominator of (3-15) is expanded so that

$$P_{(\ )_1} = \sum_{j=0}^{\infty} \int_{\xi_A}^{\xi_B} A(z, z_s; \xi)(R_u^k R_d^N)^j e^{-i\left[\phi_k^z - \phi_k^{z_s} - 2j\phi_k^{z_N} + \xi r\right]} \quad (3\text{-}18)$$

The interval of integration is divided into a number of unequal sections based upon the number of rays traced (which is an input parameter). The value of ξ for some of these sub-sections is sufficiently far from a stationary phase point so that their contribution is excluded. Although stationary phase techniques are not used, the stationary phase points are available from ray calculations. The justification for neglecting such sub-sections is involved with the spiral-like nature of the cumulative result for the field. When a subsection does not meet this criteria the phase term is approximated by a quadratic expression in ξ. The amplitude of the kernel is assumed to be slowly varying over the sub-interval so that it can be evaluated at an interior point and removed outside the integral. The resulting integral can be expressed in terms of Fresnel integrals by a suitable transformation. The Fresnel integrals are then evaluated numerically. Fresnel integrals can be used to evaluate the integrals over the sub-intervals because of the smallness of the integration interval. If larger intervals were used the computation time would increase due to the need of evaluating incomplete Airy functions.

(U) The series given by (3-18) represents the multipath expansion of (3-15). The advantage of (3-18) is that not only are the upgoing-downgoing paths delineated but the number of cycles that a ray (wave) undergoes is counted by the index j. In RAYMODE X the number of cycles necessary for a ray path to reach a given range is calculated so that the infinite series in (3-18) may be approximated by summing only a few j's. For example, if the ξ-partition corresponds to convergence zone paths and one is interested only in the first CZ, then terms for j>>1 would only yield fine structure effects on a propagation loss versus range curve.

Transmission Loss (U)

(U) The acoustic pressure field as determined from (3-17) and (3-18) is modified by a beampattern attenuation factor characterizing the off-axis beam position of an equivalent ray. This beampattern attenuation is similarly applied to the other three pressure components $P_{(\ )_2}$, $P_{(\ )_3}$ and $P_{(\ )_4}$ for each ξ-partition. The real and imaginary components of pressure,
$\mathrm{Re}\{P_{(\ )i}\}$ and $\mathrm{Im}\{P_{(\ )i}\}$
are then used to form a rms intensity and a coherent intensity for each range point desired and for each ξ-partition.

(U) Transmission loss (relative to unit intensity at unit distance from source) is then calculated from the incoherent and coherent intensity sums. For example, in the case described in Fig. 3-2, the transmission loss TL is given by

$$\mathrm{TL\ (Coherent)} = -10 \log_{10} \left\{ \left(\sum_{i=1}^{4} \left[\mathrm{Re}\{P_{SD_i}\} + \mathrm{Re}\{P_{CZ_i}\} + \mathrm{Re}\{P_{BB_i}\}\right] \right)^2 + \left(\sum_{i=1}^{4} \left[\mathrm{Im}\{P_{SD_i}\} + \mathrm{Im}\{P_{CZ_i}\} + \mathrm{Im}\{P_{BB_i}\}\right] \right)^2 \right\} + \alpha r \quad (3\text{-}19)$$

and

$$\mathrm{TL} = \mathrm{(incoherent)} = -10 \log_{10} \left\{ \left(\sum_{i=1}^{4} \left[(\mathrm{Re}\{P_{SD_i}\})^2 + (\mathrm{Im}\{P_{SD_i}\})^2 + (\mathrm{Re}\{P_{CZ_i}\})^2 + (\mathrm{Im}\{P_{CZ_i}\})^2 + (\mathrm{Re}\{P_{BB_i}\})^2 + (\mathrm{Im}\{P_{BB_i}\})^2 \right] \right\} + \alpha r \quad (3\text{-}20)$$

where α is Thorp's attenuation coefficient.

3.3 (U) Summary of Basic Assumptions

- Velocity profile fit with segments such that the index of refraction squared is a linear function of depth.

- Multiple reflections due to velocity discontinuities ignored except in surface duct situations.

- Plane wave reflection coefficients assumed.

- Surface and bottom loss expressions assume the validity of experimental data, which may be questionable.

- Only a finite number of ray cycles are considered in the multipath evaluation of the pressure integrals.

- Velocity profile does not change with range.

- Harmonic source assumed.

- Density of 1 assumed.

- Only one source and receiver allowed per run.

- Constant bottom depth.

3.4 (U) Suggested Test Cases for RAYMODE X

(U) The RAYMODE X program has been compared against both experimental data and other computer programs. In general the comparisons tend to validate most of the assumptions listed in Sections 3.3 of this synopsis. However, there are a few cases that may possibly cause RAYMODE X to give unsatisfactory answers. Results for two cases are given below:

(U) Case I: Cross layer surface duct problem with source in the duct at 250 ft and receiver below the duct at 450 ft for frequencies of 10, 50 and 100 Hz. The velocity profile for this case is shown in Figure 3-4. Bottom loss is given by FNOC type 5.

(U) In this case RAYMODE does not properly account for the surfact duct (SD) contribution because only trapped modes are presently used in the UNIVAC 1108 version. Trapped modes are here defined to mean those modes whose eigenvalues are real and lie between $\xi_1 = \omega/c_1$ and $\xi_2 = \omega/c_2$, where c_1 is the velocity at the layer depth and c_2 is the larger of the source/receiver velocities. For the lower frequencies one must also allow for the leaky modes, i.e., modes whose eigenvalues are complex. The leaky modes correspond to eigenvalues between $\xi_0 = \omega/c_0$ and $\xi_\ell = (\omega/c_{source}) \cos \theta_s$, where C_0 is the velocity at the surface and θ_s is the largest source (grazing) angle. The SD part is described as allowing for both trapped and leaky modes. That is, the SD integration interval extends from ξ_0 to ξ_ℓ. However, this version does not exist on the UNIVAC 1108 although it does exist on the HP9845 and the Tektronix 4051 computers.

(U) For the in-layer case (source at 76.2 m, receiver at 45.72 m) coherent RAYMODE (Figs. 3-5 to 3-7) predicts no trapped SD modes at 50 Hz and 100 Hz. Therefore, only the direct path and bottom bounce contribute at these frequencies. In order to evaluate RAYMODE, Fast Field Program (FFP) predictions were made (Figs. 3-8 to 3-10) since the FFP considers all modes. When RAYMODE is compared with the FFP, one observes that in the first bottom bounce region the leaky mode contribution is masked by the bottom bounce energy. However, beyond the first bottom bounce region the leaky modes are the significant contribution.

(U) For the in-layer case at 200 Hz RAYMODE predicts that one (unattenuated) trapped mode exists. When compared with the FFP it is clear that RAYMODE predicts much more trapping (approximately 10 dB) than actually exists because even at 200 Hz the true trapped mode has a significant imaginary component. This imaginary part attenuates the SD mode contribution. (Note: Incoherent RAYMODE results are given in Figures 3-11 to 3-13.)

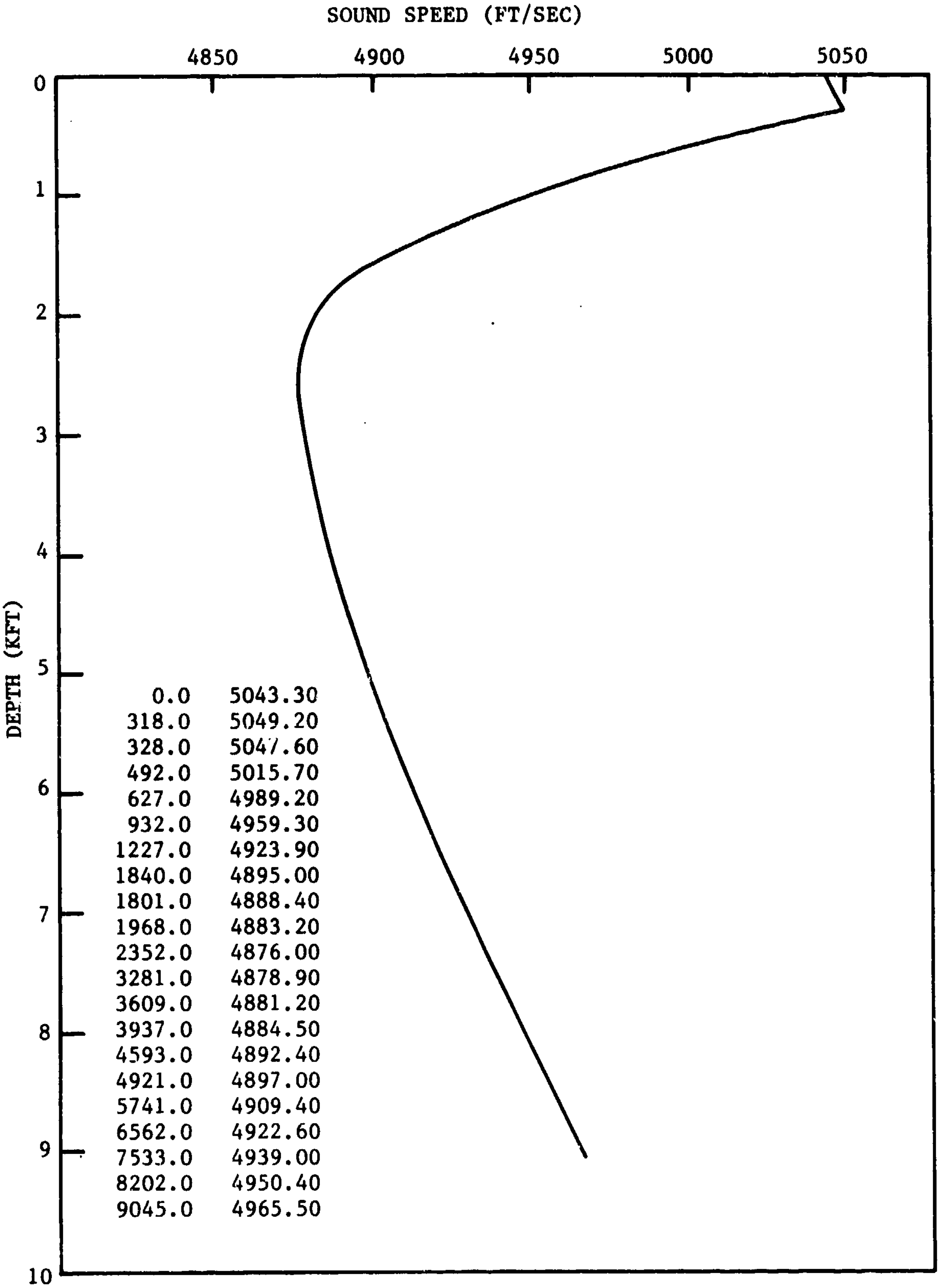

UNCLASSIFIED

Figure 3-4. (U) Velocity Depth Profile for Test Case I

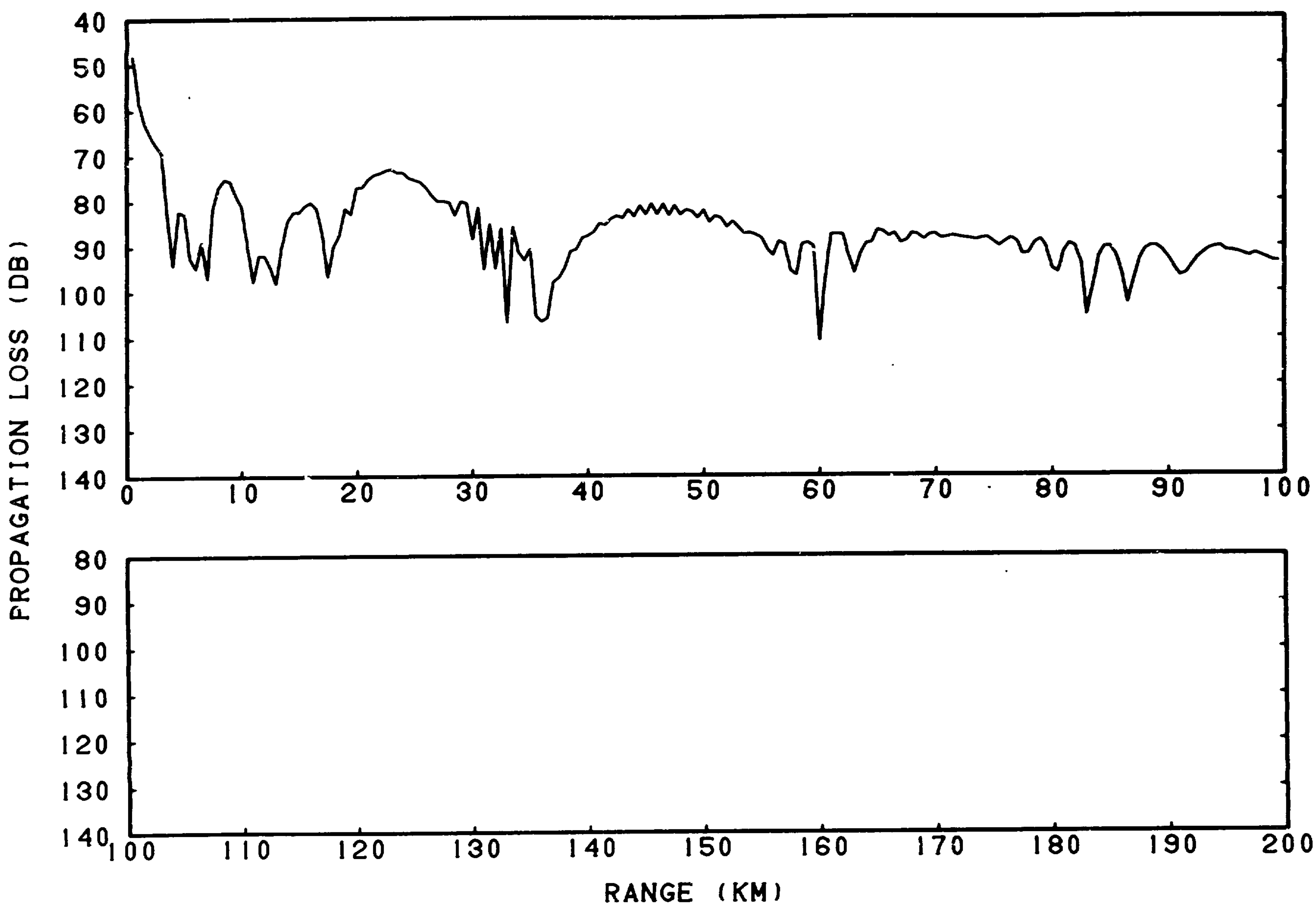

UNCLASSIFIED

Figure 3-5. (U) Case I. In-layer Geometry. RAYMODE Coherent. Source Depth = 76 m. Receiver Depth = 45 m. Frequency = 50 Hz.

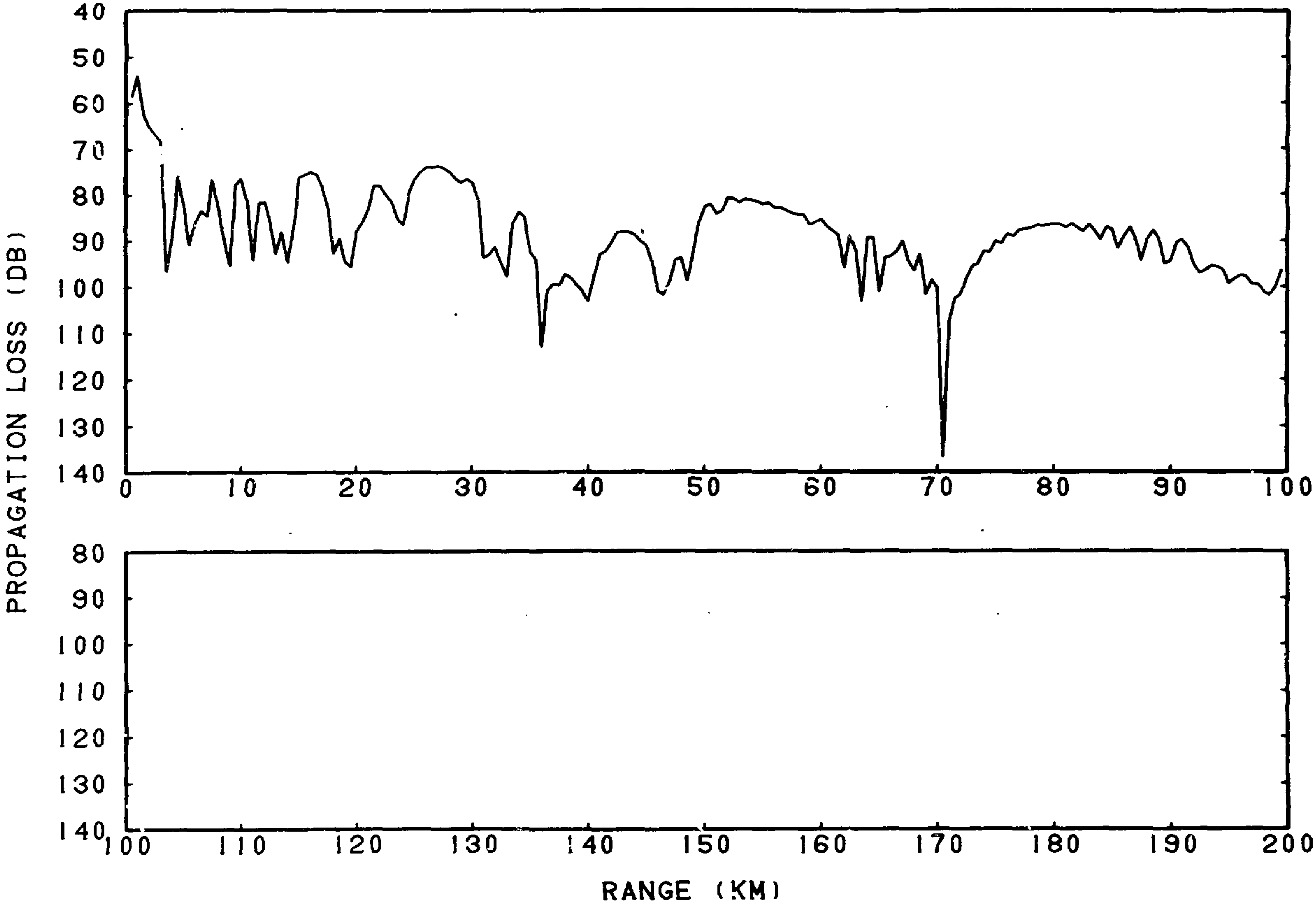

UNCLASSIFIED

Figure 3-6. (U) Case I. In-layer Geometry. RAYMODE Coherent. Source Depth = 76 m. Receiver Depth = 45 m. Frequency = 100 Hz.

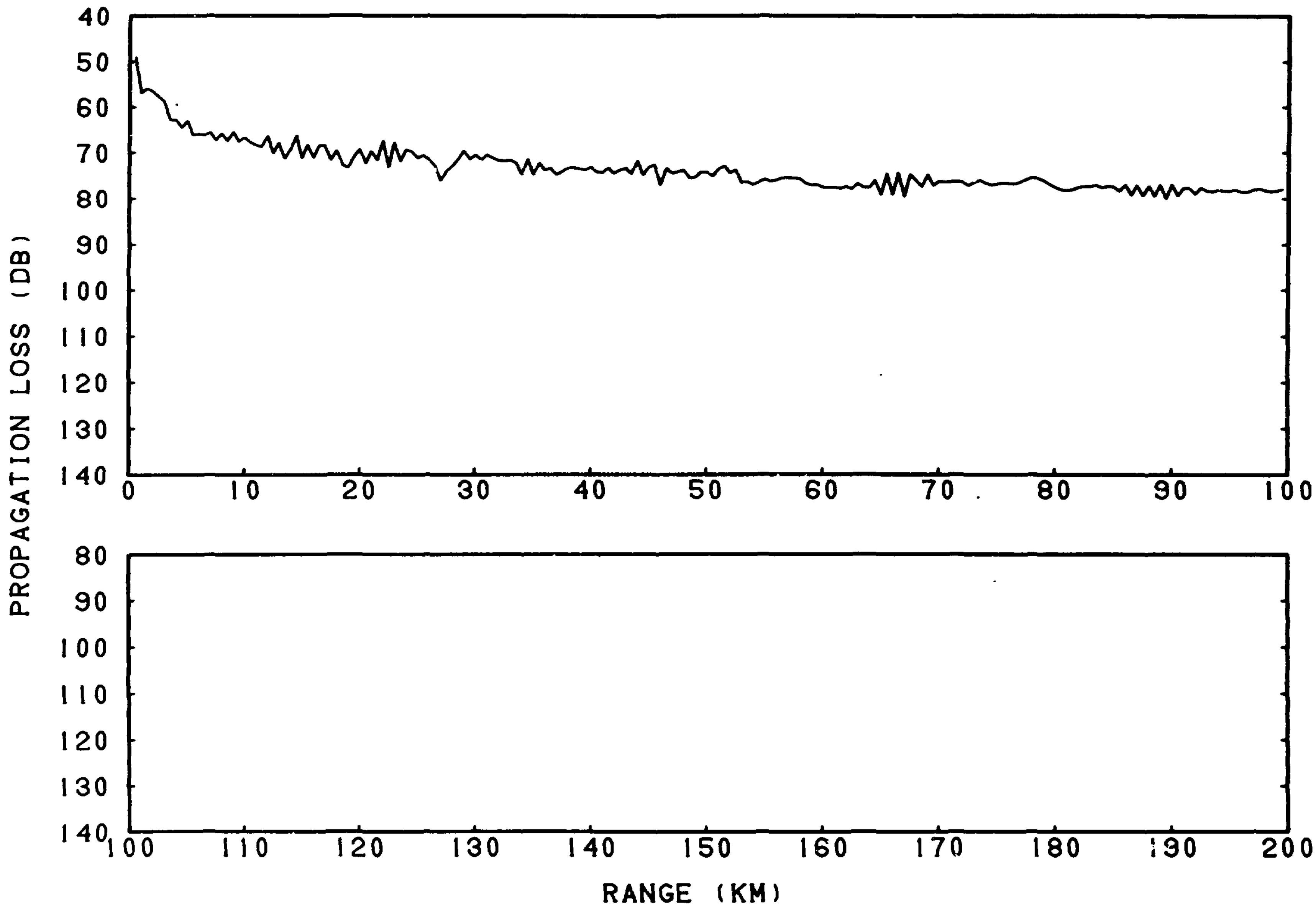

UNCLASSIFIED

Figure 3-7. (U) Case I. In-layer Geometry. RAYMODE Coherent. Source Depth = 76 m. Receiver Depth = 45 m. Frequency = 200 Hz.

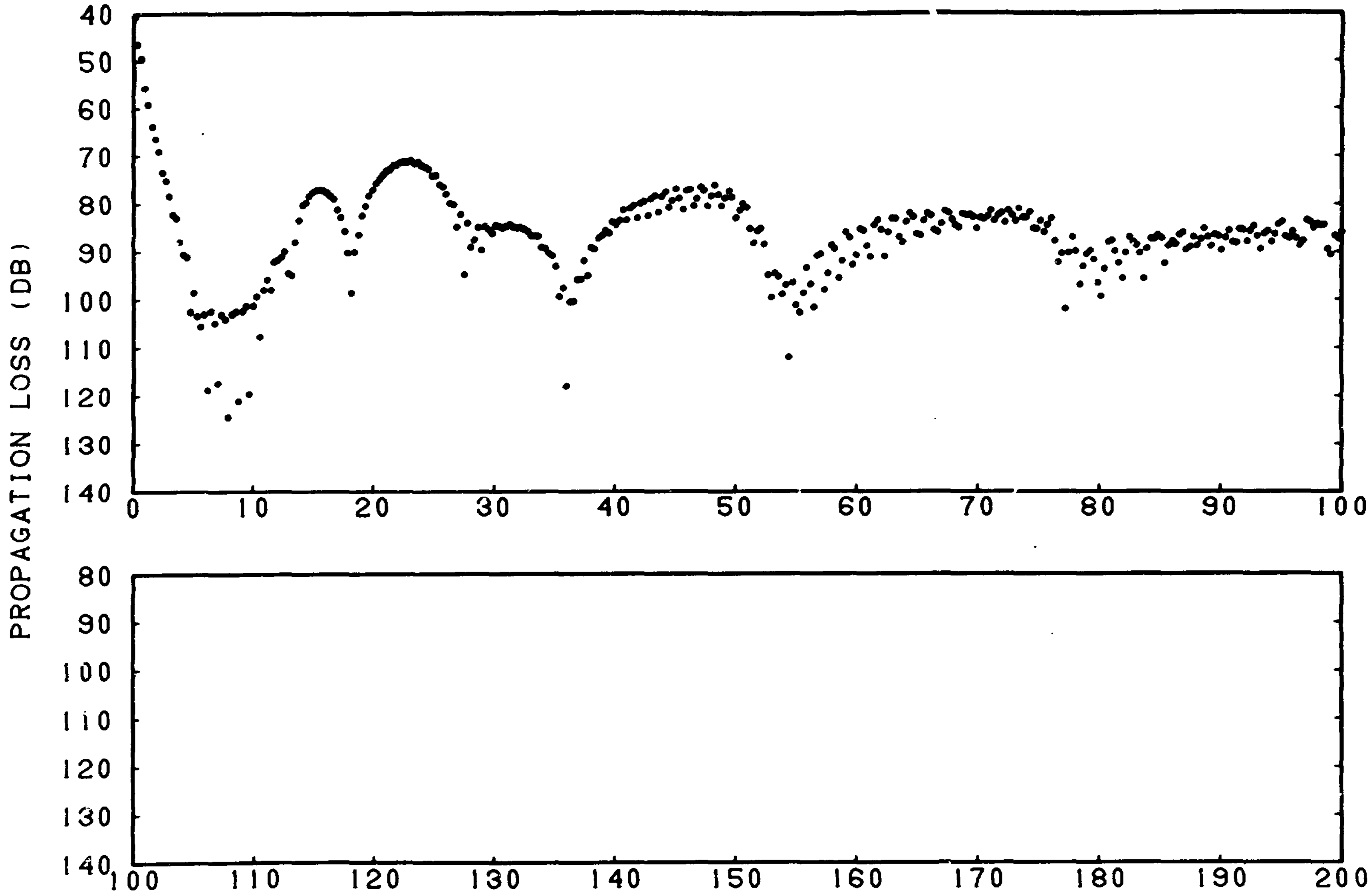

UNCLASSIFIED

Figure 3-8. (U) Case I. In-layer Geometry. FFP. Source Depth = 76 m. Receiver Depth = 45 m. Frequency = 50 Hz.

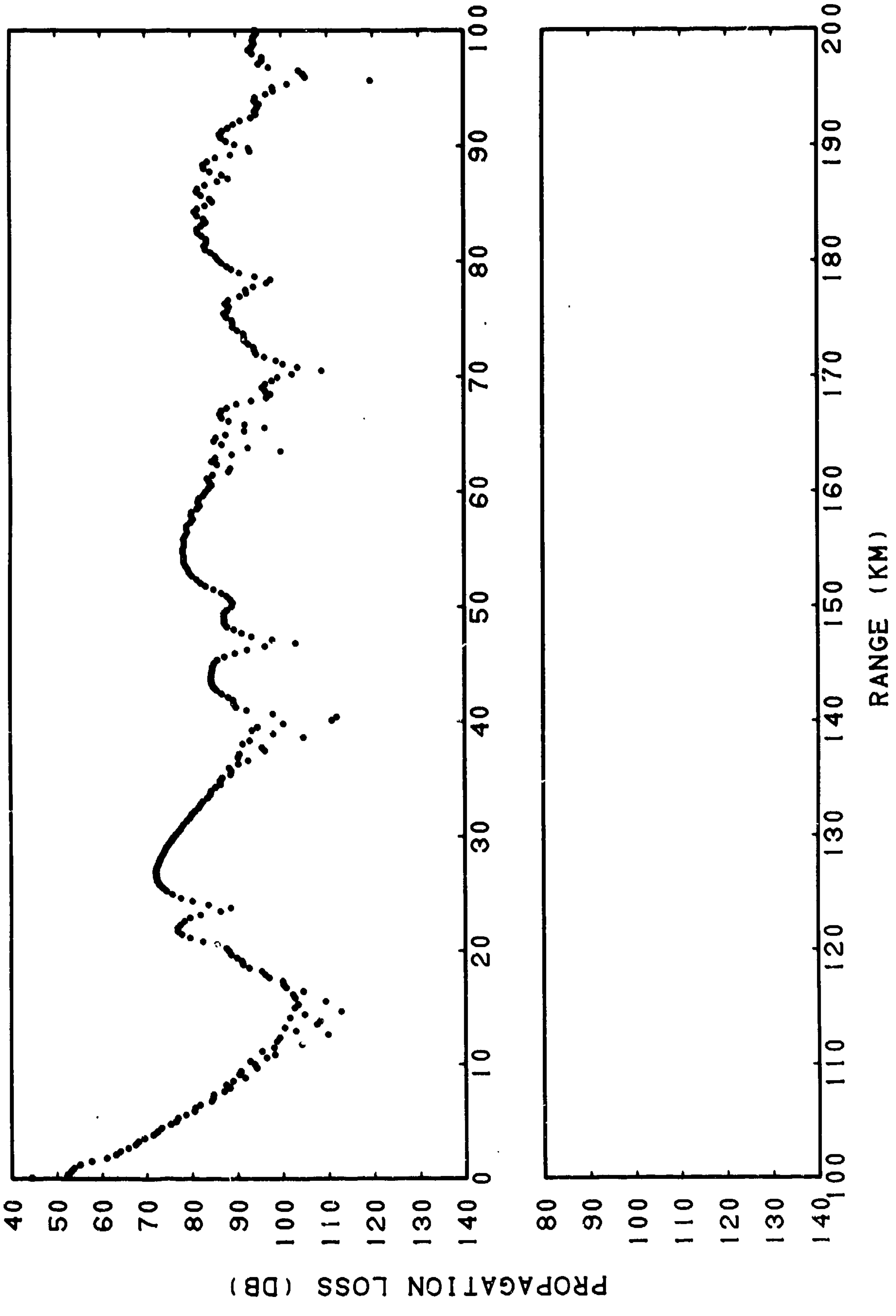

UNCLASSIFIED

Figure 3-9. (U) Case I. In-layer Geometry. FFP. Source Depth = 76 m. Receiver Depth = 45 m. Frequency = 100 Hz.

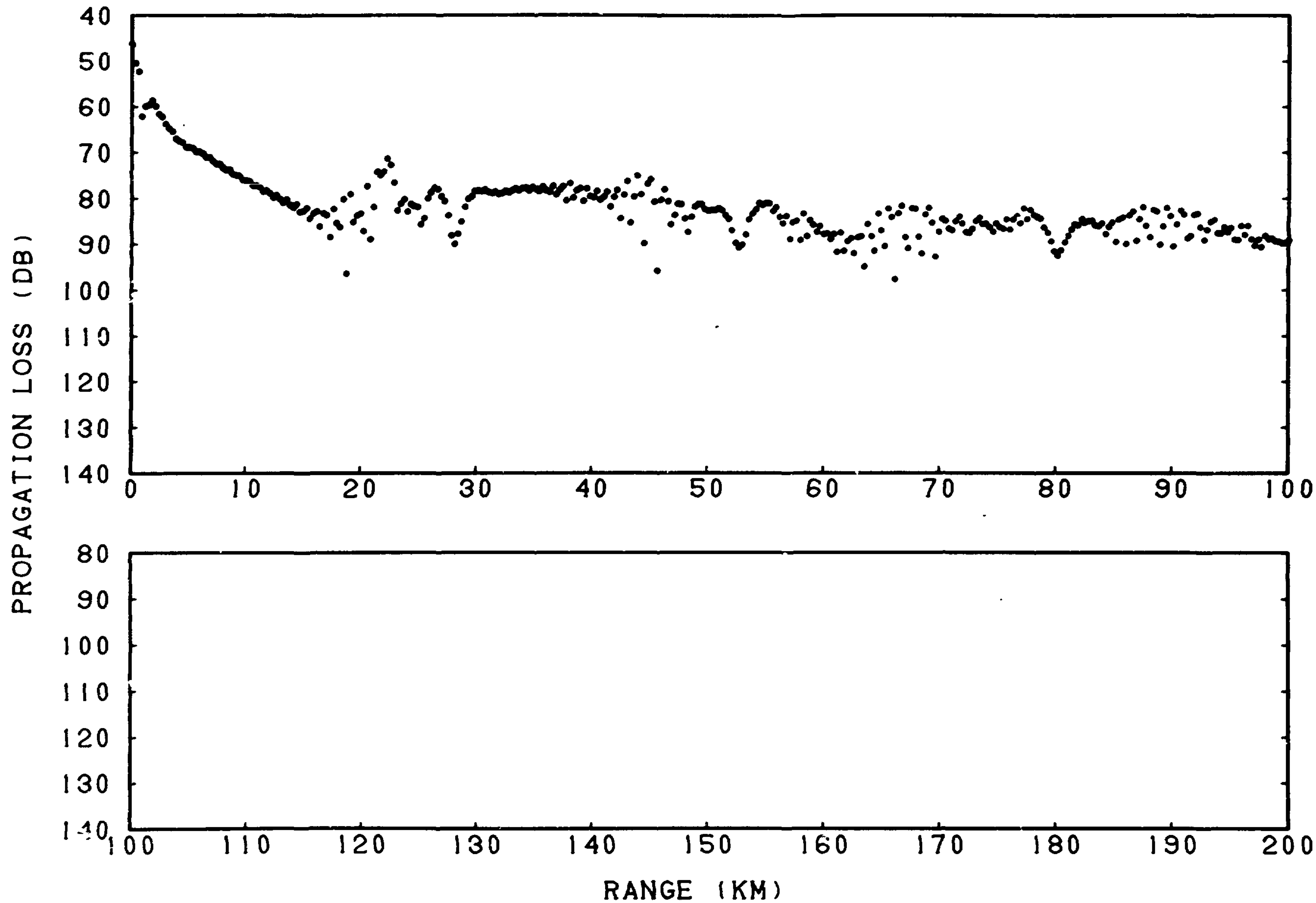

UNCLASSIFIED

Figure 3-10. (U) Case I. In-layer Geometry. FFP. Source Depth = 76 m. Receiver Depth = 45 m. Frequency = 200 Hz.

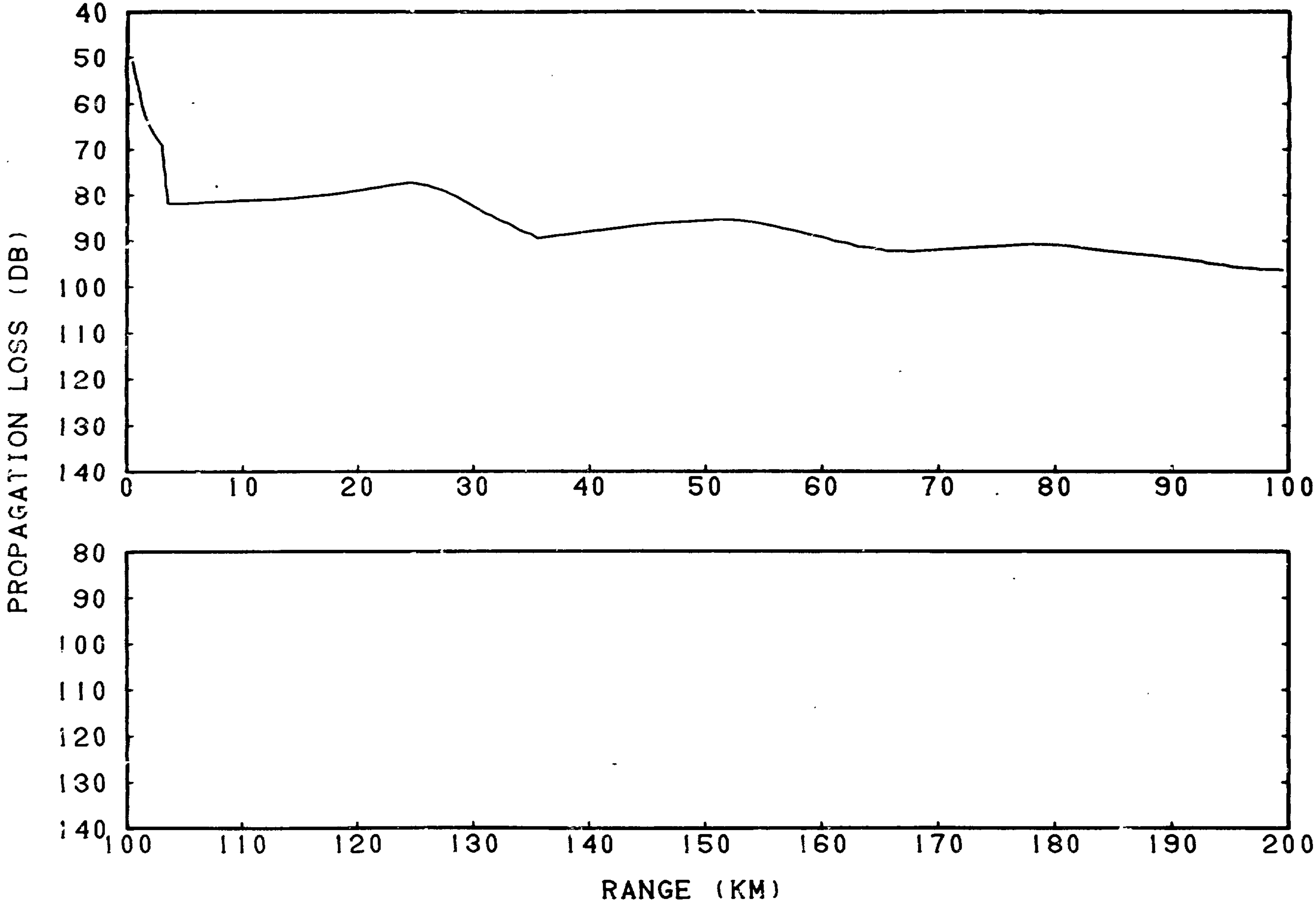

UNCLASSIFIED

Figure 3-11. (U) Case I. In-layer Geometry. RAYMODE Incoherent. Source Depth = 76 m. Receiver Depth = 45 m. Frequency = 50 Hz.

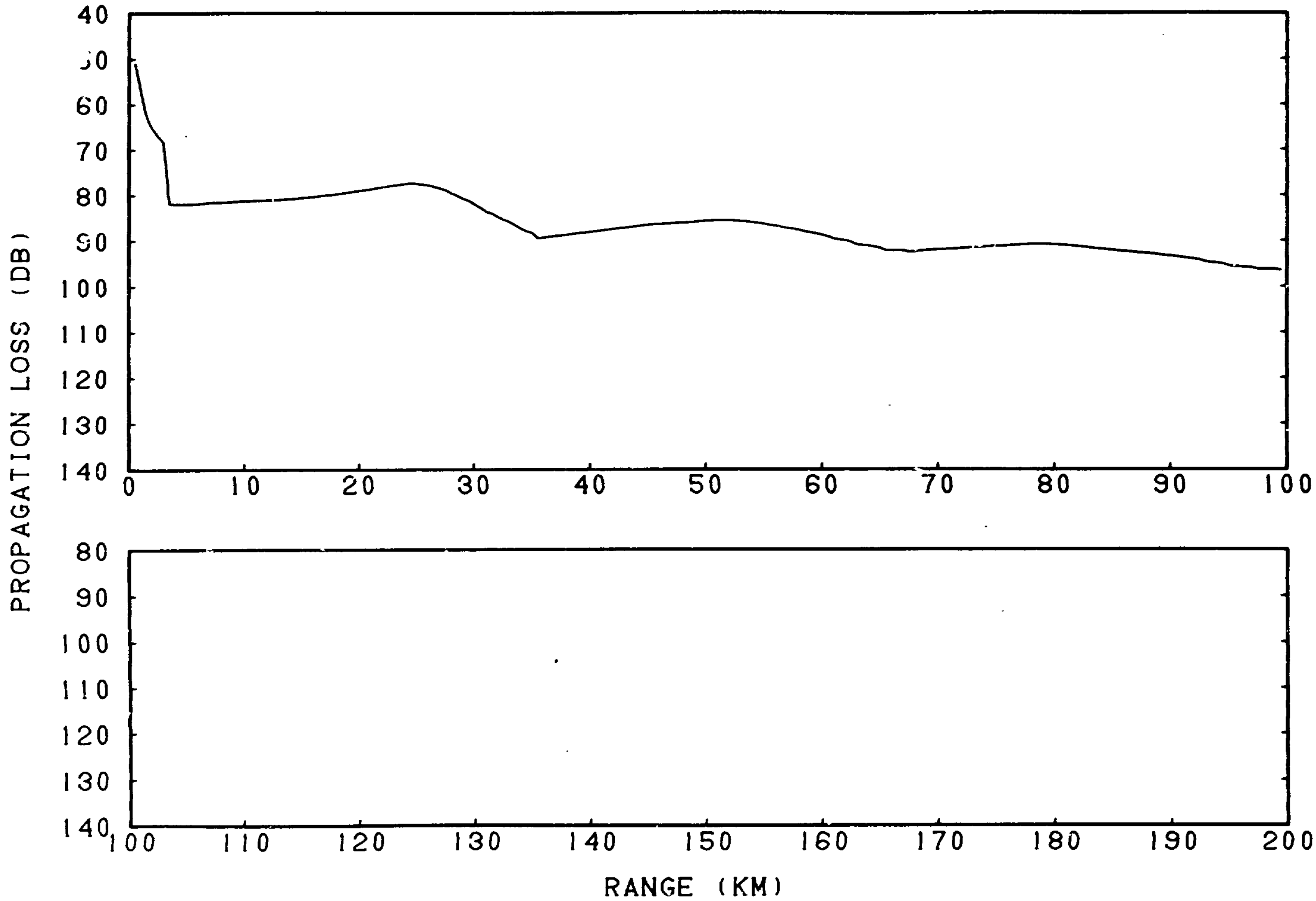

UNCLASSIFIED

Figure 3-12. (U) Case I. In-layer Geometry. RAYMODE Incoherent. Source Depth = 76 m. Receiver Depth = 45 m. Frequency = 100 Hz.

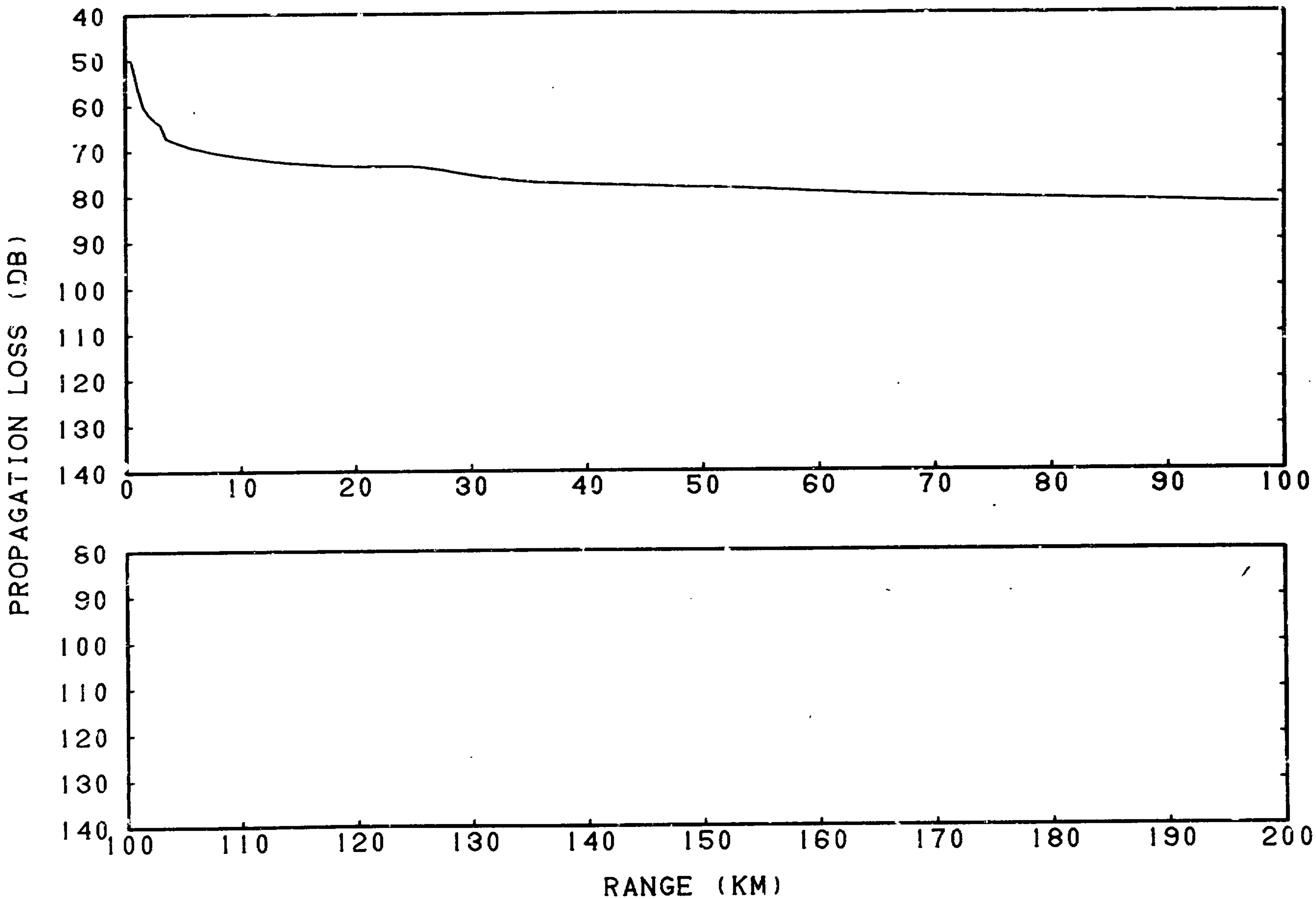

UNCLASSIFIED

Figure 3-13. (U) Case I. In-layer Geometry. RAYMODE Incoherent. Source Depth = 76 m. Receiver Depth = 45 m. Frequency = 200 Hz.

(U) In the cross-layer case (source at 76.2 m, receiver at 137.16 m) RAYMODE (Figs. 3-14 to 3-16) showed basically good results compared to the FFP (Figs. 3-17 to 3-19) for all frequencies considered despite the fact that it does not allow for below layer leakage effects. That is, in the present 1108 version it does not matter in the cross layer situation whether or not there are trapped modes in the duct since no energy is allowed to escape. (Note: RAYMODE incoherent results are given in Figures 3-20 to 3-22.)

(U) In summary, Case I shows that the present UNIVAC 1108 version of RAYMODE can yield poor surface duct results at the lower frequencies. This deficiency in RAYMODE has been recognized by Leibiger for some time, and has been corrected in the HP and Tektronix versions.

(U) Case II: Depressed sound channel problem with source and receiver both in the depressed channel at depths of 270 ft and 220 ft, respectively, and for frequencies of 10, 30, 100 and 300 Hz. Velocity profile for this case is shown in Figure 3-23. Bottom loss is given in Table 3-1.

Table 3-1. (U) Bottom Loss Versus Grazing Angle for Test Case II

Angle (degrees) θ	Bottom Loss (dB) BL(θ)
0.0	0.0
0.5	2.8
1.0	5.6
1.5	8.6
2.0	11.5
2.5	14.2
3.0	16.7
3.5	18.8
4.0	20.5
5.0	23.0
6.0	24.4
8.0	25.7
10.0	26.1
15.0	26.4
90.0	26.4

UNCLASSIFIED

(U) Case II is concerned with low frequency propagation in an environment where the velocity profile (Fig. 3-23) exhibits a depressed channel above the SOFAR channel. The source and receiver are located near the axis of the depressed channel. For a frequency of 10 Hz, RAYMODE (Fig. 3-24) does not see the depressed channel (depressed modes below phase-integral cutoff) but only some combination of convergence zone (CZ) and bottom bounce energy. The FFP (Fig. 3-27), however, seems to indicate trapping within the depressed channel. When the frequency is increased to 100 Hz, RAYMODE (Fig. 3-25) still does not calculate depressed modes but predicts more loss than at 10 Hz, which is difficult to understand since there should be more trapping at 100 Hz. The FFP for 100 Hz (Fig. 3-28) does predict more trapping within the shallow channel as well as some CZ energy at 40 km and 80 km. At 300 Hz RAYMODE (Fig. 3-26) appears now to be predicting one totally trapped depressed mode along with some CZ energy at around 43 km and 86 km. The FFP for 300 Hz (Fig. 3-29) predicts strong depressed channel trapping (approximately 12 dB less loss than RAYMODE) with only hints of the CZ energy at 40 km and 80 km. (Note: RAYMODE incoherent results are given in Figs. 3-30 to 3-32.) In summary RAYMODE does not properly account for depressed channel propagation at the lower frequencies (<300 Hz). The exact reasons are not clear but seem to be related to the fact that in RAYMODE there is no consideration of partial trapping of energy within the depressed channel. This low frequency trapping, however, is masked many times by low loss bottom bounce energy.

Appendix 3A. Depth Dependent Solutions for a Segmented Velocity Profile (U)

(U) The RAYMODE method assumes that the sound speed profile c(z) can be approximated by segments such that q(z) is a linear function of z in each segment (layer). Therefore, within each layer segment, independent traveling wave solutions of (3.4 are) exactly given by

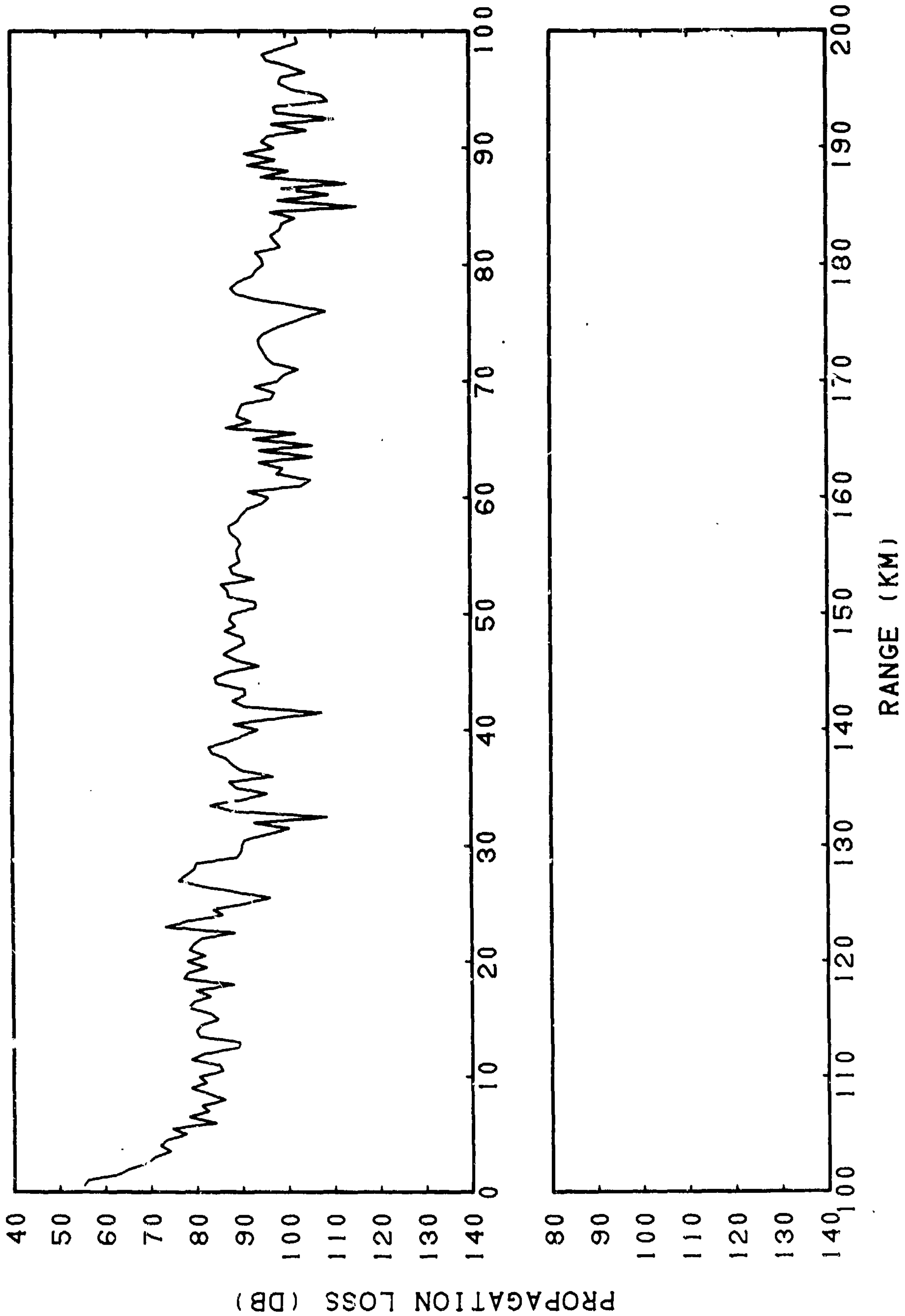

UNCLASSIFIED

Figure 3-14. (U) Case I. In-layer Geometry. RAYMODE Coherent. Source Depth = 76 m. Receiver Depth = 137 m. Frequency = 50 Hz.

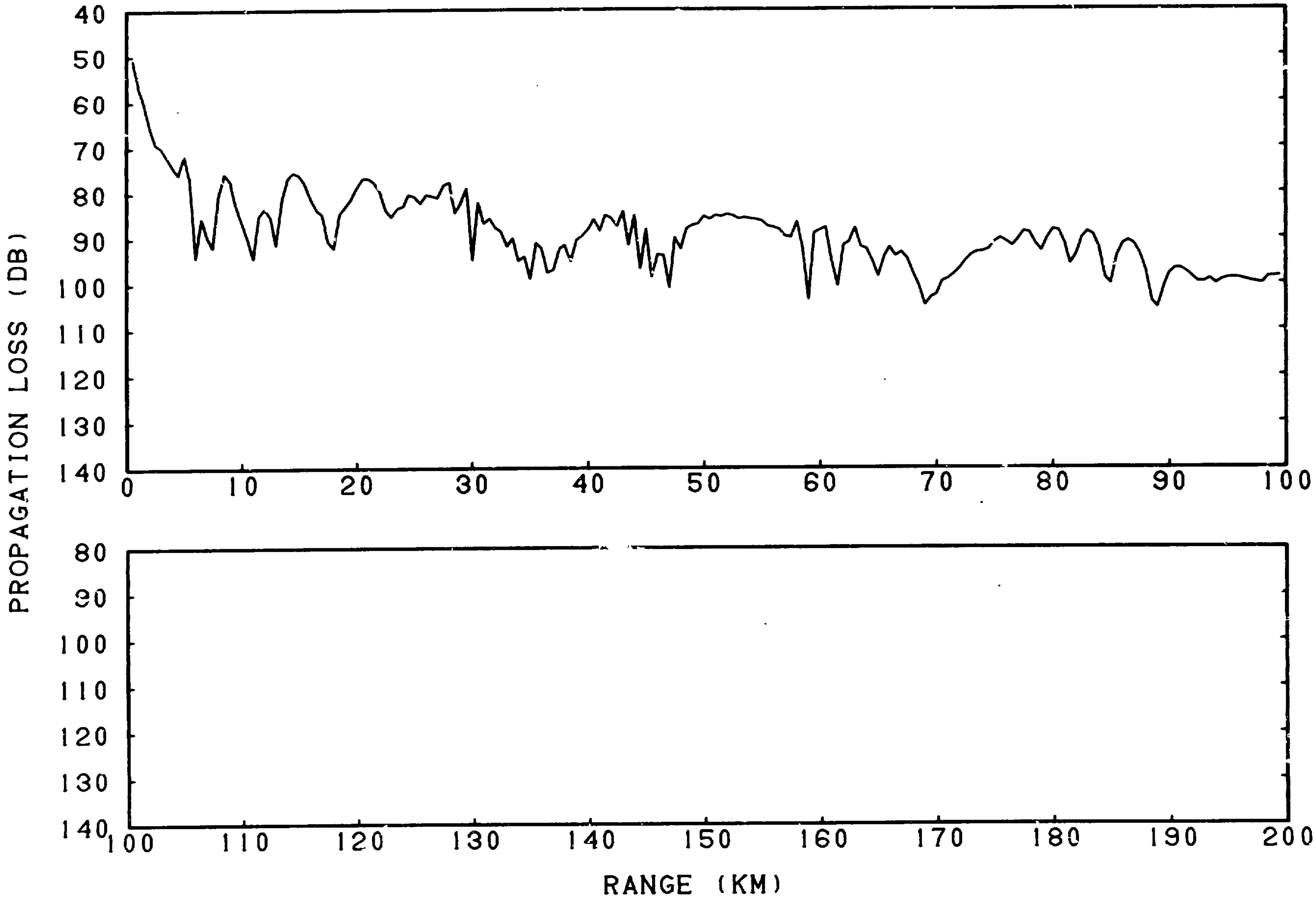

UNCLASSIFIED

Figure 3-15. (U) Case I. In-layer Geometry. RAYMODE Coherent. Source Depth = 76 m. Receiver Depth = 137 m. Frequency = 100 Hz.

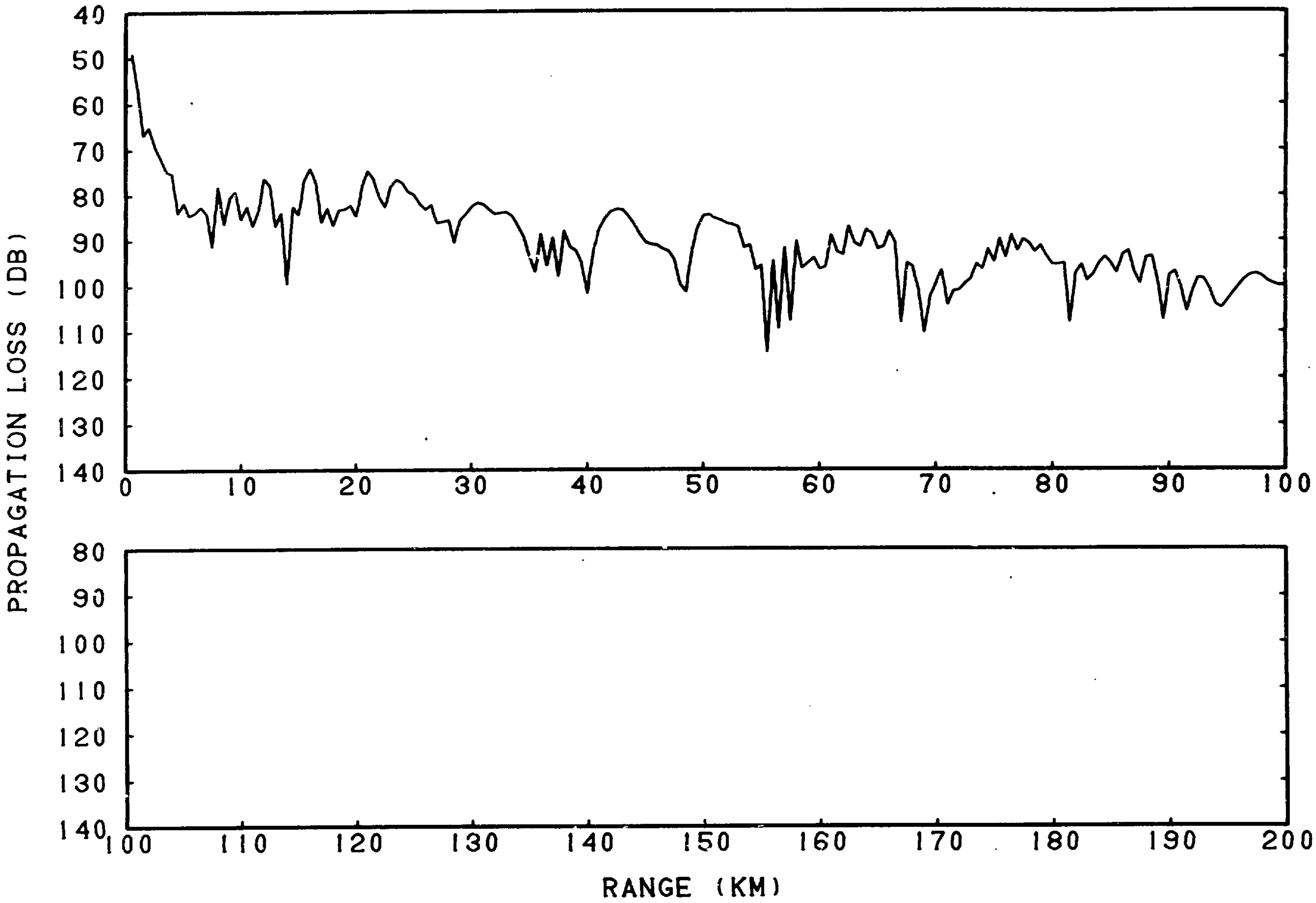

UNCLASSIFIED

Figure 3-16. (U) Case I. In-layer Geometry. RAYMODE Coherent. Source Depth = 76 m. Receiver Depth = 137 m. Frequency = 200 Hz.

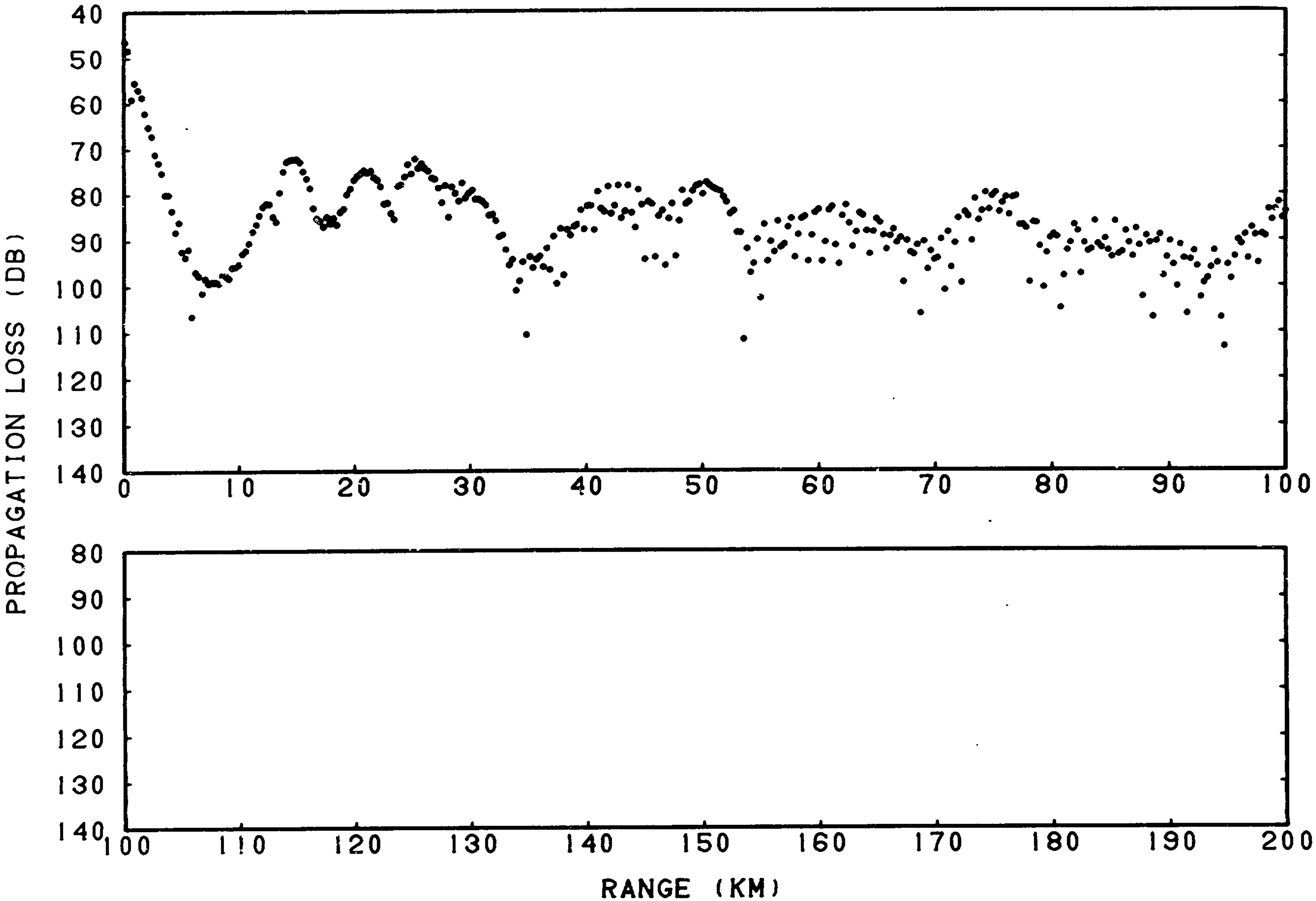

UNCLASSIFIED

Figure 3-17. (U) Case I. Cross-layer Geometry. FFP. Source Depth = 76 m. Receiver Depth = 137 m. Frequency = 50 Hz.

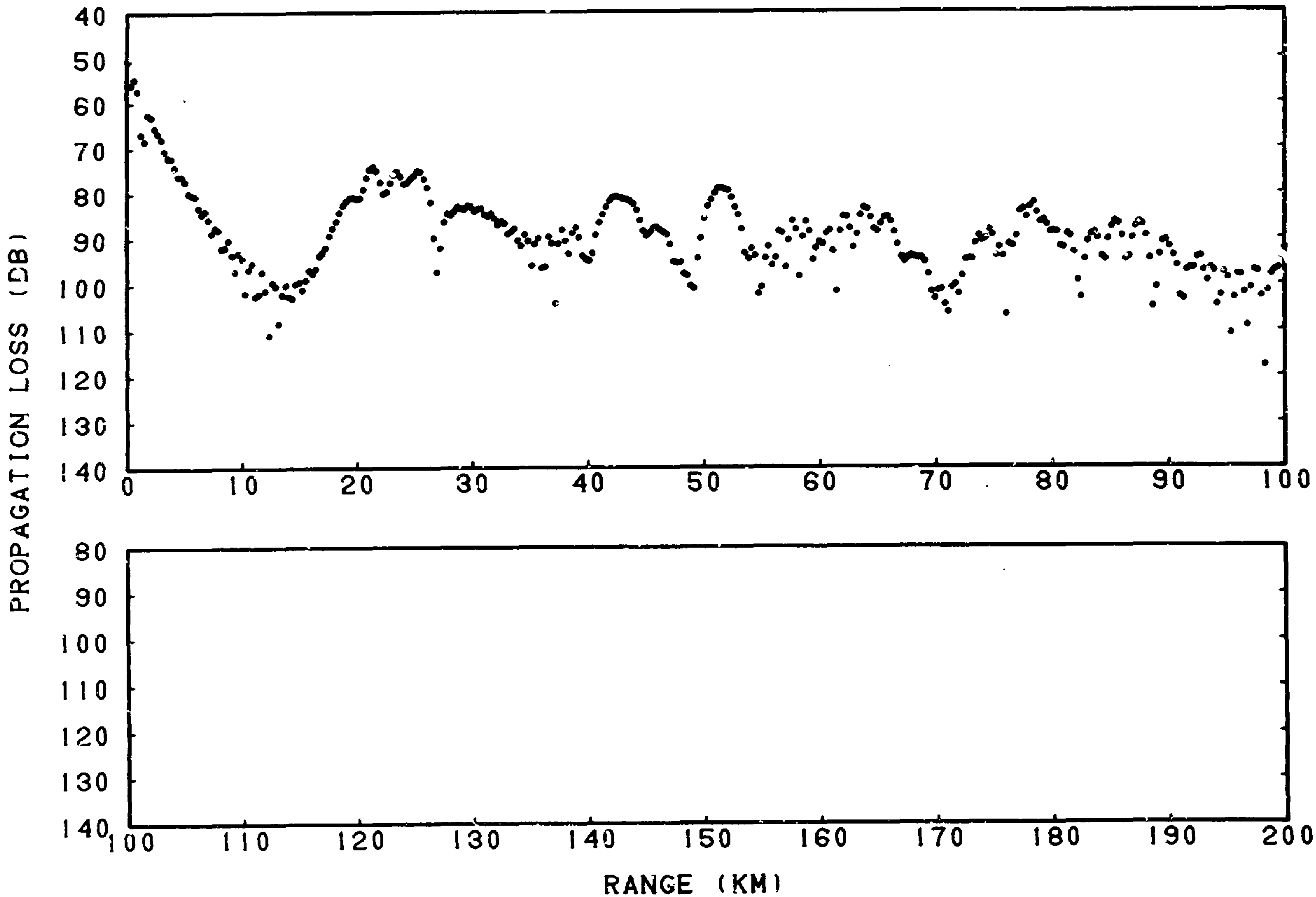

UNCLASSIFIED

Figure 3-18. (U) Case I. Cross-layer Geometry. FFP. Source Depth = 76 m. Receiver Depth = 137 m. Frequency = 100 Hz.

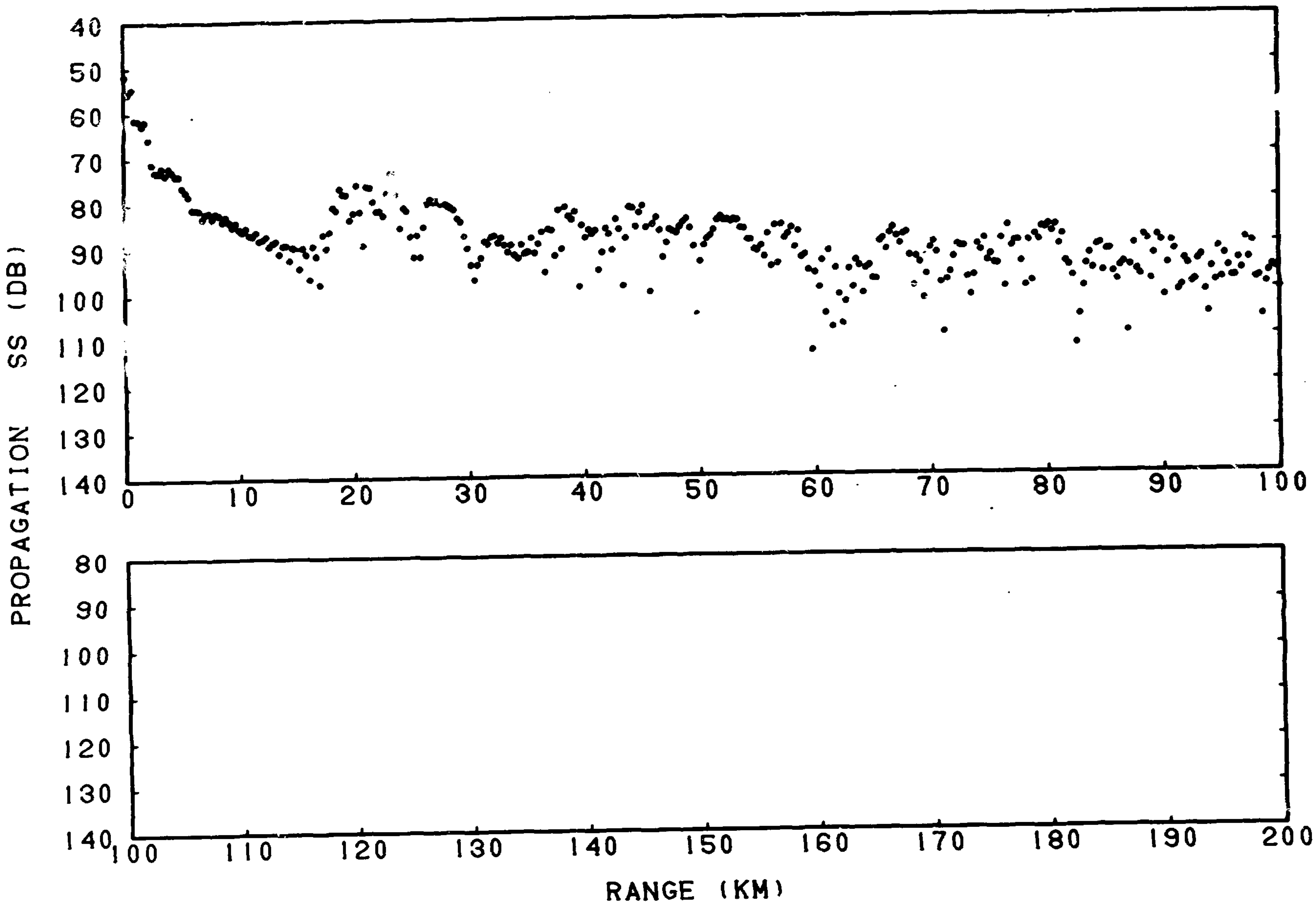

UNCLASSIFIED

Figure 3-19. (U) Case I. Cross-layer Geometry. FFP. Source Depth = 76 m. Receiver Depth = 137 m. Frequency = 200 Hz.

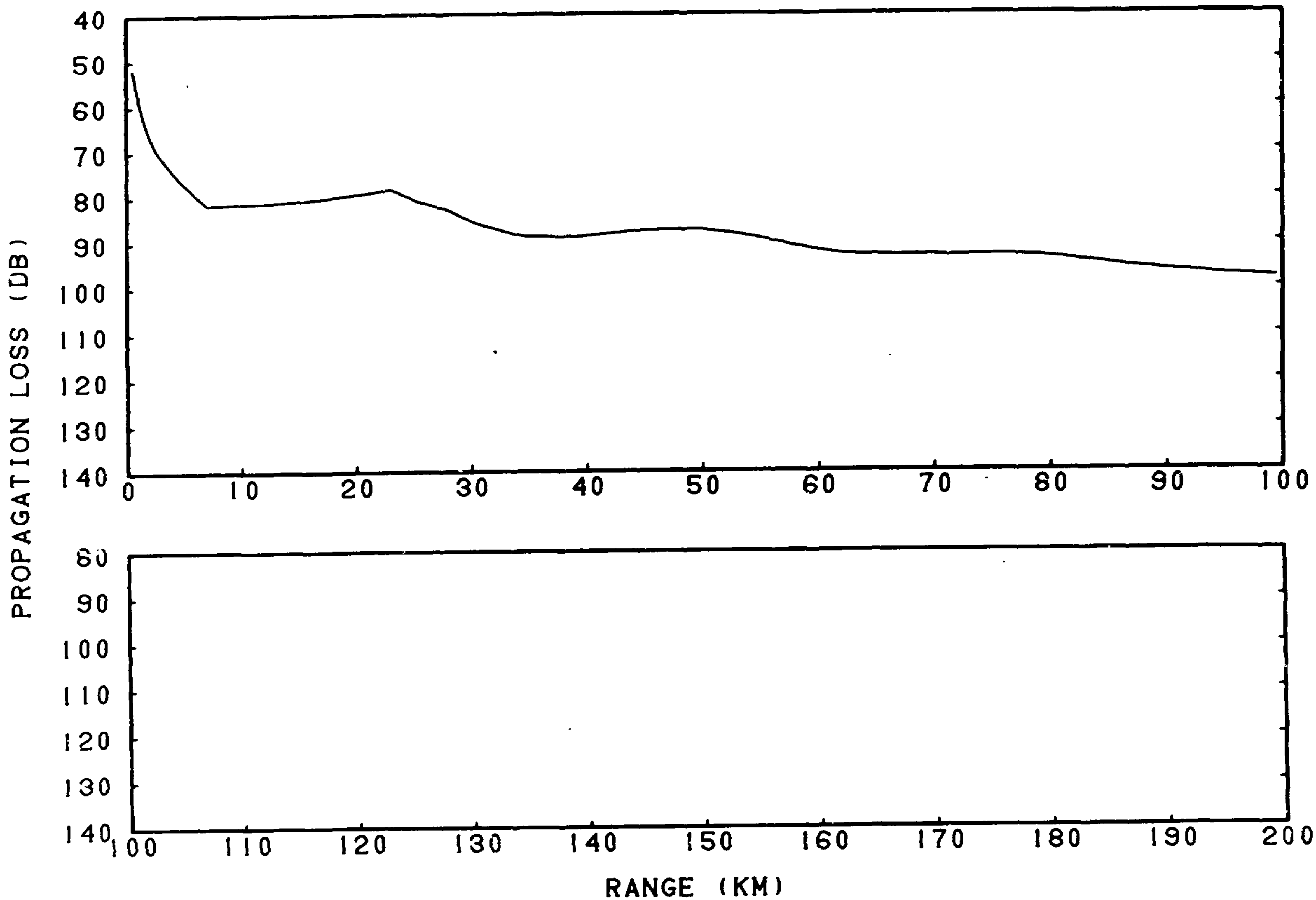

UNCLASSIFIED

Figure 3-20. (U) Case I. Cross-layer Geometry. RAYMODE Incoherent. Source Depth = 76 m. Receiver Depth = 137 m. Frequency = 50 Hz.

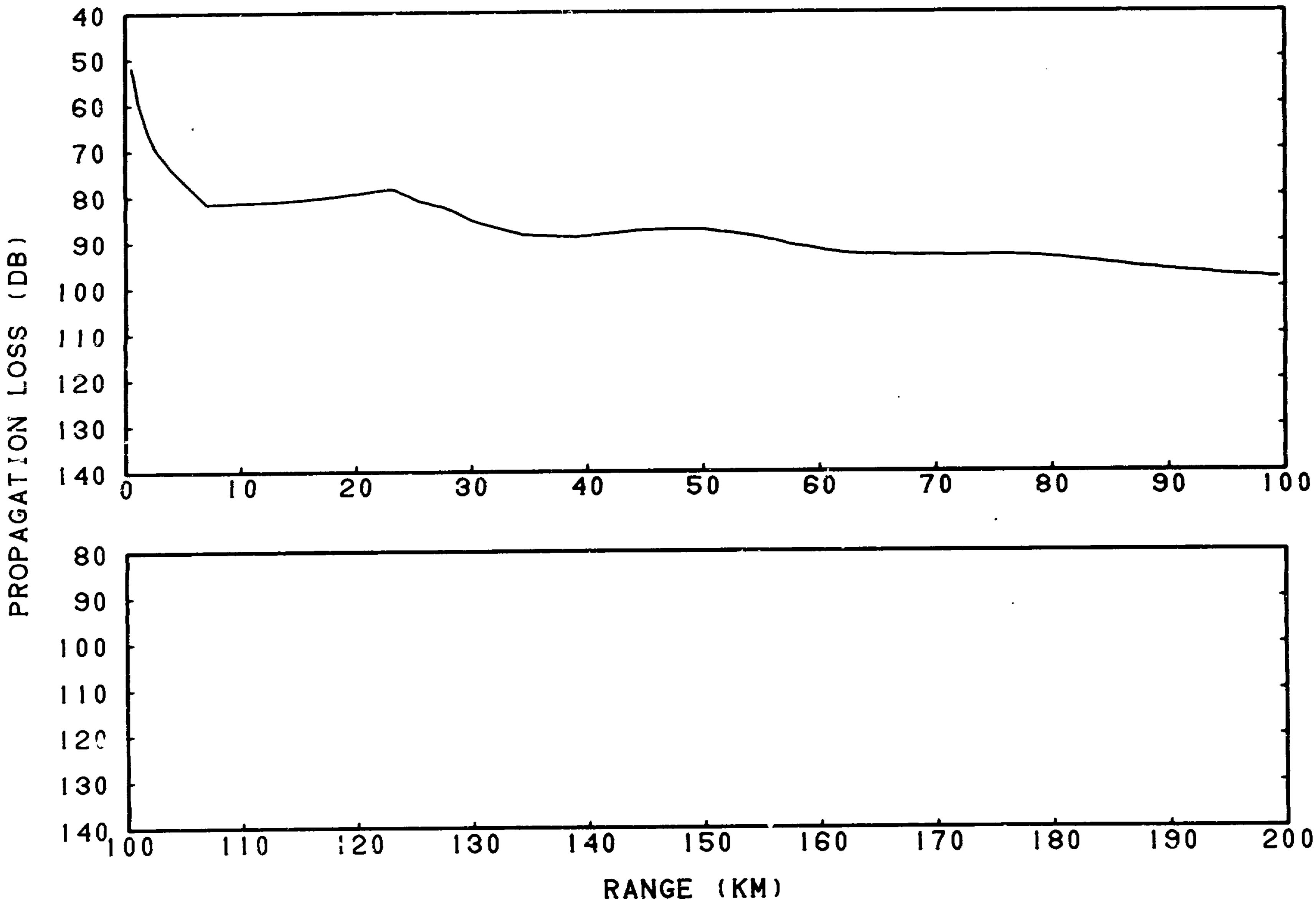

UNCLASSIFIED

Figure 3-21. (U) Case I. Cross-layer Geometry. RAYMODE Incoherent. Source Depth = 76 m. Receiver Depth = 137 m. Frequency = 100 Hz.

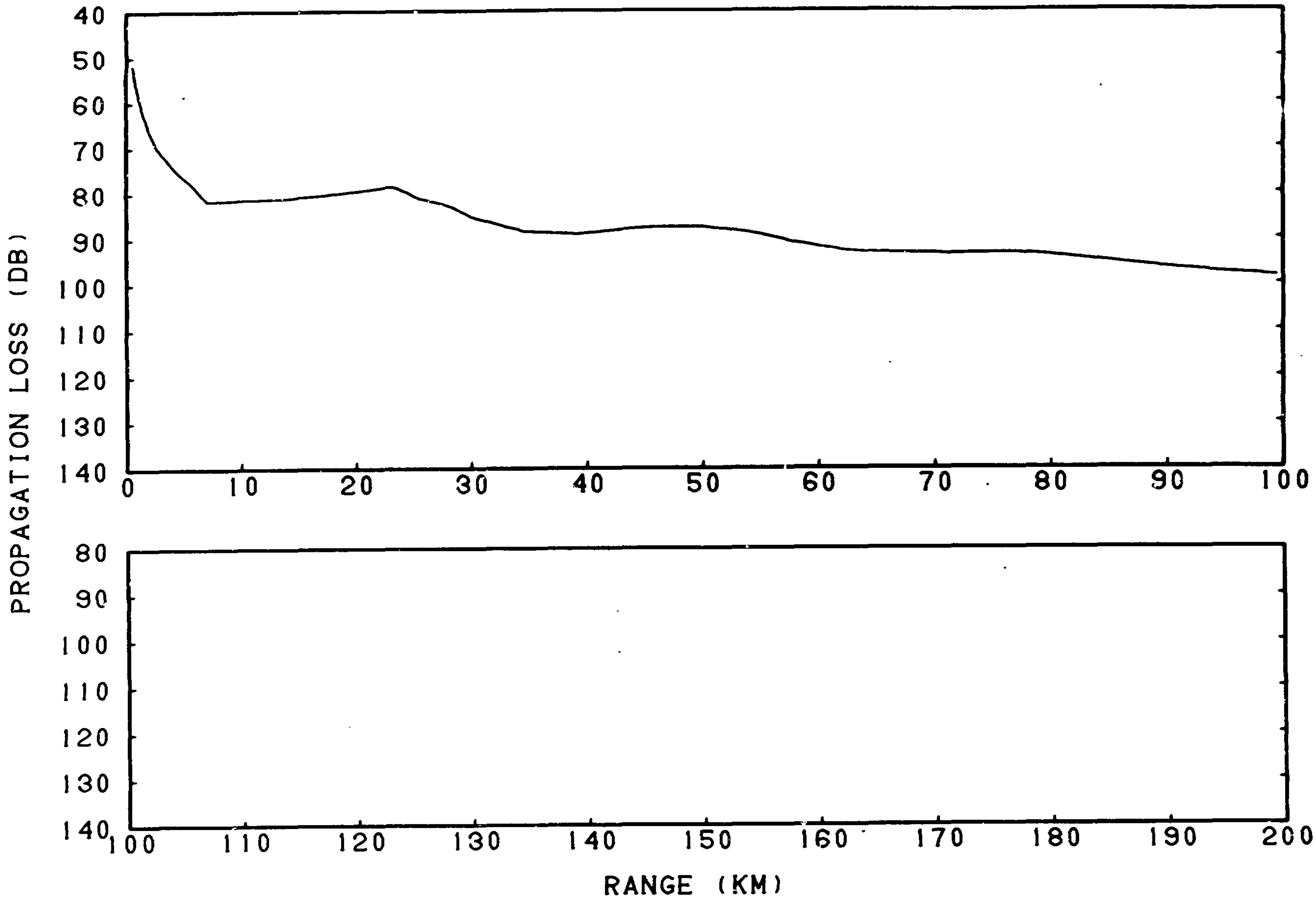

UNCLASSIFIED

Figure 3-22. (U) Case I. Cross-layer Geometry. RAYMODE Incoherent. Source Depth = 76 m. Receiver Depth = 137 m. Frequency = 200 Hz.

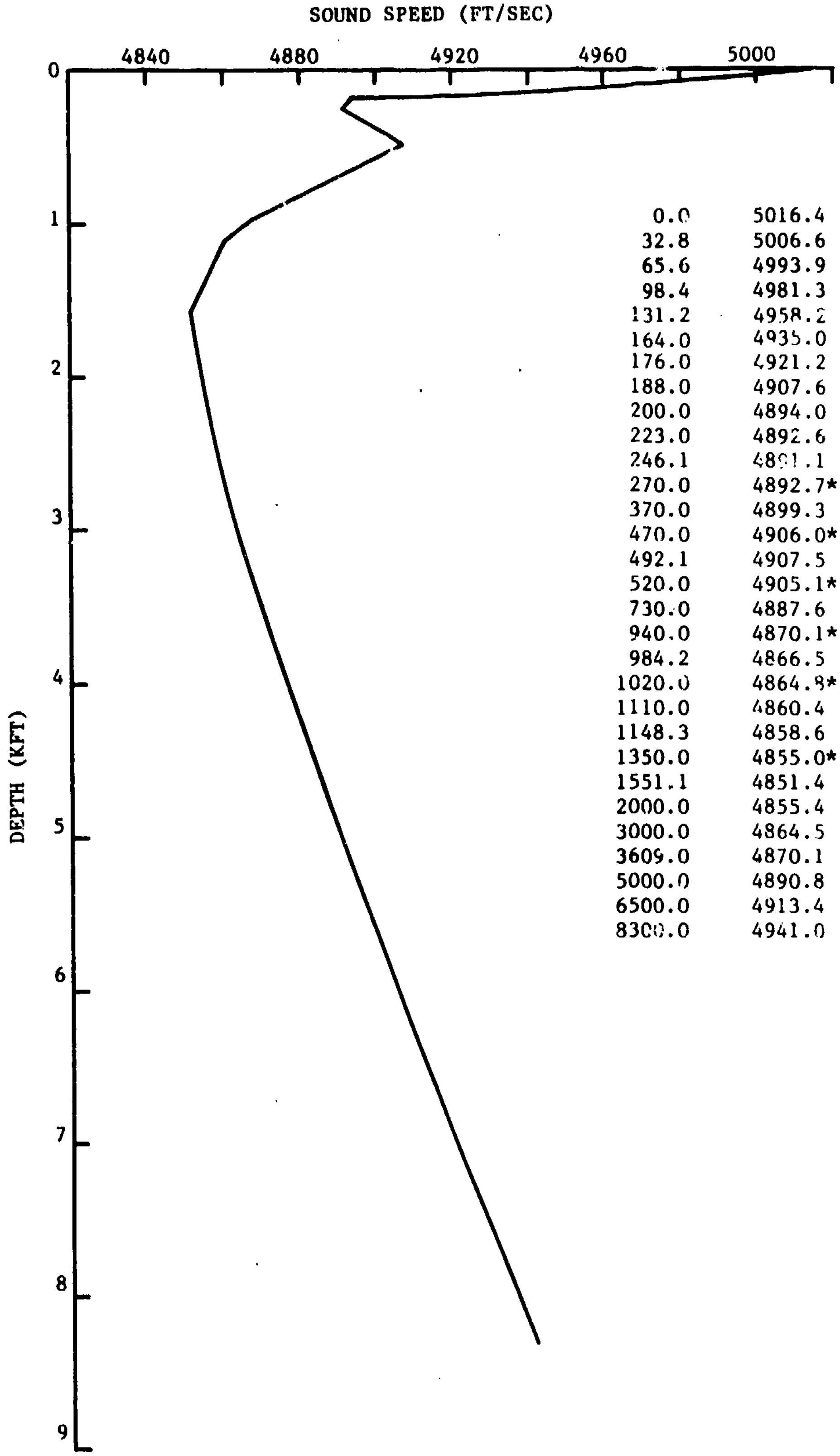

UNCLASSIFIED

Figure 3-23. (U) Velocity Depth Profile for Test Case II

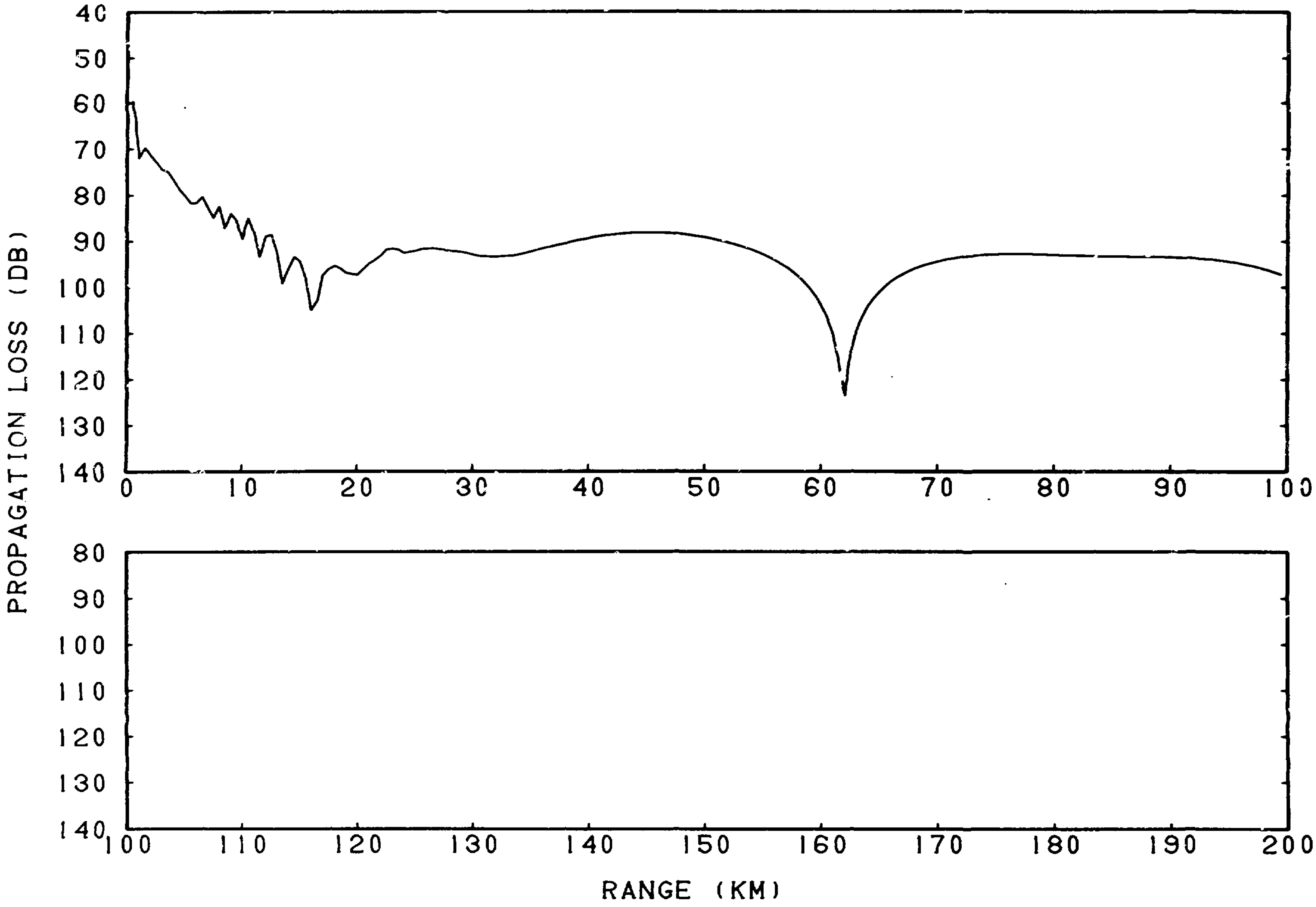

UNCLASSIFIED

Figure 3-24. (U) Case II. RAYMODE Coherent. Source Depth = 82 m. Receiver Depth = 67 m. Frequency = 10 Hz.

CONFIDENTIAL

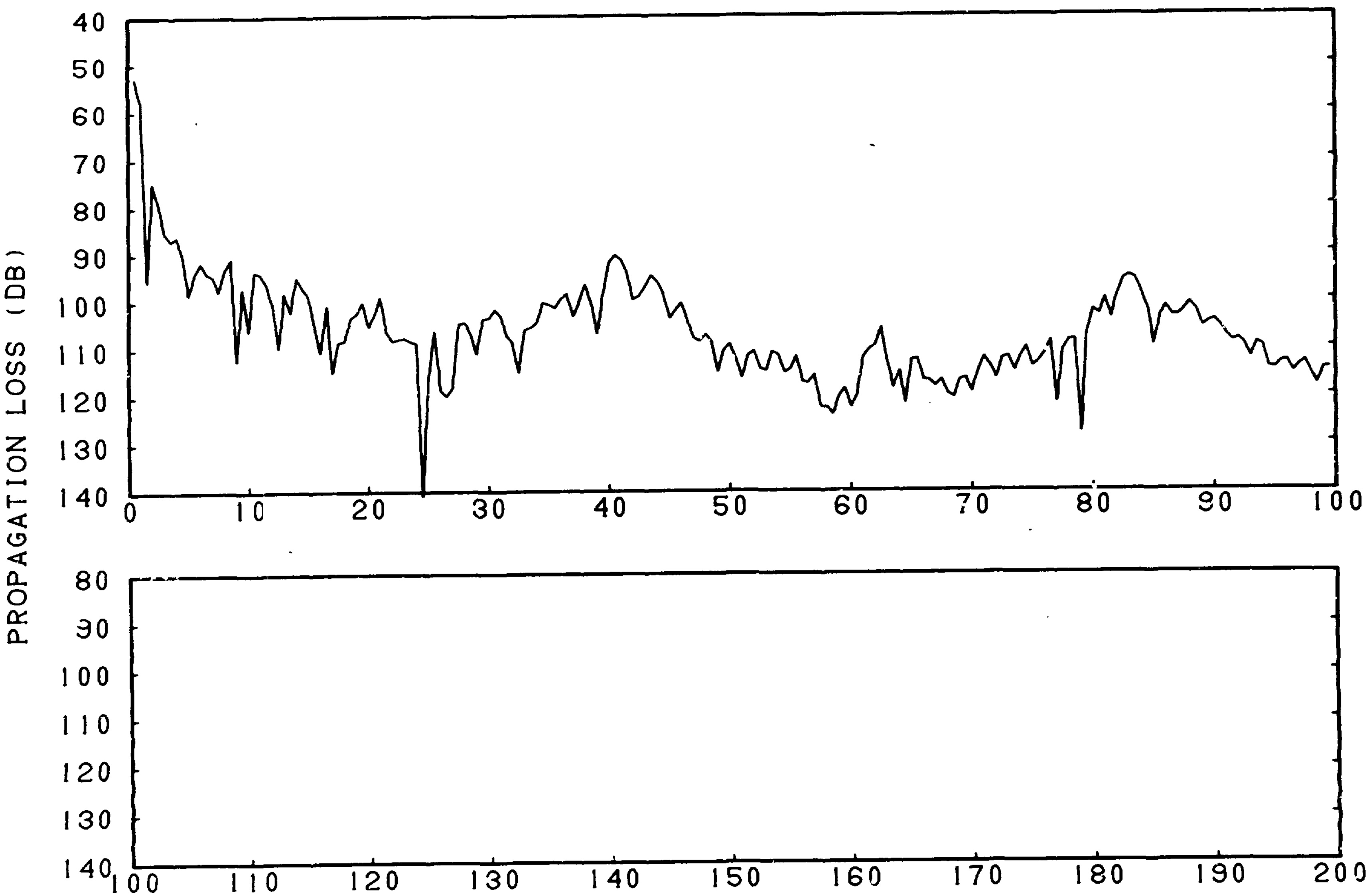

UNCLASSIFIED

Figure 3-25. (U) Case II. RAYMODE Coherent. Source Depth = 82 m. Receiver Depth = 67 m. Frequency = 100 Hz.

CONFIDENTIAL

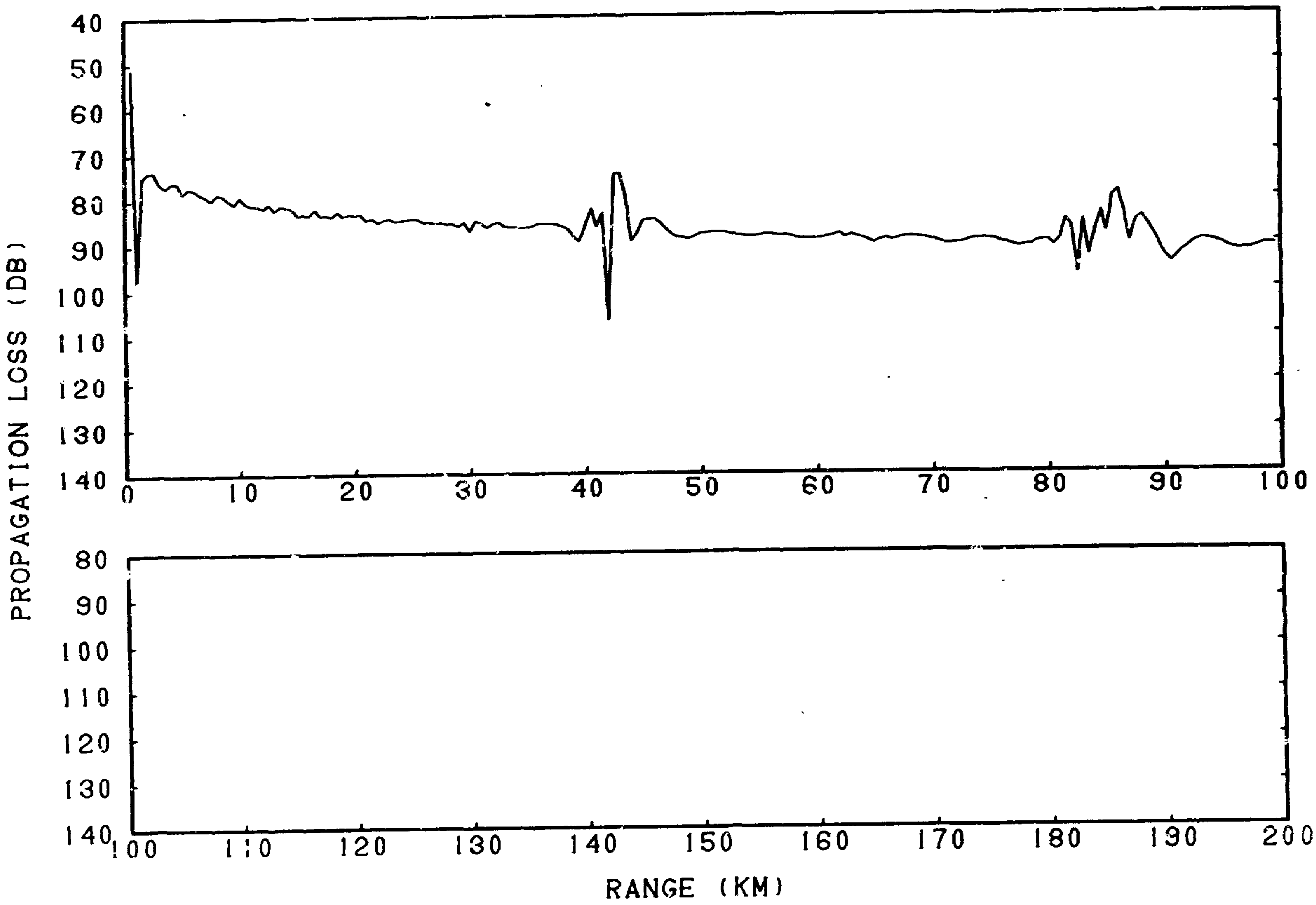

UNCLASSIFIED

Figure 3-26. (U) Case II. RAYMODE Coherent. Source Depth = 82 m. Receiver Depth = 67 m. Frequency = 300 Hz.

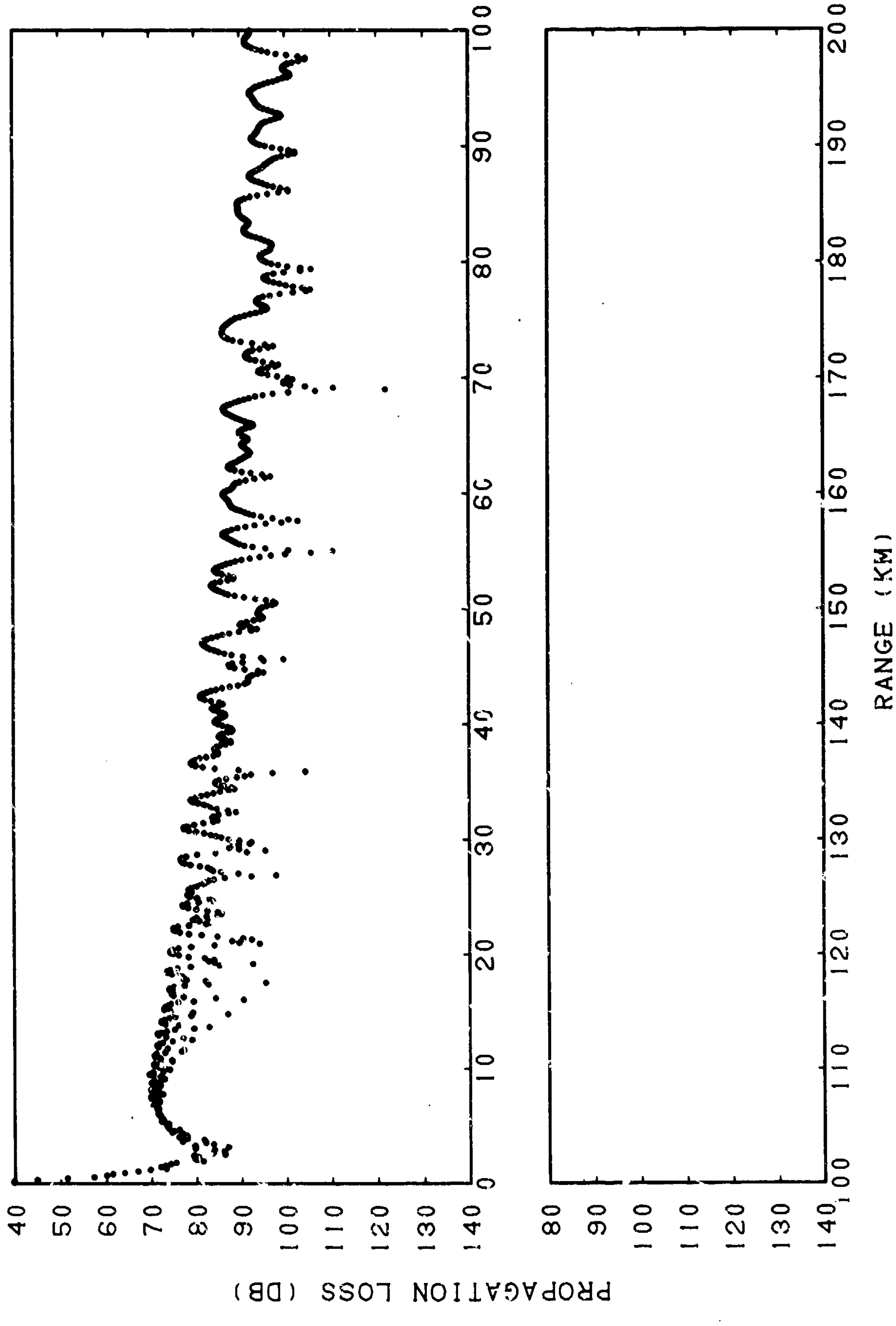

UNCLASSIFIED

Figure 3-27. (U) Case II. FFP. Source Depth 82 m. Receiver Depth = 67 m.
Frequency = 10 Hz.

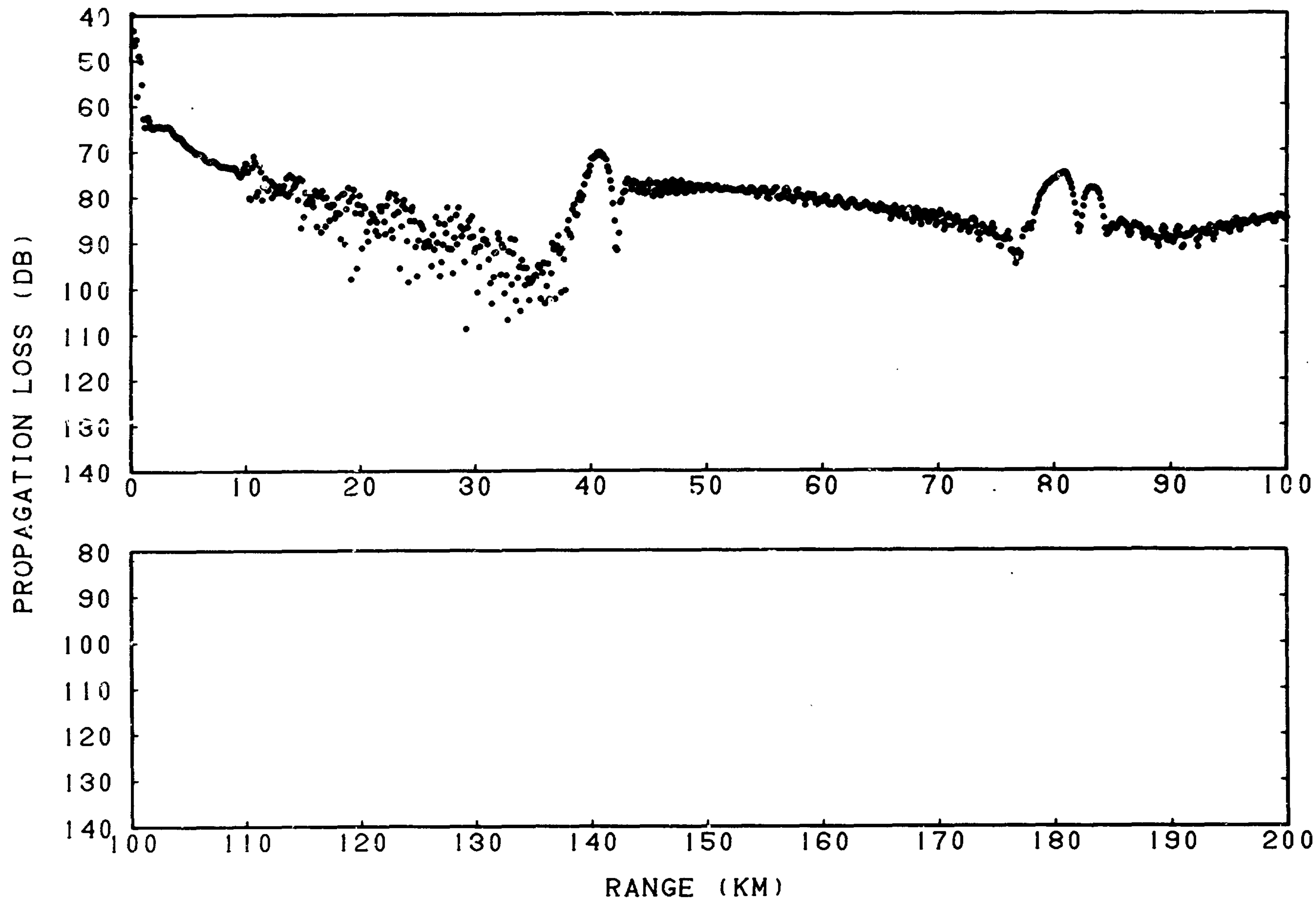

UNCLASSIFIED

Figure 3-28. (U) Case II. FFP. Source Depth = 82 m. Receiver Depth = 67 m. Frequency = 100 Hz.

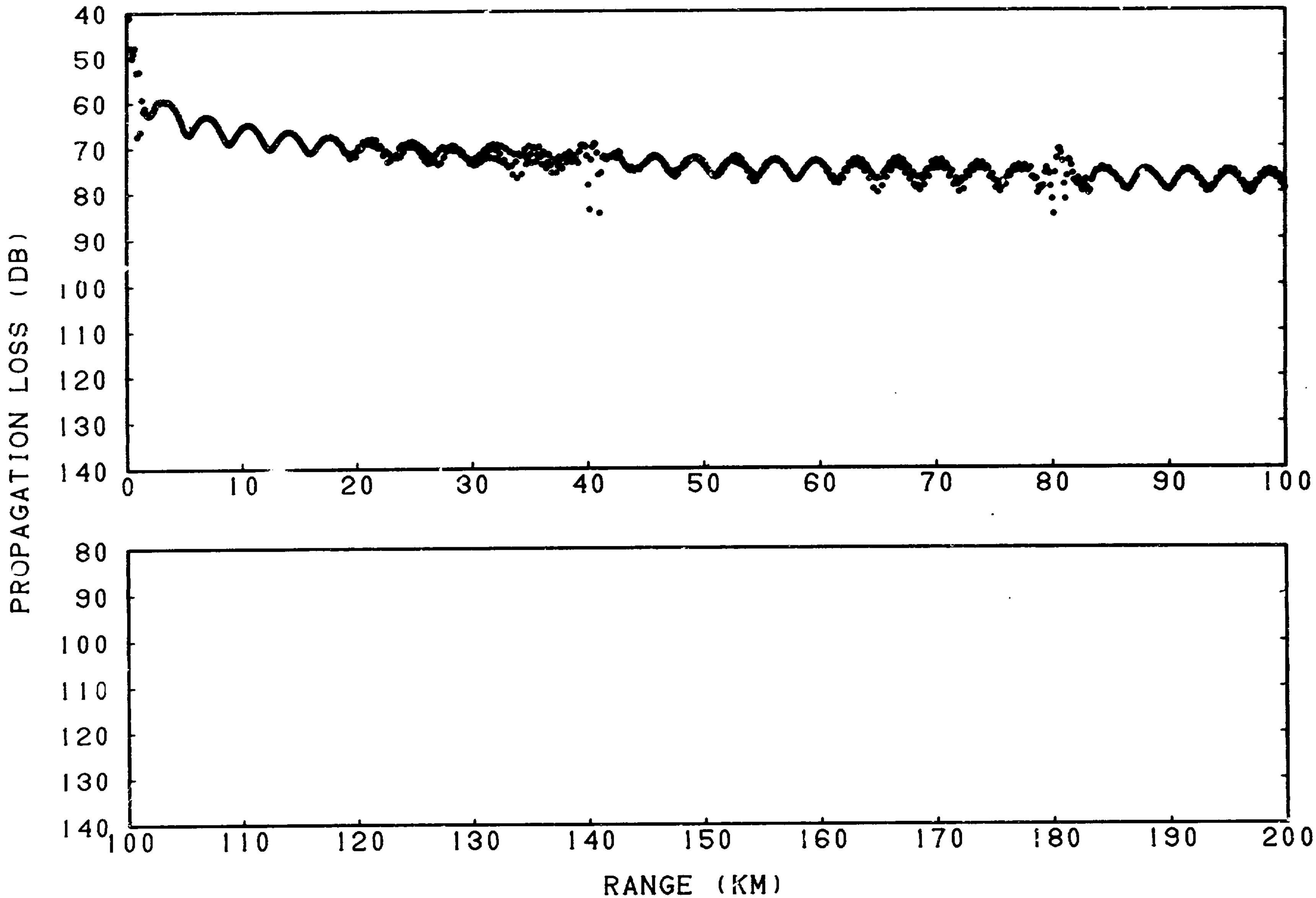

UNCLASSIFIED

Figure 3-29. (U) Case II. FFP. Source Depth = 82 m. Receiver Depth = 67 m. Frequency = 300 Hz.

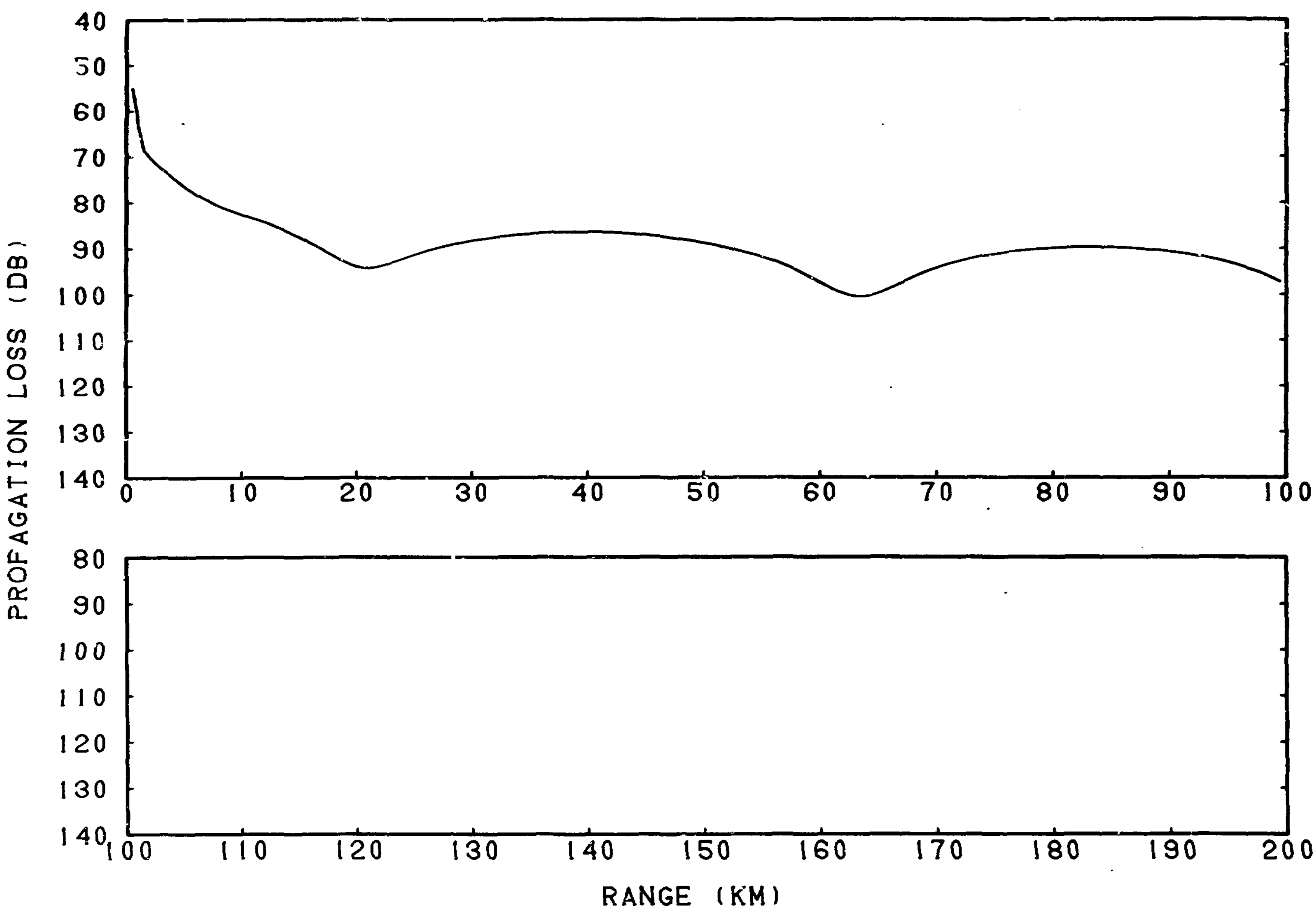

UNCLASSIFIED

Figure 3-30. (U) Case II. RAYMODE Incoherent. Source Depth = 82 m. Receiver Depth = 67 m. Frequency = 10 Hz.

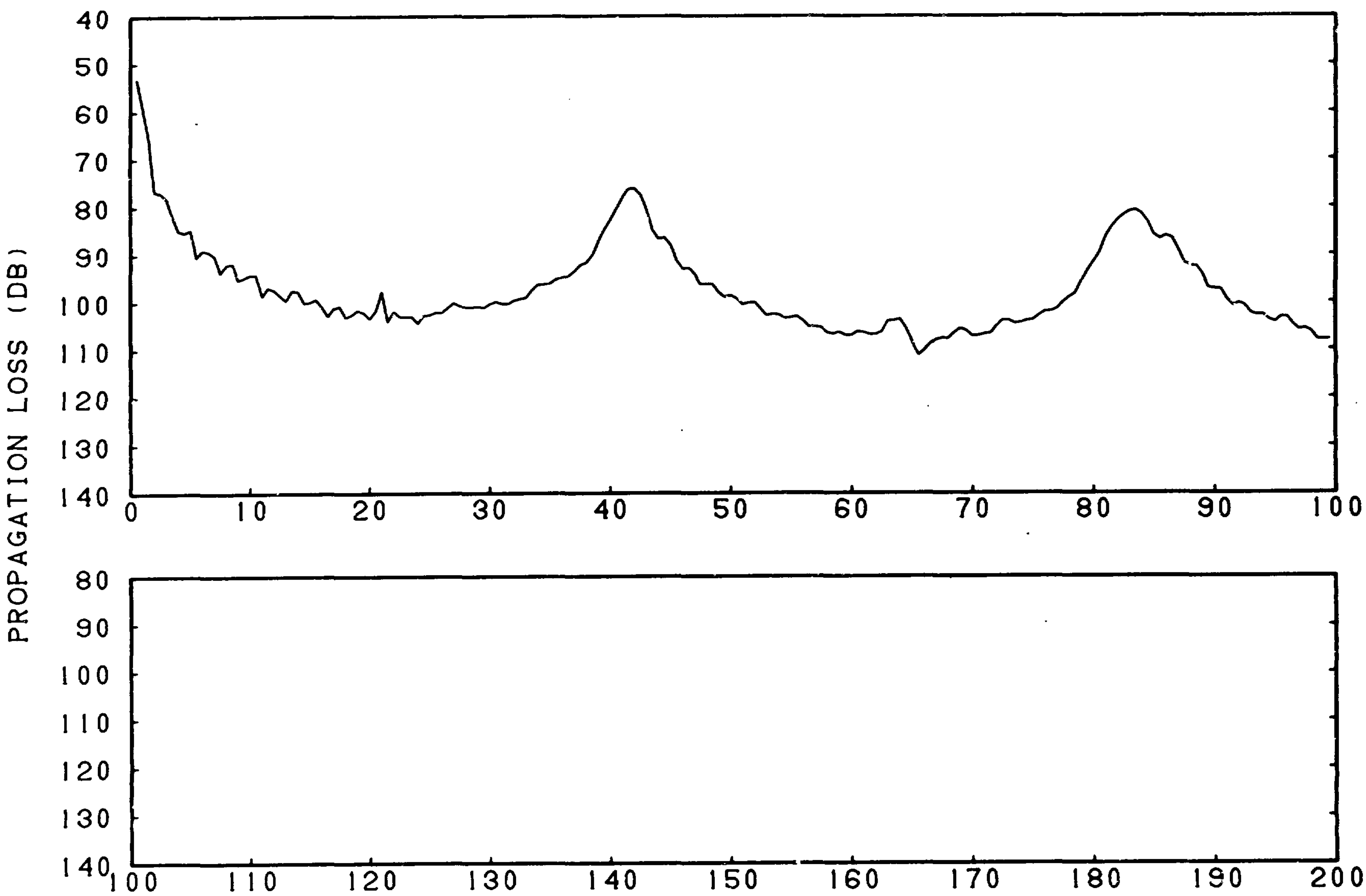

UNCLASSIFIED

Figure 3-31. (U) Case II. RAYMODE Incoherent. Source Depth = 82 m. Receiver Depth = 67 m. Frequency = 100 Hz.

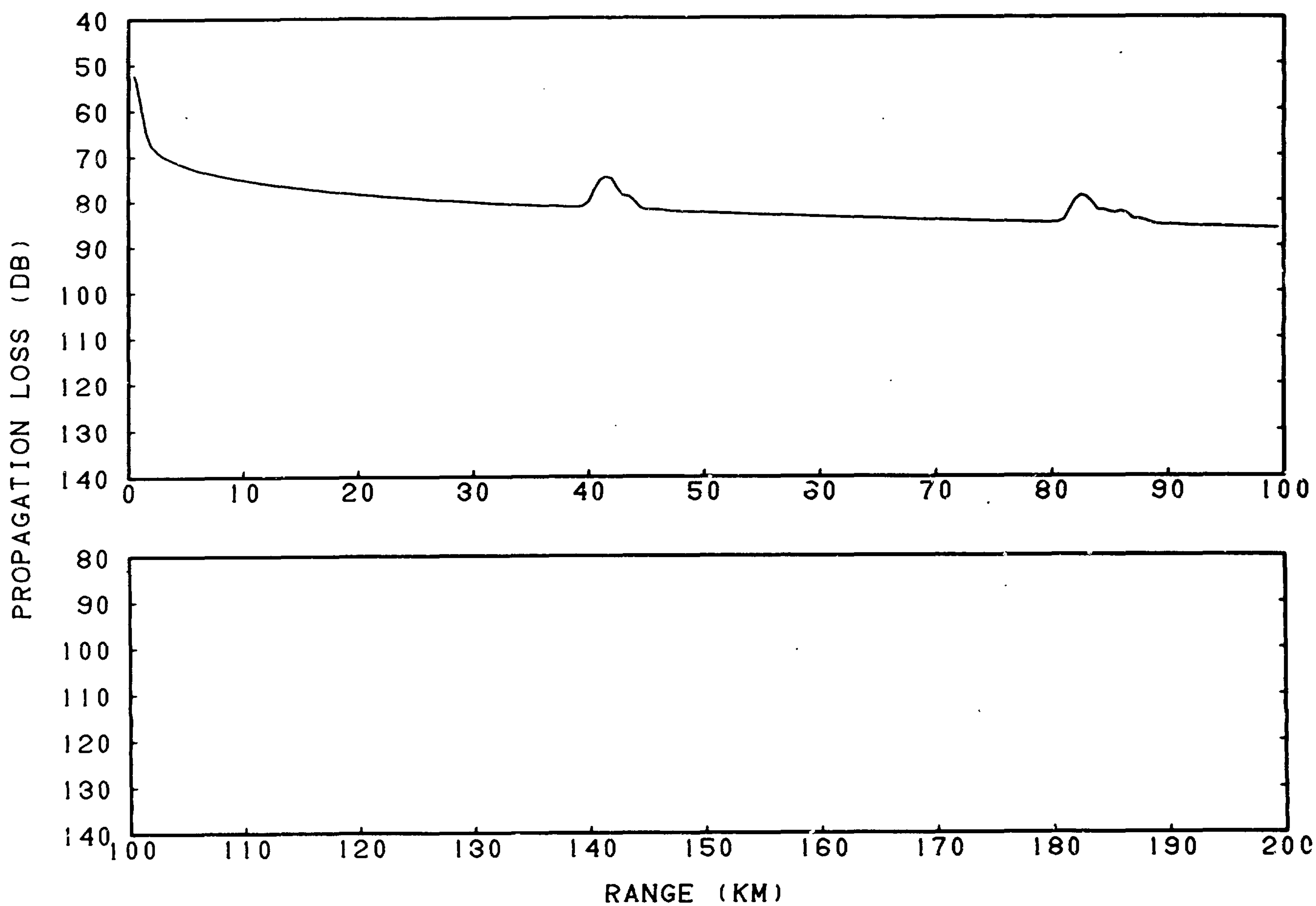

UNCLASSIFIED

Figure 3-32. (U) Case II. RAYMODE Incoherent. Source Depth = 82 m. Receiver Depth = 67 m. Frequency = 300 Hz.

$$f(z) = T \left(\frac{\phi_k^z}{q^{1/2}}\right)^{1/2} H_{1/3}^{(2)}(\phi_k^z) \quad (3A\text{-}1)$$

$$= V(z)e^{-i\phi_k^z} \quad (3A\text{-}2)$$

and

$$g(z) = T^* \left(\frac{\phi_k^z}{q^{1/2}}\right)^{1/2} H_{1/3}^{(1)}(\phi_k^z) \quad (3A\text{-}3)$$

$$= V^*(z)e^{i\phi_k^z} \quad (3A\text{-}4)$$

where $H_{1/3}$ are Hankel functions of order 1/3; T and V(z) are complex quantities defined by

$$T = \sqrt{\frac{\pi}{2}}\, e^{-i5\pi/12} \quad (3A\text{-}5)$$

$$V(z) = T \left(\frac{\phi_k^z}{q^{1/2}}\right)^{1/2} H_{1/3}^{(2)}(\phi_k^z)e^{i\phi_k^z} \quad (3A\text{-}6)$$

T* and V*(Z) represent the complex conjugates of T and V(Z). The phase ϕ_k^z is defined as

$$\phi_k^z = \int_{z_k}^{z} \left[\frac{\omega^2}{c^2(z)} - \xi^2\right]^{1/2} dz$$

which is identical to (3-5) but for variable reference depth.

(U) The traveling wave solutions f and g can thus be written in generalized WKB form,

$$f(z) = V(z) \exp\left\{-i\int_{z_k}^{z} q^{1/2}(z)\, dz\right\} \quad (3A\text{-}7)$$

$$g(z) = V^*(z) \exp\left\{i\int_{z_k}^{z} q^{1/2}(z)\, dz\right\} \quad (3A\text{-}8)$$

and still be exact within any given layer.

Appendix 3B. Surface Scattering Loss (U)

(U) Surface loss in RAYMODE X assumes two scattering mechanisms: a high frequency, large roughness loss, SL_1, and a low frequency loss, SL_2. The total surface scattering loss is then given by the sum $SL_1 + SL_2$. It is not clear what the physical basis is for these two processes. I suggest that it would be profitable if this aspect of RAYMODE X be examined (especially since a user of RAYMODE X may input his own surface loss table). The large roughness SL_1 is given by

$$SL_1 = -10 \log_{10}\left\{1 - \int_0^{2\pi}\int_0^{\pi/2} \sigma \cos\phi_r \, d\phi_r \, d\theta_r\right\} \quad (3B\text{-}1)$$

where the angles are defined by the geometry shown in Figure 3B-1. Equation (3B-1) is based on the assumption that an intensity scattering (reflection) coefficient R should obey the equation

$$R + \int_0^{2\pi}\int_0^{\pi/2} \sigma \cos\phi_r \, d\phi_r \, d\theta_r = 1 \quad (3B\text{-}2)$$

(U) Therefore, if surface loss is defined by $-10 \log_{10}|R|$, then (3B-2) yields the loss formula given by (3B-1). The scattering coefficient σ is the usual one given when the Fraunhofer phase approximation is assumed (for example, see Beckman and Spizzichino, (1963). In the large roughness limit σ can be written in terms of the distribution of slopes as

$$\sigma = \left\{e^{-\cot^2\beta_0 \hat{f}(\phi_r,\theta_r)}\right\} \frac{\cot^2\beta_0}{\pi} \frac{F^2}{(\sin\phi_i + \sin\phi_r)^2} \quad (3B\text{-}3)$$

where the mean square slope is $\frac{1}{2}\tan^2\beta_0$ and

$$\cot^2\beta_0 = \left[2(.003 + 2.6 \times 10^{-3}WS)\right]^{-1}$$

$$\hat{f}(\phi_r,\theta_r) = \frac{\cos^2\phi_i - 2\cos\phi_i\cos\phi_r\cos\theta_r + \cos^2\phi_r}{(\sin\phi_i + \sin\phi_r)^2} \quad (3B\text{-}4)$$

$$F = \frac{1 + \sin\phi_i\sin\phi_r - \cos\phi_i\cos\phi_r}{(\sin\phi_i + \sin\phi_r)}$$

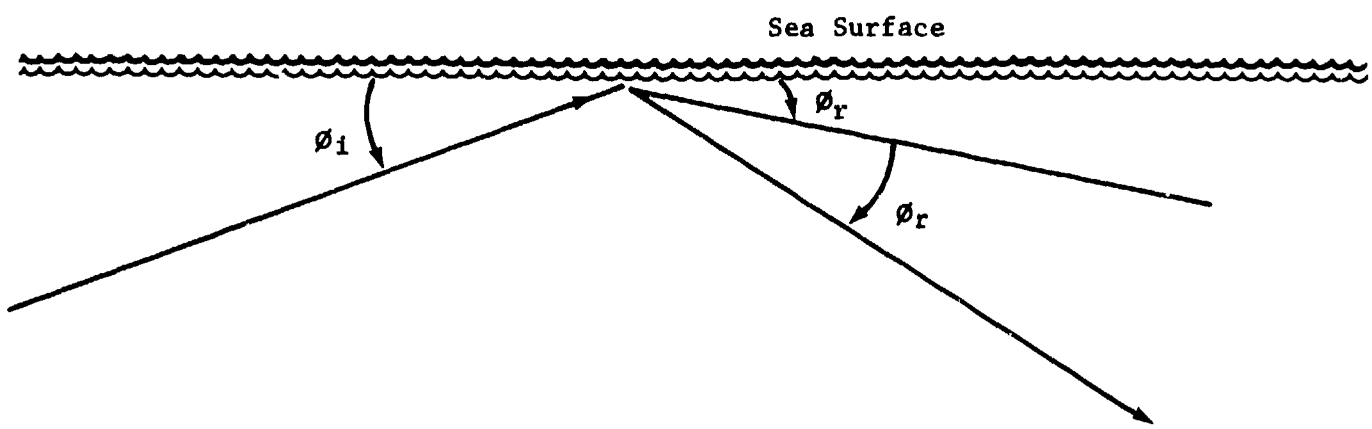

UNCLASSIFIED

Figure 3B-1. (U) Rough Surface Scattering Geometry

and WS is the windspeed in knots. When (3B-3) is used in (3B-1) and the integrations performed, the surface loss SL_1 is approximately given by

$$SL = -20 \log (1-V3)^{\frac{1}{2}} \qquad (3B-5)$$

where

$$V3 = \text{maximum of} \begin{cases} \sin\theta - \dfrac{\exp\left(\dfrac{a\theta^2}{4}\right)}{(\pi a)^{\frac{1}{2}}} \dfrac{\sin\theta}{\theta} \\ \dfrac{\sin\theta}{2} \end{cases} \qquad (3B-6)$$

and $a = \cot^2 \beta_0$; θ is the grazing angle in radians. If V3 is larger than .99, then V3 is set equal to .99.

(U) The "low frequency" surface loss term SL_2 is based on surface duct scattering data given by Marsh and Schulkin (1962). A suitable equation describing this experimental data is given by

$$SL_2 = -20 \log_{10} \left\{ .3 + \frac{.7}{1 + \left(\frac{fH}{10^4}\right)^2} \right\} \qquad (3B-7)$$

where f represents the frequency in Hz and H is the average wave height in feet. Eugene Podeszwa* at NUSC/NL has analyzed some results of Vine and Volkmann (Woods Hole, 1950) and arrived at the following relationship between wave height (H) in feet and wind speed, WS, in knots:

$$H = 2.04 \times 10^{-2} WS^2 . \qquad (3B-8)$$

(U) When this formula of Podeszwa's is used in (3B-7), the surface loss SL_2 in terms of wind speed becomes

$$SL_2 = -20 \log_{10} \left\{ .3 + \frac{.7}{1 + .01(2 \cdot f \cdot WS \cdot 10^{-5})^2} \right\} \qquad (3B-9)$$

*Private Communication

However, there is something unusual about (3B-8), because according to Sverdrup and Munk (1947) the significant wave height $H_{1/3}$ is given by

$$H_{1/3}(ft) = 2.32 \times 10^{-2} WS^2 (knot), \qquad (3B-10)$$

and if the Pierson-Moskowitz (1964) spectrum is used, $H_{1/3}$ becomes

$$H_{1/3}(ft) = 1.86 \times 10^{-2} WS^2 (knot). \qquad (3B-11)$$

(U) The usual relationship between the average wave height H and the significant wave height $H_{1/3}$ is given by

$$H = .625 H_{1/3}. \qquad (3B-12)$$

(U) When (3B-12) is used in (3B-10) and (3B-11) one obtains

$$H(ft) = 1.45 \times 10^{-2} WS^2 (knot) \qquad (3B-13)$$
(Sverdrup-Munk)

and

$$H(ft) = 1.16 \times 10^{-2} WS^2 (knot) \qquad (3B-14)$$
(Pierson-Moskowitz)

(U) If the average height given by (3B-13) and (3B-14) is compared with Podeszwa's (3B-8), it would appear that Podeszwa's "wave height" corresponds more closely to the significant wave height $H_{1/3}$.

(U) However, in describing the Marsh-Schulkin data it is necessary to use the average wave height. Because of the above discrepancy, it is felt that the use of an alternate formula should be considered.

Appendix 3C. Normal Mode Eigenvalues and Eigenfunction Normalization (U)

(U) The complex eigenvalues ξ_m associated with the normal mode (residue) expansion (3-17) are found from the zeros

of the denominator of (3-15). Explicitly they are assumed to be single poles obtained by solving the equation

$$W(\xi_m) = \left(1 - R_u^k R_d^N e^{-2i\phi_k^{z_N}}\right) = 0 \tag{3C-1}$$

If the reflection coefficients are defined in terms of magnitude and phase (θ_K and θ_N) then the above eigenvalue equation becomes

$$\begin{gathered} \left|R_u^k\right| \left|R_d^N\right| = e^{2\,\mathrm{Im}\{\phi_k^{z_N}\}} \\ \theta_k + \theta_N + 2\,\mathrm{Re}\{\phi_k^{z_N}\} = 2m\pi, \quad m = 0,1,2,\ldots \end{gathered} \tag{3C-2}$$

The real part of the eigenvalue, $\hat{\xi}_m = \mathrm{Re}\{\xi_m\}$ is found by solving (3C-2) without recourse to iterative methods which results in a considerable savings in execution time. To accomplish this the extreme mode numbers (N_A, N_B) are determined by substituting ξ_A and ξ_B (the end points of a given ξ-partition) into the second part of (3C-2) and solving form. In addition, differentiation yields

$$\frac{dm}{d\xi} = \frac{1}{2\pi}\left[Rc(m) - \frac{\partial\theta_k}{\partial\xi} + \frac{\partial\theta_N}{\partial\xi}\right] \tag{3C-3}$$

where

$$Rc(m) = -\frac{\partial}{\partial\xi}\left(2\,\mathrm{Re}\{\phi_k^{z_N}\}\right)\Big|_{\hat{\xi}} \tag{3C-4}$$

is the cycle range associated with the mode eigenvalue $\hat{\xi}_m$. The value of $R_c(m)$ is available in closed form due to the assumed sound speed variation within each layer. If one assumes that the phase of the reflection coefficients is a slowly varying function of ξ, the above equation may then also be solved for the extreme values ξ_A and ξ_B. Thus a curve of $\hat{\xi}_m$ vs. mode number m passing through the end points (ξ_A, N_A), (ξ_B, N_B) and having the slopes prescribed above, can be obtained. This curve is approximated by a cubic polynomial and the unknown coefficients are determined by interpolation. This expression is then evaluated for each integer such that $N_A < \xi_m < N_B$ for a direct (non-iterative) evaluation of the real part of the eigenvalues.

(U) The imaginary part of the eigenvalues ξ_m is approximately given by

$$\mathrm{Im}\{\xi_m\} \simeq \frac{-\log_e \left|R_u^k\right| \left|R_d^N\right|}{Rc(m)} \tag{3C-5}$$

The normal mode residue expansion associated with (3-15) then becomes

$$P_{(\ )_1}(r,z,z_s) \simeq 2\pi i \sum_{m=N_A}^{N_B} \frac{A(z,z_s;\xi_m)}{\left.\frac{\partial w}{\partial\xi}\right|_{\xi_m}} e^{-i(\phi_k^z - \phi_k^{z_s} + \xi_m r)} \tag{3C-6}$$

The normalization term in the denominator can be approximately written as

$$\left.\frac{\partial w}{\partial\xi}\right|_{\xi_m} = \left(-\frac{1}{R_u^k}\frac{\partial R_u^k}{\partial\xi}\right) + \left(\frac{1}{R_d^N}\frac{\partial R_d^N}{\partial\xi}\right) - i\,Rc(m) \tag{3C-7}$$

and further approximated by retaining only the term involving R_C. The final form of the residue normal mode series is obtained by expanding the phase terms (e.g., ϕ_k^z and $\phi_K^{z_s}$) in a Taylor series about $\hat{\xi}_m$ and retaining only the first two terms, since for trapped modes (Im$\{\xi_m\}$ is small. Then

$$\begin{aligned} P_{(\ )_1}(r,z,z_s) \simeq 2\pi i \sum_{m=N_A}^{N_B} \Bigg[& \frac{A(z,z_s;\xi_m)}{Rc(m)} e^{-i(\phi_k^z - \phi_k^{z_s} - \hat{\xi}_m r)} \\ & \times e^{-\mathrm{Im}\{\xi_m\}\left[r(z_k,z) - r(z_k,z_s) - r\right]} \Bigg] \end{aligned} \tag{3C-8}$$

where $r(z_K,z)$ and $r(z_K,z_s)$ are the horizontal ranges (obtained from ray theory) from z_K to z and to z_K to z_s, respectively.

References (U)

3.1 Leibiger, G. A. (1978). The Acoustic Propagation Model RAYMODE: Theory and Numerical Treatment. NUSC Tech. Rpt., Naval Underwater Systems Center, New London, Conn., in preparation.

3.2 Yarger, D. F. (1976). The User's Guide for the Raymode Propagation Loss Program. Tech. Memo 222-10-76, Naval Underwater Systems Center, New London, Conn.

3.3 Beckmann, P. and A. Spizzichino (1963). The Scattering of Electromagnetic Waves from Rough Surfaces. (The MacMillan Company, New York, New York).

3.4 Marsh, H. W. and M. Schulkin (1962). Underwater Sound Transmission. AVCO Marine Electronics Office, p. 47-48, November (U).

3.5 Christensen, R. E., O. Kaufman, and J. Frank (1973). Preliminary Analysis of 100 Hz Bottom Loss Data (U). Naval Oceanographic Office, Technical Note 9320-02-73, 20 February (CONFIDENTIAL).

3.6 Sverdrup, H. U. and W. H. Munk (1947). Wind, Sea, and Swell: Theory of Relations for Forecasting. U.S. Hydrographic Office Publication No. 601, U.S. Hydrographic Office, Washington, D.C.

3.7 W. J. Pierson, Jr. and L. Moskowitz (1964). A Proposed Spectra Form for Fully Developed Wind Seas Based on the Similarity Theory of S. A. Kitaigorodskii. J. Geophys. Res. 69(24), 5181-5190 (December).

4.0 (U) Running Time

(U) The running times for the cases examined in the RAYMODE X evaluation are given in Table 4-1. Running times are the total of simultaneously exercising the incoherent and coherent phase addition options. All running times were obtained on the UNIVAC 1108 computer at the New London Laboratory. Input variables for these runs were allowed to assume default variables (except for most environmental inputs.

Table 4-1. (U) RAYMODE X Run Times on Univac 1108

Data Set	Case	Source Depth (m)	Receiver Depth (m)	Frequency (Hz)	Number of Points	Run Time (Sec)
HAYS-MURPHY	I	24.4	137.2	35.0	400	9.6
	II	24.4	137.2	67.5	400	51.9
	III	24.4	137.2	100.0	400	53.7
	IV	24.4	137.2	200.0	400	56.0
	V	24.4	106.7	35.0	400	10.3
	VI	24.4	106.7	100.0	400	55.2
FASOR	I (FIG)	6.1	37.0	1500.0	200	13.4
	II (OAK)	23.0	37.0	1500.0	200	3.1
	III (THORN)	23.0	37.0	1500.0	200	4.8
	IV (REDWOOD)	6.1	37.0	1500.0	200	14.5
PARKA	I	152.4	91.4	50.0	400	29.2
	II	152.4	91.4	400.0	300	54.1
BEARING STAKE	I	91.0	496.0	25.0	300	6.5
	II	91.0	1685.0	25.0	300	6.9
	III	91.0	3320.0	25.0	300	6.6
	IV	91.0	3350.0	25.0	300	6.7
	V	18.0	496.0	140.0	300	5.4
	VI	18.0	1685.0	140.0	300	5.1
	VII	18.0	3320.0	140.0	300	5.4
	VIII	18.0	3350.0	140.0	300	5.3
	IX	18.0	496.0	290.0	300	5.6
	X	18.0	1685.0	290.0	300	5.9
	XI	18.0	3320.0	290.0	300	6.0
	XII	18.0	3350.0	290.0	300	5.4
JOAST	I	6.1	18.3	3700.0	200	16.5
	II	6.1	79.2	3700.0	200	18.1
	III	6.1	163.1	3700.0	200	16.7
	IV	6.1	18.3	3700.0	200	23.6
	V	6.1	79.2	3700.0	200	24.6

CONFIDENTIAL

Table 4-1 (cont.). (U) RAYMODE X Run Times on Univac 1108

Data Set	Case	Source Depth (m)	Receiver Depth (m)	Frequency (Hz)	Number of Points	Run Time (Sec)
JOAST (cont.)	VI	6.1	163.1	3700.0	200	24.2
	VII	6.1	18.3	3700.0	200	15.8
	VIII	6.1	79.2	3700.0	200	15.4
	IX	6.1	163.1	3700.0	200	15.9
	X	6.1	18.3	3700.0	200	15.8
	XI	6.1	163.1	3700.0	200	15.8
	XII	6.1	18.3	3700.0	200	16.2
	XIII	6.1	79.2	3700.0	200	16.2
	XIV	6.1	304.8	3700.0	200	16.2
SUDS	I	45.0	17.0	400.0	400	21.5
	II	45.0	112.0	400.0	400	22.3
	III	42.0	43.0	1000.0	400	22.3
	IV	42.0	112.0	1000.0	400	22.4
	V	41.0	6.0	1500.0	400	21.9
	VI	41.0	59.0	1500.0	400	25.9
	VII	41.0	6.0	2500.0	400	41.1
	VIII	41.0	59.0	2500.0	400	22.1
	IX	45.0	17.0	3500.0	400	23.5
	X	45.0	112.0	3500.0	400	22.4
	XI	42.0	17.0	5000.0	400	17.5
	XII	42.0	112.0	5000.0	400	18.2
Gulf of Alaska	I (Run 140)	30.5	30.5	1500.0	250	30.3
	II (Run 140)	30.5	304.8	1500.0	250	32.1
	III (Run 143)	30.5	30.5	1500.0	250	31.3
	IV (Run 143)	30.5	304.8	1500.0	250	31.5
	V (Run 124)	30.5	30.5	1500.0	250	30.0
	VI (Run 124)	30.5	304.8	1500.0	250	32.4
	VII (Run 112A)	1066.8	30.5	2500.0	250	28.4
	VIII (Run 112A)	1066.8	304.8	2500.0	250	26.2
	IX (Run 112B)	1066.8	30.5	2500.0	250	27.2

CONFIDENTIAL

Table 4-1 (cont.). (U) RAYMODE X Run Times on Univac 1108

Data Set	Case	Source Depth (m)	Receiver Depth (m)	Frequency (Hz)	Number of Points	Run Time (Sec)
Gulf of Alaska (cont.)	X (Run 112B)	1066.8	304.8	2500.0	250	28.1
	XI (Run 107)	304.8	30.5	2500.0	250	18.0
	XII (Run 107)	304.8	304.8	2500.0	250	17.7
	XIII (Run 108)	304.8	30.5	2500.0	250	26.8
	XIV (Run 108)	304.8	304.8	2500.0	250	28.9
LORAD	IA	15.2	30.5	530.0	300	23.0
	IB	15.2	30.5	530.0	300	23.0
	IC	15.2	30.5	530.0	300	24.9
	ID	15.2	30.5	530.0	300	24.9
	IE	15.2	30.5	530.0	300	24.3
	IF	15.2	30.5	530.0	300	24.3
	IG	15.2	30.5	530.0	300	24.3
	IIA	15.2	304.8	530.0	300	22.4
	IIB	15.2	304.8	530.0	300	22.4
	IIC	15.2	304.8	530.0	300	24.7
	IIC	15.2	304.8	530.0	300	24.7
	IIE	15.2	304.8	530.0	300	24.2
	IIF	15.2	304.8	530.0	300	24.2
	IIG	15.2	304.8	530.0	300	24.2

CONFIDENTIAL

5.0 (U) Core Storage Requirements

(U) The number of decimal words of core storage for RAYMODE is presented in Table 5-1 in four ways for each of two different sets of parameters used in dimensioning data arrays. Core storage was calculated both with and without the IGS plotting routines, but including other normal input/output functions. These numbers have been broken down into data and code size for the RAYMODE program routines alone and for the program with the UNIVAC system routines necessary to execute it. The program stored is sized according to the first set of parameters to accommodate even large problems; the second set shows the effect of reducing these parameters to a still reasonable size.

Table 5-1. (U) RAYMODE Storage Size

Method	Parameters	Code	Data	Total
With plots and systems	dimensioned for	22213	11927	34140
With plots, without system	400 ranges	7084	5547	12631
Without plots, with system	and 50 modes and	10236	7083	17319
Without plots and system	ray pts	3928	4533	8461
With plots and system	dimensioned for	22213	10502	32715
With plots, without system	200 ranges	7084	4122	11206
Without plots, with system	and 25 modes and	10236	5658	15894
Without plots and system	ray pts	3928	3108	7036

UNCLASSIFIED

6.0 (U) Program Flow

(U) The following flowchart for the RAYMODE model was obtained from D. F. Yarger of the Naval Underwater Systems Center, New London Laboratory.

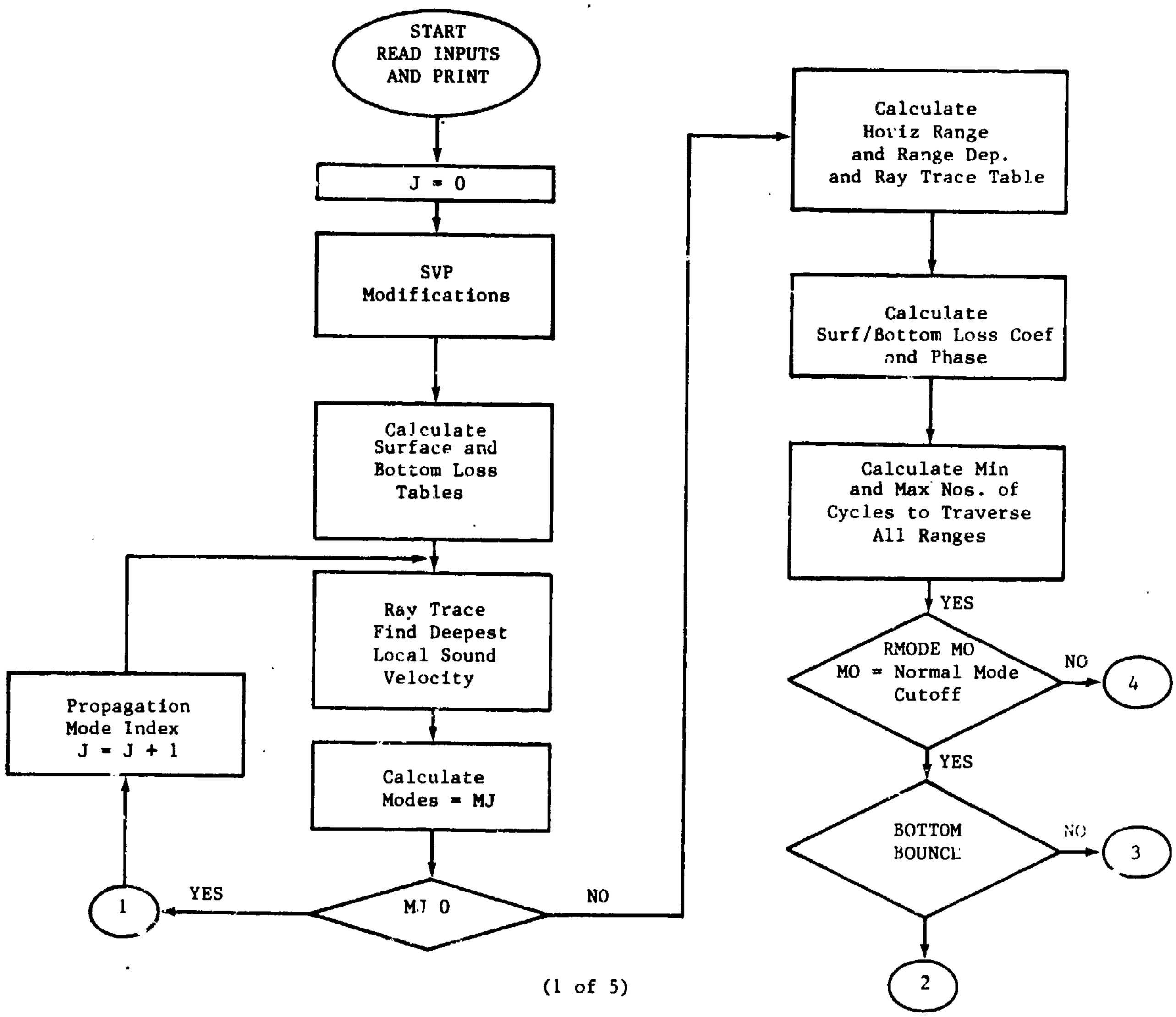

(1 of 5)

UNCLASSIFIED

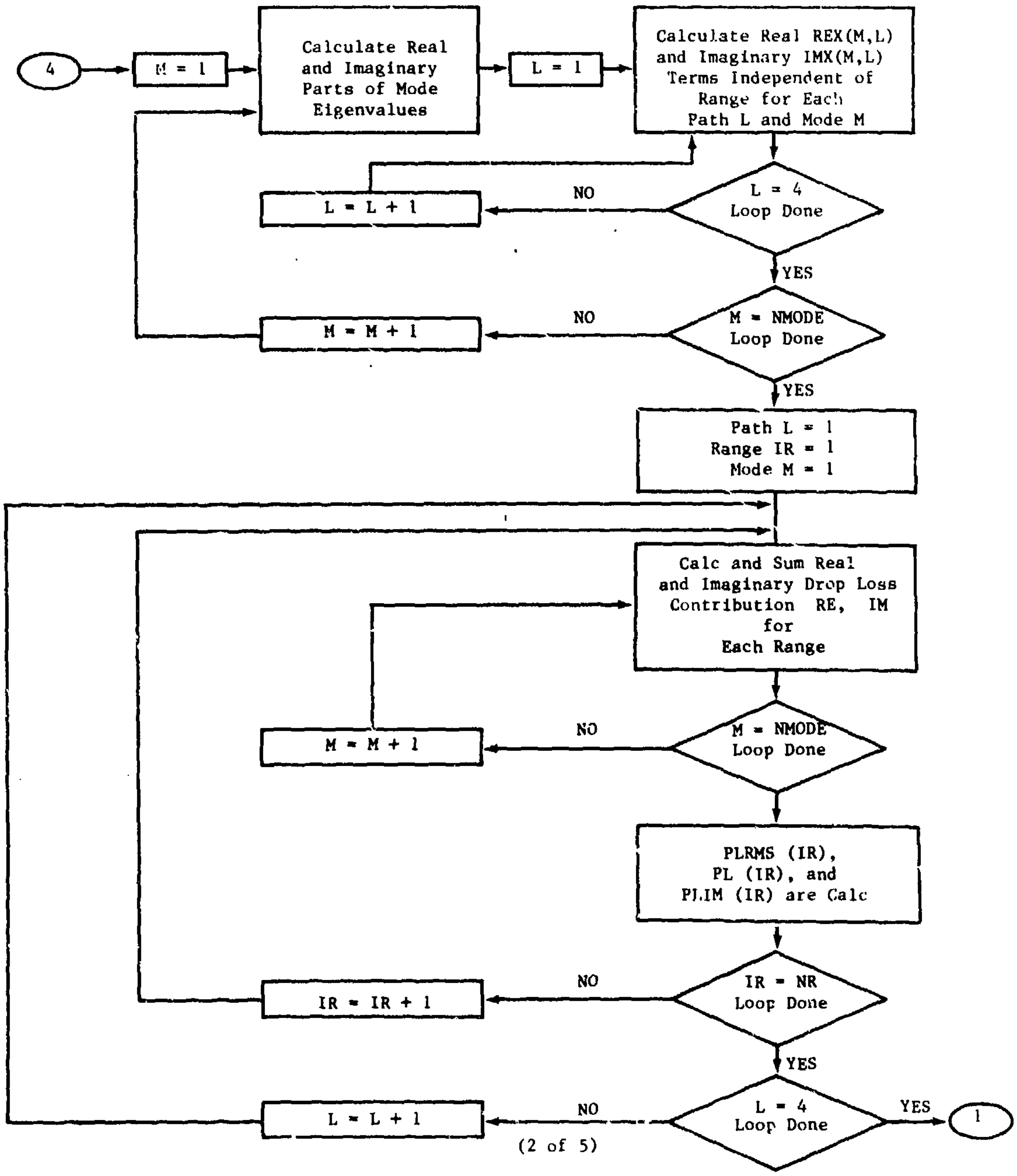

(2 of 5)

UNCLASSIFIED

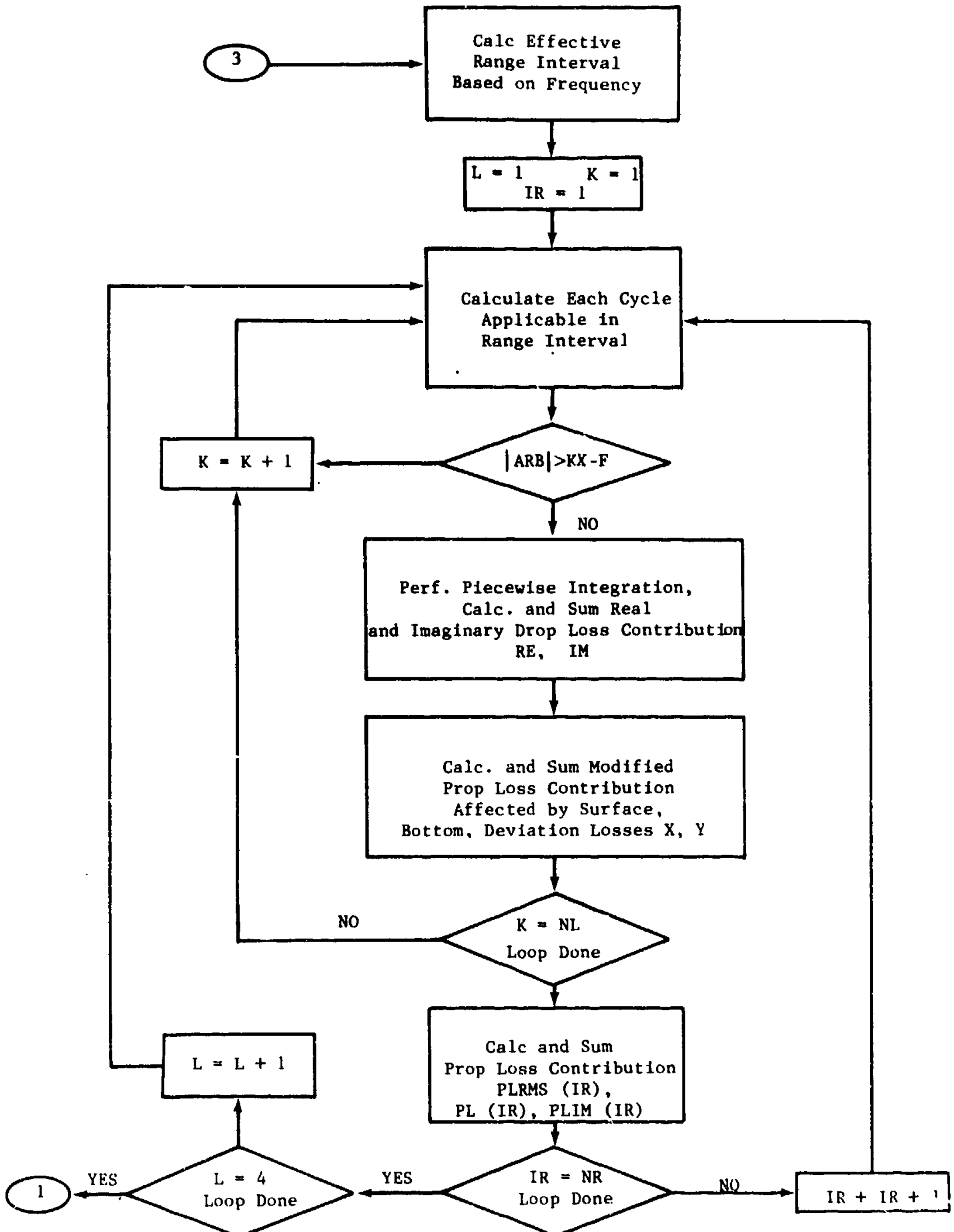

(3 of 5)

UNCLASSIFIED

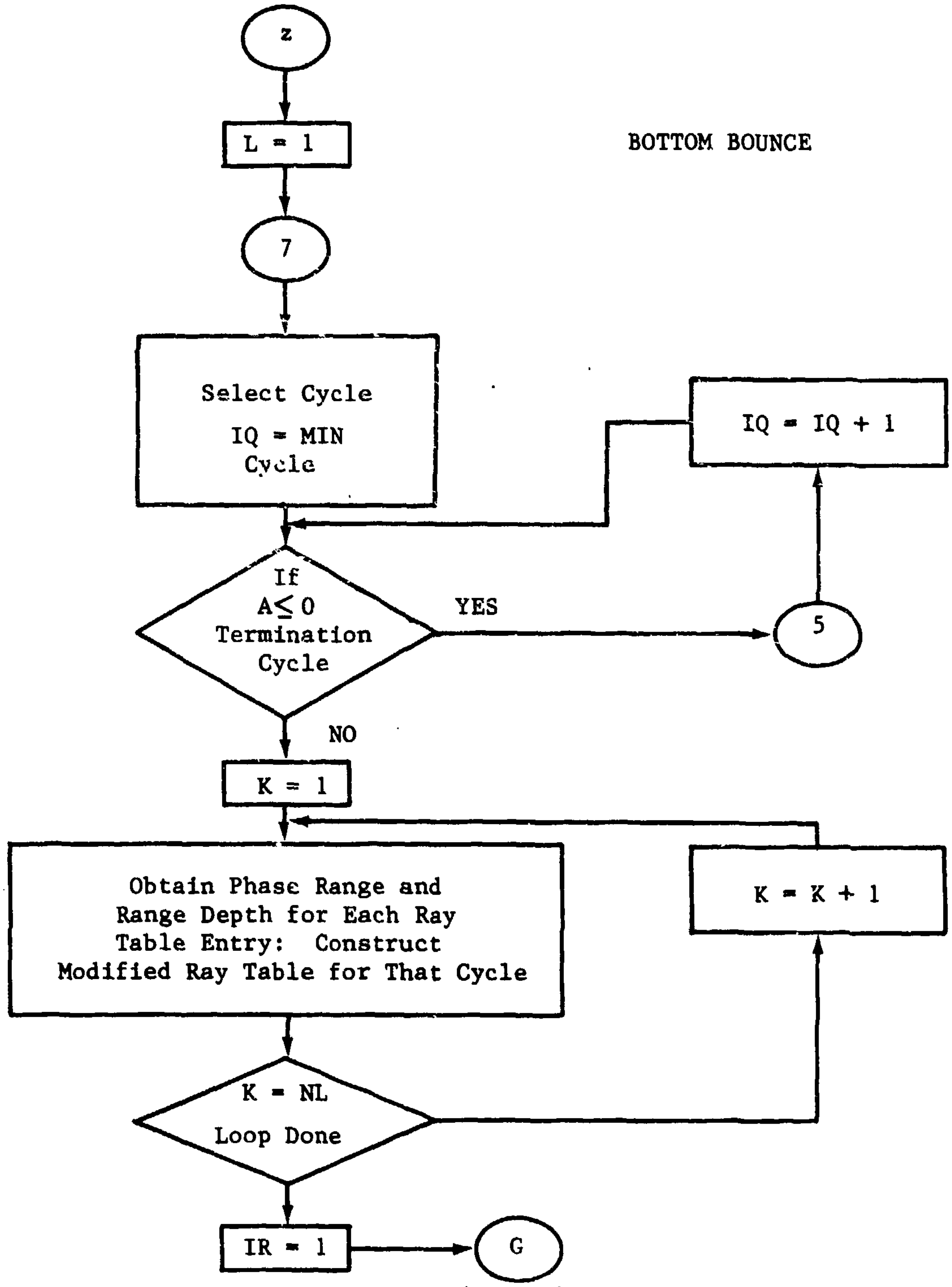

(4 of 5)

UNCLASSIFIED

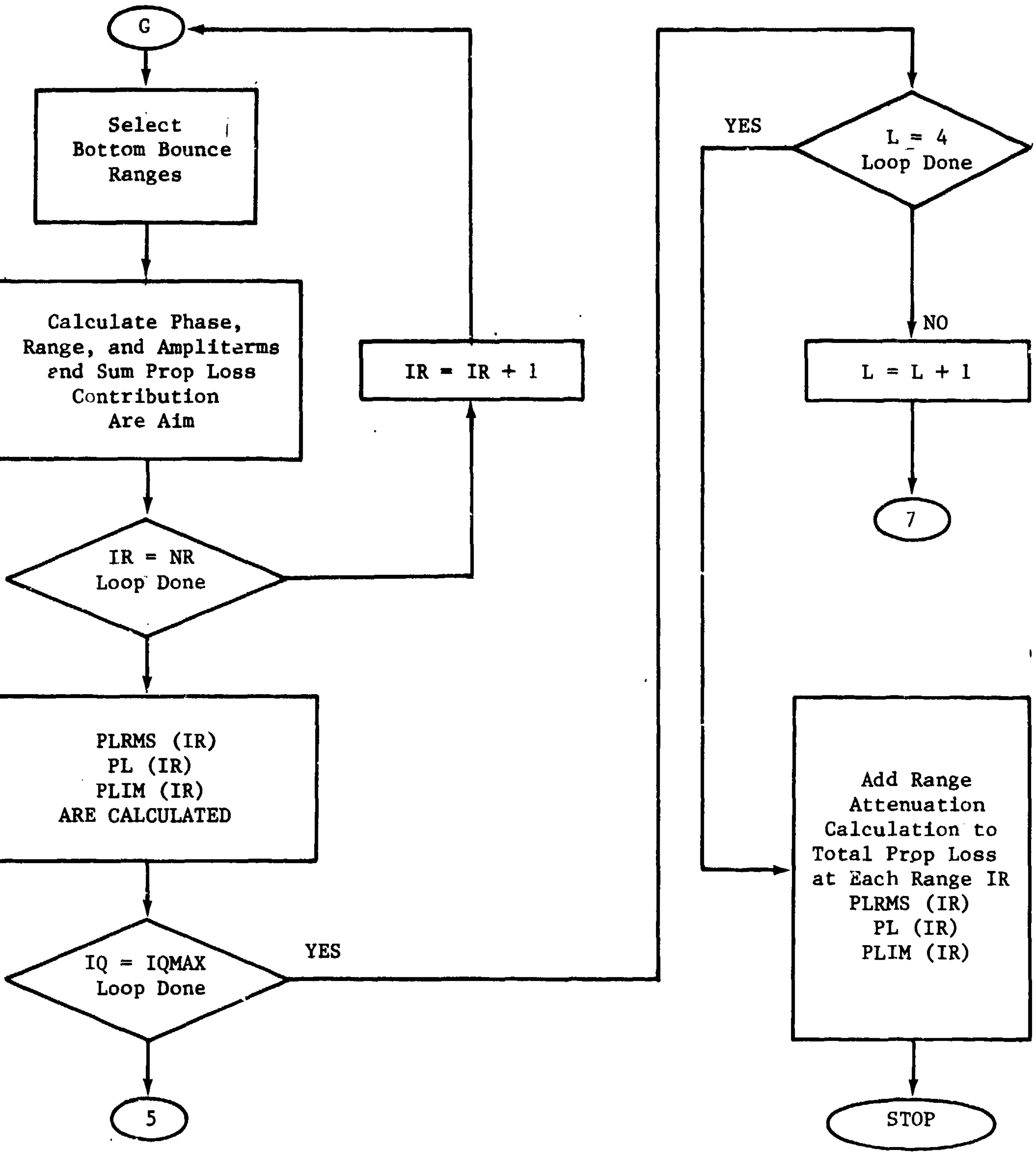

(5 of 5)

UNCLASSIFIED

7.0 (U) RAYMODE X Inputs

(U) RAYMODE X inputs and their discussion by Yarger (1976) are presented below. Some editorial liberties, including rearrangement and rewriting of some text as necessitated by the format of this report, have been undertaken. Also, detailed discussion of inputting historical velocity profiles (HVPs) has been omitted.

7.1 (U) RAYMODE Control Card and Data Deck Requirements

(U) RAYMODE is presently running on the UNIVAC 1108 computer at NUSC/NL under the EXEC VIII executive system. The propagation model is stored on catalogued file TEN*RAYMØD and should be executed from the absolute element RAMO DXA. The control stream for running RAYMODE is shown in Figure 7-1, which also contains a sample multi-case data deck.

(U) If a historical velocity profile (HVP) is to be called, the user must assign the correct tape-to-tape unit 1 before execution. The tape number to be

```
@RUN      ...,run-time,max-pages        (run-time  .5n, max-pages  20n for n cases)   }
@ASG,A    TEN*RAYMOD                                                                  } UNIVAC
@ASG,T    HVTAPE,U,U796 (or U544)       }only if HVP                                  } EXEC VIII
@USE      1.,HVTAPE.                    }to be used                                   } Control
@XQT      TEN*RAYMOD.RAMODXA                                                          } Cards
          NORTH ATLANTIC - WINTER                     (heading card)                  }
 $INPUTS                                              (in col. 2-8)                   }
          IOCEAN = 2, IPROFL = 10,  ISEASN = 4,       (historical profile)            }
          ZS = 20., ZR = 200.,                        (source & receiver)             } Sample
          F = 500.,                                   (frequency)                     } Case 1
          MGSOP = 3, WS = 15.,                        (bottom loss & wind speed)      }
          R= 1000., DELTAR = 1000., RMAX = 100000.,   (range determinants)            }
 $END                                                 (in col. 2-5)                   }
          NORTH ATLANTIC - WINTER                                                     }
 $INPUTS                                                                              } Case 2
          F = 1000.,                                  (change frequency)              }
 $END
      •
      •
      •
      •
      •
      •
          NORTH ATLANTIC - WINTER                                                     }
 $INPUTS                                                                              } Case n
      •                                                                               }
      •                                                                               }
      •                                                                               }
 $END
@FIN
```

UNCLASSIFIED

Figure 7-1. (U) RAYMODE Control and Data Deck Structure

referenced depends on the unit system of the data, English or metric; where

Tape U769 contains HVP's in ft and ft/s (English system).

Tape U544 contains HVP's in m and m/s (metric system).

The tape will automatically position itself to the proper HVP even when calling several different ones in the same execution.

(U) Following the UNIVAC control instructions as outlined in Figure 7-1, each separate case requires

- a heading card in format 12A6
- the required NAMELIST inputs inserted between the indicators $INPUTS and $END.

(U) The input information to be supplied by the user consists of:

(1) Sound velocity profile: input directly or form historical velocity profile tape.

(2) Source and Receiver depths: ZS, ZR or indices NU, MU.

(3) Frequency: F.

(4) Horizontal range determinants: R, RMAX, DELTAR

(5) Bottom loss: MGS province number of table.

(6) Wind speed: WS.

(7) Source and/or Receiver beam patterns (defaulted omnidirectional).

(8) Program controls (defaulted for general use).

(9) Output options (defaulted "on").*

*Editors Note: See section 7.2 for RAYMODE X output options.

(U) A discussion of the use of NAMELIST and the particular RAYMODE inputs within each of the above categories is included in this section. The NAMELIST method offers an advantage when running more than one case. For the first case, the user needs to include only those input variables not supplied by defaults plus the ones for which the defaults are not suitable for his application; for each case after the first, the user needs to include only those input variables which differ from the ones previously set. The illustration in Figure 7-1 shows that a typical case in the English unit system (default) using any of the historical velocity profiles (3 inputs) for any source/receiver combination (2), frequency (1), MGS province (1), wind speed (1), and set of ranges (3) with omnidirectional source and receiver (default) and calling for all available output (default) requires exactly 11 inputs to be defined with the appropriate numerical values. To change only frequency for a second case merely requires another heading card and another NAMELIST $INPUTS deck with the new frequency assigned. Therefore, although the NAMELIST list of inputs may appear somewhat formidable because it includes up to three variable names (eight of which are arrays with up to 50 entries each), the usual cases are handled quite simply with the program defaults. The extensive list of inputs, however, allows for great flexibility of the program control in special applications. User inputs are not modified internally. A summary of RAYMODE inputs with their limits and defaults is provided in Table 7-1.

(U) The specific input requirements for execution of each RAYMODE case are discussed below:

1. (U) Heading Card

(U) The first card required for each RAYMODE data case is an alphanumeric heading card read in format 12A6. The comment on this card is intended to be the title of the case and will be printed at the beginning of the printed

Table 7-1. (U) Summary of Raymode Inputs

INPUT	DEFINITION	UNITS	LIMITS	DEFAULTS	COMMENT	PAGE
Metric	option for system of units		0 or 1*	0 (Eng.)		9
N	no. of profile points input		2<N≤47			9
Z(1)	array of profile depths	ft or yd; m*	0. to bottom		set IOCEAN = 0	9
C(1)	array of profile velocity or temperature	ft/s, yd/s;m/s* %F; %C*	>100. ≤100.			9
SALNTY	salinity	0/00		35.	for BT conversion	9-10
IOCEAN	ocean code for HVP		IOCEAN≤2	0		10
IPROFL	profile index for HVP		1≤IPROFL≤69 or 77			10
ISEASN	season index for HVP		1≤ISEASN≤4			10
ZB	bottom depth	ft or yd; m*		0.		10-11
NU	source depth index		1<NU<N	0		11
MU	receiver depth index		1<MU<N	0		11
ZS	source depth	ft or yd; m*	0.<ZS<Z(N)			11
ZR	receiver depth	ft or yd; m*	0.<ZR<Z(N)			11
F	frequency	Hz	F≥0			11
R	range minimum	yd or m*	R>0.			12
RMAX	range maximum	yd or m*	RMAX≥R			12
DELTAR	range increment	yd or m*	DELTAR>0.			12
MGSOP	MGS bottom loss province		0≤MGSOP≤9	0		12
ITAB	no. of bottom loss points		0≤ITAB≤50	0		12
THETA(1)	array of bottom loss angles	deg	0. to ANGLE	X	set MGSOP = 0	12
BL(1)	array of bottom losses	dB	≥0.	X		12

UNCLASSIFIED

* - Historical Velocity Profile

Table 7-1 (cont.). (U) Summary of Raymode Inputs

INPUT	DEFINITION	UNITS	LIMITS	DEFAULTS	COMMENT	PAGE
WS	wind speed	kts	≥0.	0.		12
IDL	no. of source deviation points		0≤IDL≤50			12-13
THEDA(1)	array of source deviation angles	deg	-ANGLE to ANGLE	X		12-13
DL(1)	array of source deviation losses	dB	≥0.	X		12-13
JDL	no. of receiver deviation points		0≤JDL≤50	0		12-13
THEDA2(1)	array of receiver deviation angles	deg	-ANGLE to ANGLE	X		12-13
DL2(L)	array of receiver deviation losses	dB	≥0.	X		12-13
LAMMIN	minimum no. of cycles		LAMMIN<50	-1		14
LAMDA	maximum no. of non-BB cycles		LAMDA<50	-1		14
LAMDAB	maximum no. of BB cycles		LAMDAB<50	-1		14
ANGLO	minimum sonar angle or corresponding velocity	deg ft/s, yd/s; m/s*	0.≤ANGLO<90.	0.		14-15
ANGLE	maximum sonar angle or corresponding velocity	deg ft/s, yd/s; m/s*	ANGLE<ANGLE<90.	60.		14-15
MINMOD	minimum mode number		1≤MINMOD≤50	1		15-16
MAXMOD	maximum mode number		MAXMOD≤50	0		15-16
MO	mode cutoff		3≤MO≤50	10		15-16
NL	no. of pts in ray tables		2<NL≤50	10		16
IPRINT	ray print option			1 ("on")		16-18
PLOTCZ	integer plot option for SVP			1 ("on")		18-20

UNCLASSIFIED

* - Historical Velocity Profile

TABLE 7-1 (cont.). (U) Summary of Raymode Inputs

INPUT	DEFINITION	UNITS	LIMITS	DEFAULTS	COMMENT	PAGE
PLOTOP	integer plot option for ray diagrams			3 ("on")		18-20
PLOTTI	integer plot option for travel time			1 ("on")		18-20
PLOTPL	integer plot option for prop loss			3 ("on")		18-20
PLO	minimum for PL loss scale	dB	$PLO \geq 0.$	40		18-20

UNCLASSIFIED

output and at the bottom of any selected plots. For best results on the plots, any comment should be centered within the first 72 columns. If no title is desired, a blank card must be used.

2. (U) NAMELIST $INPUTS Deck

(U) A detailed discussion of the NAMELIST procedure is contained in the FORTRAN V manual, reference (e). In brief, the first card of the NAMELIST deck will be $INPUTS in columns 2-8 and the last will be $END in columns 2-5; in between, the inputs are defined in equation form and separated by commas, for example:

(a) in the case of a constant

F=50.,

and

(b) in the case of an array using a subscript and listing the elements

THETA(1) = 0., 5., 10., ..., 55., 60.,

(U) The inputs defined in this way afford convenience to the user in checking data for later review. For this reason a print of the data deck itself is meaningful, hence is provided as part of the output as shown in the examples below. Variables within the NAMELIST deck may be assigned in any order and need not be in special fields or on separate cards with the exception that the use of column 1 should be avoided. Each variable must be of the appropriate type, integer or real. For RAYMODE each input variable is typed according to the name rule (i.e., real unless beginning with the letters I-N) with the exception of the 4 plot options which are integers. Arrays are distinguished by the subscript (1).

(U) The particular input categories are discussed in the following section.

Sound Velocity Profile (U)

(U) A sound velocity profile may be input directly from cards listing such point from surface to bottom using N, Z, C, SALNTY <u>or</u> be accessed from a historical velocity profile tape by providing the three parameter values IØCEAN, IPRØFL, ISEASN.

a. (U) Selection of Units: METRIC

(U) The systems of units to be used for input and output is controlled by the integer METRIC.

METRIC = 0 implies the English system (default)
= 1 implies the Metric system.

b. (U) Directly Input Profile: N, Z, C, SALNTY

(U) When using the English system if the depth units are feet, a profile may be made up of a mixture of velocities in ft/s and temperatures in °F in order to easily merge bathythermograph (BT) data with an SVP. When using the metric system, a profile may be made up of a mixture of velocities in m/s and temperatures in °C for the same reason. The program automatically converts temperature data to sound velocity measure in the appropriate units to complete the SVP. Adjacent equal velocities or temperatures are accepted by the program but are slightly modified for internal use to avoid a zero gradient condition. The user inputs for a directly inserted SVP are:

N = no. of pts in SVP, $2 < N \leq 47$.

Z(1) = depth entries from surface to bottom in increasing order in ft or yd if METRIC = 0, in m if METRIC = 1.

C(1) = velocity entries corresponding to Z depths in ft/s or yd/s if METRIC = 0, in m/s if METRIC = 1, <u>or</u> temperatures in °F if depth in ft and METRIC = 0, in °C if METRIC = 1, $C_1 \leq 100.$ when temperature.

SALNTY = salinity in parts per thousand for conversion of temperatures to velocities if any temperatures are entered in C array above (default 35).

3. (U) Access Historical SVP: IOCEAN, IPROFL, ISEASN

(U) The historical velocity profile tape was developed from the seasonal profiles selected by E. Podeszwa (February, 1976; April, 1976).

IOCEAN = ocean code (default 0).
$\leq$ 0 implies that SVP is input directly as in b above.
> 0 implies that historical profile is to be used.
= 1 selects the North Pacific Ocean
= 1 selects the North Atlantic Ocean.

IPROFL = profile index as obtained from area charts.

ISEASN = season index 1 $\leq$ISEASN $\leq$4.
= 1 for winter (Jan-Mar).
= 2 for spring (Apr-Jun).
= 3 for summer (Jul-Sep).
= 4 for fall (Oct-Dec).

4. (U) Bottom Depth ZB

(U) Bottom depth may be inserted directly in the same units as the profile depths input. This input is particularly required for use with a historical velocity profile, since a fixed bottom depth of 21,000 feet (or 6400 meters) is assumed for the stored profiles. The program truncates or extends the stored HVP to conform to the selected bottom depth. Since charted depths are often uncorrected, the user is responsible for any correction to bottom depth before entering it. The input bottom depth will be used as the last point of the profile when >0.; if $\geq$0., the last profile depth is assumed to be the bottom.

ZB = bottom depth in ft, yd, or m corresponding to depth units.
$\leq$ 0. implies Z(N) is bottom depth.
$\geq$ 0. implies bottom depth input specifically.

Source and Receiver Depths (U)

(U) Source and receiver depths may be identified by the indices of these depths in the profile using NU or MU or by the actual depths using ZS and ZR, respectively.

a. (U) Indices of Source and Receiver Depths: NU, MU

(U) When the source and receiver depths are both points in the profile, the user may identify these depths by using the appropriate indices.

NU = index of source depth, 1>NU>N.
= 0 implies ZS and ZR to be used.

MU = index of receiver depth, 1>MU>N.

b. (U) Source and Receiver Depths: ZS,ZR

(U) When either source or receiver depths are not points in the profile or when using a historical profile, the user may insert the depths directly in the same units as the profile depths input. When using this method, set NU = 0.

ZS = source depth in ft, yd, or m corresponding to depth units, 0.<ZS<bottom depth.

ZR = receiver depth in same units as ZS, 0.<ZR<bottom depth.

Frequency: F (U)

(U) RAYMODE has been run for frequencies as low as 10 Hz and as high as 100 kHz.

F = frequency in Hz, F>0.

Range Determinants: R, RMAX, DELTAR (U)

(U) The program will accommodate up to 400 ranges.

R = range minimum in yd if METRIC=0.
in m if METRIC=1, R>0.

RMAX = range maximum in same units as R, RMAX≥R.

DELTAR = range increment in same units as R, DELTAR>0.

Bottom Loss (U)

a. (U) MGS Bottom Loss Province MGSØP

(U) When an MGS bottom loss province number is entered, the program generates a bottom loss table for grazing angles every 2° from 0° to the maximum sonar angle ANGLE discussed later.

MGSØP = MGS bottom loss province 0≤MGSØP≤9 (default 0).

b. (U) Bottom Loss Table: ITAB, THETA, BL

(U) Set MGSØP = 0 when an input bottom loss table is desired.

ITAB = no. of pts in input bottom loss table, 0≤ITAB≤50 (default 0).

THETA (1) = angles in degrees for bottom loss table to be supplied from 0° to ANGLE in increasing order.

BL(1) = bottom losses in dB≥0. corresponding to THETA angles.

Wind Speed: WS (U)

(U) For a positive wind speed input, the program will generate a surface loss vs. grazing angle table every 2° from 0° to ANGLE.

WS = wind speed in knots, WS≥0. (default 0).

Beam Patterns for Source and/or Receiver (U)

(U) Vertical beam patterns in the form of deviation loss vs. angle may be applied to the source and/or receiver. The absence of a deviation loss table indicates an omnidirectional pattern. In defining the deviation loss table downward-directed angles from the horizontal (0°) are interpreted by the program as being positive, upward-directed angles as negative.

a. (U) Source Deviation Loss Table: IDL, THEDA, DL

IDL = no. of pts in source deviation table, 0≤IDL≤50 (default 0).

THEDA(1) = angles in degrees for source deviation loss table from -ANGLE to ANGLE in increasing order.

DL(1) = source deviation losses in dB≥0. corresponding to THEDA angles.

b. (U) Receiver Deviation Loss Table: JDL, THEDA2, DL2

JDL = no. of pts in receiver deviation table, 0≤JDL≤50 (default 0).

DL2(1) = receiver deviation losses in dB≥0. corresponding to THEDA2 angles.

Program Controls (U)

(U) As previously noted, the default values of the program control parameters and those controls which are internally generated by the program itself are adequate for usual applications of the model. Program control is provided for the user who is sufficiently familiar with certain pertinent aspects of the model to employ successfully the input parameters described in this section. These controls generally vary the amount of computation performed in the execution of the model and therefore impact the computation time and associated

cost. Some of the controls affect the accuracy of the computation so that the user may run the model in accordance with his own specific accuracy/running time requirements. Generally, the greater the required accuracy the greater the running time. Thus, if a user has many cases to run and is not overly concerned with providing the maximum attainable accuracy, he may set the program controls to process each case rapidly, thereby keeping the total accumulated run-time for all cases within some acceptable limit.

(U) Another use of the program controls involves the possibility of separate examination of distinct contributors to the total acoustic field. For example, the user may desire to compare the relative effect of surface duct and convergence zone propagation on the total propagation loss, or to compare the relative contributions of single normal modes or subsets of modes. The employment of program controls in the manner described below allows such special model applications to be processed.

a. (U) Control of Number of Ray Cycles: LAMMIN, LAMDA, LAMDAB

(U) The RAYMODE program will compute the minimum and maximum number of ray cycles necessary for both nonbottom bounce (e.g., surface duct or convergence zone) and bottom bounce propagation loss computations by using selected cycle range values. The user may wish to assign his own cycle values to reduce execution time or to isolate selected propagation paths, e.g., first convergence zone). Negative cycle inputs indicate the cycles are under program control only.

LAMMIN = minimum number of ray cycles for all propagation modes if computed minimum, LAMMIN<50 (default -1).

LAMDA = maximum number of ray cycles for all propagation modes other than bottom bounce if > computed maximum, LAMMIN$\leq$LAMDA<50 (default -1).

LAMDAB = maximum number of ray cycles for bottom bounce if < computed maximum, LAMMIN$\leq$LAMDAB<50 (default -1).

(U) Therefore, if the user enters LAMMIN = 1, LAMDA = 1, LAMDAB = 2, the program will compute one ray cycle for all nonbottombounce propagation paths with one and two bottom reflections only. Setting LAMMIN = 0 will cause the program to include the short range direct and surface-reflected propagation paths (cycle 0).

b. (U) Control of Source Angle Limits: ANGLO, ANGLE'

(U) Selection of angle limits will restrict the computation of propagation loss to that portion of the source energy emitted within the ray angle limits defined by ANGLO, ANGLE. Thus, the user can isolate that portion of the total propagation structure influencing surface duct (SD), convergence zone (CZ), and bottom bounce (BB) for separate examination.

(U) For user convenience ANGLO and/or ANGLE may be entered in terms of sound velocities in the same units as the profile velocity inputs. The chart below illustrates how to select these limits for particular combinations of propagation paths.

C_O = max sound velocity on the SVP between and including ZS and ZR.

C_L = surface layer velocity.

C_N = bottom velocity.

C_X = maximum velocity on entire SVP.

ANGLO = positive and negative minimum sonar angle in degrees, 0.$\leq$ANGLO<90. (default 0).

Propagation Type	ANGLO if angle	or	ANGLO if vel	ANGLE if angle	or	ANGLE if vel
SD:	0°		C_0	$\cos^{-1}\left(\frac{C_0}{C_L}\right)$		C_L
CZ:	$\cos^{-1}\left(\frac{C_0}{C_L}\right)$		C_L	$\cos^{-1}\left(\frac{C_0}{C_N}\right)$		C_N
BB:	$\cos^{-1}\left(\frac{C_0}{C_X}\right)$		C_X	max angle		$\frac{C_0}{\cos(\text{max angle})}$
SD + CZ:	0°		C_0	$\cos^{-1}\left(\frac{C_0}{C_N}\right)$		C_N
CZ + BB:	$\cos^{-1}\left(\frac{C_0}{C_L}\right)$		C_L	max angle		$\frac{C_0}{\cos(\text{max angle})}$
SD + CZ + BB:	0°		C_0	max angle		$\frac{C_0}{\cos(\text{max angle})}$

Restriction: ANGLO < ANGLE when in same units.

UNCLASSIFIED

or velocity limit in same units as profile velocities.

ANGLE = positive and negative maximum sonar angle in degrees, ANGLO<ANGLE<90. (default 60).

c. (U) Control of Modes Processed: MINMØD, MAXMØD, MO

(U) The specification of inputs to control mode selection will result in the program evaluation of propagation loss for only the normal modes between and including the indicated limit values. This control can therefore be used to examine the field strength of individual modes or subsets of the total mode set by setting limits MINMØD and MAXMØD when the total number of modes trapped is ≤MO, the cutoff for normal mode processing. A value of 0 for MAXMØD will result in the program computing relative mode numbers from MINMØD to the largest mode number for trapped modes (NMODE).

(U) Thus, if MINMØD = 5, MAXMØD = 5 and MO = 10, the program will treat only the fifth mode of the sequence 1, ..., NMODE, ignoring the remaining NMODE - 1 modes in the determination of propagation loss.

MINMØD = first relative normal mode processed by mode summation, 1≤MINMØ50 (default 1).

MAXMØD = last relative normal mode processed by mode summation, MAXMØD ≤50 (default 0).

MO = maximum number of modes processed by mode summation, 1≤MO≤50 (default 10).

d. (U) Number of Points in Ray Tables: NL

(U) Selection of the number of points in the ray tables controlled by the integer input NL greatly influences running time and, to a lesser extent, the accuracy of the model results. A preliminary step

leading to propagation loss evaluation is the construction of tabular data involving repeated application of a ray tracing algorithm. Once obtained, the information is processed sequentially as required in the propagation loss routine. The larger the NL the more accurate the propagation loss results but, as expected, the longer the run-time. Values of NL as high as 50 provide the most precise results but are rarely needed. Accuracy suffers little in reducing NL to 20 while improving run-time by more than a factor of two. For typical applications NL = 10 is almost always satisfactory, with errors in propagation loss being limited to approximately 0.5 dB; hence, this value of NL is used as the default condition. Reducing NL to values of five or less yields exceedingly rapid execution times with errors expected in the 1-2 dB region at worst.

NL = number of points in ray tables,
$2 < NL \leq 50$ (default 10).

(U) An example of the input data deck for a RAYMODE run using a Pacific Ocean sound speed profile from cards in the English system is given in Table 7-2. Table 7-3 gives the input data deck for an example which accesses a historical sound speed profile from the North Atlantic Ocean in the metric system.

7.2 (U) RAYMODE X Outputs

(U) RAYMODE X outputs and their discussion as presented by Yarger (1976) are presented below. Some editorial liberties, including rearrangement and rewriting of some text as necessitated by the format of this report, have been undertaken.

(U) Tables 7-4 and 7-5 give the printed outputs for the examples corresponding to the inputs of Tables 7-2 and 7-3, respectively. The RAYMODE model will provide printout of the selected inputs and tabulated propagation loss versus range and optionally provide ray information tables. The printout will be titled with the comments used on the heading card. The velocity profile input from cards or accessed from tape will be printed in its original units followed by source, receiver, and bottom depths; then the velocity profile used internally by the program in yd with source, receiver, and bottom depths inserted is printed. The other prints related to input are frequency, wind speed with the generated surface loss table if WS>0.; MGS province and its generated bottom loss table or the bottom loss table input directly, if any; the source deviation loss table, if any; the receiver deviation loss table, if any; sonar angle limits; mode inputs; and, finally, a computed reference velocity C_0 used for ray computations. Printouts of the ray information will follow if this option is chosen. Finally the output table of Range (R) in kyd or kilometers, depending on the unit system used, versus coherent phase propagation loss (PL), which represents the coherent summation of all computed propagation paths and random phase propagation loss (PLRMS), which represents an intensity summation over all propagation paths in units of decibels relative to one yard from the source (dB//1 yd), is produced for the number of ranges selected. A maximum of twenty printed pages will be produced per case.

(U) The model will also automatically plot propagation loss versus range when used in conjunction with the NUSC/NL graph plotting facility, the Information International FR 80, which utilizes the Integrated Graphics System (IGS) software; there are four other available plots that the user may select. The execution time addition for the total plot set is less than ten seconds. The set of available output plots furnishes the most convenient means for intepretation of RAYMODE results; however, the potential user employing the model at a computing facility without the IGS graph plotting capability must rely on the printed version of the output. Such a user will have little difficulty in interpreting the printed output after some scrutinization of the sample plots in

Table 7-2. (U) Example 1

The input data deck for Example 1 is presented below:

PARKA Data

```
$INPUTS
      N = 29,
      Z(1) = 0.,50.,100.,131.2,164.,180.5,200.,229.7,246.1,262.5,
      278.9,300.,400.,500.,600.,800.,1200.,1312.3,1968.5,2500.,
      3280.8,4921.2,6561.7,8202.1,9842.5,11482.9,13123.3,16404.2,
      18044.6,
      C(1) = 5022.17,5022.99,5023.81,5024.33,5024.87,5025.14,5025.46,
      5025.95,5026.22,5026.5,5024.32,5018.87,4995.16,4983.05,4971.65,
      4953.37,4922.25,4913.93,4876.22,4861.85,4857.19,4876.77,4894.18,
      4918.49,4947.27,4973.6,5002.04,5060.12,5089.61,
      NO = 14,  MU = 12,  F = 50.,  MGSOP = 4,  WS = 5.,
      R = 1000.,   DELTAR = 1000.,  RMAX = 26000.,
$END
```

Output prints follow in Table 7-4.

UNCLASSIFIED

Table 7-3. (U) Example 2

The input data deck for Example 2 is presented below:

North Atlantic Historical Profile

```
$INPUTS
      METRIC = 1
      IOCEAN = 2,  IPROFL = 16,  ISEASN = 2,
      ZB = 6500.,
      ZS = 20.,  ZR = 50.,
      P = 3500.,  MGSOP = 2,  WS = 15.,
      R = 500.,  DELTAR = 500.,  RMAX = 80000.,
      IDL = 47,
      THEDA(1) = -60.,-29.,-28.,-26.,-25.,-23.,-22.,-21.,-20.,-18.5,-17.5,
      -16.,-15.,-14.,-13.,-12.,-11.,-10.,-8.,-6.,-5.,-3.,-1.,0.,1.,3.,5.,
      6.,8.,10.,11.,12.,13.,14.,15.,16.,17.5,18.5,20.,21.,22.,23.,25.,
      26.,28.,29.,60.,
      DL(1) = 30.,30.,20.,15.,13.,11.5,2*11.,11.5,13.,15.,20.,30.,28.,20.,
      14.,10.,8.,5.,2.7,1.8,.8,.2,0.,.2,.8,1.8,2.7,7.5.,8.,10.,14.,20.,28.,
      30.,20.,15.,13.,11.5,2*11.,11.5,13.,15.,20.,30.,30.,
$END
```

Output prints follow in Table 7-5.

UNCLASSIFIED

TABLE 7-4. (U) Printed Outputs for Example 1

PROFILE UNITS (FT.FT/S OR DEG F):

VELOCITY PROFILE:

N	Z	C OR T
1	.0000	5022.1700
2	50.0000	5022.9900
3	100.0000	5023.8100
4	131.2000	5024.3300
5	164.0000	5024.8700
6	180.5000	5025.1400
7	200.0000	5025.4600
8	229.7000	5025.9500
9	246.1000	5026.2200
10	262.5000	5026.5000
11	278.9000	5024.3200
12	300.0000	5018.8700
13	400.0000	4995.1600
14	500.0000	4983.0500
15	600.0000	4971.6500
16	800.0000	4953.3700
17	1200.0000	4922.2500
18	1312.3000	4913.9300
19	1968.5000	4876.2200
20	2500.0000	4861.8500
21	3280.8000	4857.1900
22	4921.2000	4876.7700
23	6581.7000	4894.1800
24	8202.1000	4918.4900
25	9842.5000	4947.2700
26	11482.9000	4973.6000
27	13123.3000	5002.0400
28	16404.2000	5060.1200
29	18044.6001	5089.6100

SOURCE DEPTH: 500.00

RECEIVER DEPTH: 300.00

VELOCITY PROFILE (YD.YD/S):

N	DEPTH	VELOCITY
1	.0000	1674.0566
2	16.6667	1674.3300
3	33.3333	1674.6033
4	43.7333	1674.7767
5	54.6667	1674.9566
6	60.1667	1675.0467
7	66.6667	1675.1533
8	76.5667	1675.3167
9	82.0333	1675.4066
10	87.5000	1675.5000
11	92.9667	1674.7733
12	100.0000	1672.9566
13	133.3333	1665.0533
14	166.6667	1661.0166
15	200.0000	1657.2167
16	266.6667	1651.1233
17	400.0000	1640.7500
18	437.4333	1637.9767
19	656.1667	1625.4066
20	833.3333	1620.6166
21	1093.6000	1619.0633
22	1640.4000	1625.5900
23	2187.2333	1631.3933
24	2734.0333	1639.4966
25	3280.8333	1649.0900
26	3827.6333	1657.8666
27	4374.4333	1667.3466
28	5468.0666	1686.7066
29	6014.8666	1696.5367

FREQUENCY (HZ): 50.00

WIND SPEED (KTS): 5.00

SURFACE LOSS TABLE (DEG.DB):

I	ANGLE	LOSS
1	.0000	.0000
2	2.0000	.0765
3	4.0000	.1542
4	6.0000	.2332
5	8.0000	.3133
6	10.0000	.4311
7	12.0000	.6388
8	14.0000	.8578
9	16.0000	1.0872
10	18.0000	1.3259
11	20.0000	1.5729
12	22.0000	1.8275
13	24.0000	2.0890
14	26.0000	2.3571
15	28.0000	2.6317
16	30.0000	2.9130
17	32.0000	3.2016
18	34.0000	3.4981
19	36.0000	3.8035
20	38.0000	4.1189
21	40.0000	4.4457
22	42.0000	4.7853
23	44.0000	5.1392
24	46.0000	5.5091
25	48.0000	5.8969
26	50.0000	6.3044
27	52.0000	6.7340
28	54.0000	7.1862

29	56.0000	7.6698
30	58.0000	8.1822
31	60.0000	8.7293

MGS PROVINCE: 4

BOTTOM LOSS TABLE (DEG.DB):

I	ANGLE	LOSS
1	.0000	.0000
2	2.0000	.0000
3	4.0000	.0000
4	6.0000	.0000
5	8.0000	.0000
6	10.0000	.4581
7	12.0000	1.0666
8	14.0000	1.6430
9	16.0000	2.1884
10	18.0000	2.7040
11	20.0000	3.1909
12	22.0000	3.6502
13	24.0000	4.0829
14	26.0000	4.4899
15	28.0000	4.8723
16	30.0000	5.2309
17	32.0000	5.5666
18	34.0000	5.8804
19	36.0000	6.1730
20	38.0000	6.4452
21	40.0000	6.697[illegible]
22	42.0000	6.9314
23	44.0000	7.1468
24	46.0000	7.3446
25	48.0000	7.5254
26	50.0000	7.6898
27	52.0000	7.8384
28	54.0000	7.9716
29	56.0000	8.0899
30	58.0000	8.1938
31	60.0000	8.2857

SOURCE ANGLES (DEG) FROM .00 to 60.00

NORMAL MODES FROM 1 to 10

REFERENCE VELOCITY CO (YD): 1672.9666

UNCLASSIFIED

CONFIDENTIAL

PROPAGATION MODE INDEX J = 1

VELOCITY INTERVAL FROM CMIN = 1672.97 TO CMAX = 1675.50 YDS/SEC

NO OF MODES = 3 FROM 51 to 53

UPPER PHASE CHANGE PHI1 = 1.571
LOWER PHASE CHANGE PHI2 = 1.571

NO. OF CYCLES FROM 0 TO 5

ANGLES (DEG) VS. RANGE (YDS) VS. TRAVEL TIME (SEC) FOR ONE CYCLE:

K	SOURCE ANGLE	RECVR ANGLE	PATH1 RANGE	PATH1 TTIME	PATH2 RANGE	PATH2 TTIME	PATH3 RANGE	PATH3 TTIME	PATH4 RANGE	PATH4 TTIME	CYCLE RANGE	CYCLE TTIME
1	7.54	3.16	63611.84	39.04912	66029.37	40.50081	62536.95	38.40709	64954.48	39.85879	64283.16	39.45395
2	7.03	1.59	62563.30	38.42302	64549.32	39.61709	62204.23	38.20841	64190.24	39.40248	63376.77	38.91275
3	6.85	.20	62250.57	38.23610	64229.84	39.42614	62205.79	38.20934	64185.06	39.39938	63217.82	38.81774

RANGE AT CYCLE Q FOR PATH N = (PATHN RANGE) + (Q-1)*(CYCLE RANGE) FOR A FIXED K
TTIME AT CYCLE Q FOR PATH N = (PATHN TTIME) + (Q-1)*(CYCLE TTIME) FOR A FIXED K

UNCLASSIFIED

CONFIDENTIAL

PROPAGATION MODE INDEX J = 2

VELOCITY INTERVAL FROM CMIN = 1675.51 TO CMAX = 1696.54 YDS/SEC

NO OF MODES = 25 FROM 55 to 79

UPPER PHASE CHANGE PHI1 = -3.142
LOWER PHASE CHANGE PHI2 = 1.571

NO. OF CYCLES FROM 0 TO 4

ANGLES (DEG) VS. RANGE (YDS) VS. TRAVEL TIME (SEC) FOR ONE CYCLE:

K	SOURCE ANGLE	RECVR ANGLE	PATH1 RANGE	PATH1 TTIME	PATH2 RANGE	PATH2 TTIME	PATH3 RANGE	PATH3 TTIME	PATH4 RANGE.	PATH4 TTIME	CYCLE RANGE	CYCLE TTIME
1	11.75	9.56	69057.05	42.28847	70989.79	43.46186	67821.44	41.54107	69754.18	42.71447	69405.62	42.50147
2	11.00	8.62	68027.07	41.68057	70169.81	42.97792	66640.73	40.84422	6873.484	42.14157	68405.27	41.91107
3	10.29	7.70	67232.88	41.21070	69632.87	42.66026	65656.33	40.26178	68056.32	41.71135	67644.60	41.46102
4	9.64	6.79	66674.09	40.87933	69396.53	42.52010	64850.43	39.78389	67572.87	41.42466	67123.48	41.15200
5	9.05	5.93	66247.39	40.62588	69386.13	42.51397	64091.04	39.33279	67229.78	41.22087	66738.59	40.92338
6	8.54	5.11	66120.07	40.55014	69817.58	42.77071	63495.37	38.97838	67192.88	41.19894	66656.48	40.87454
7	8.12	4.38	66376.96	40.70320	70864.17	43.39419	63044.44	38.71638	67542.75	41.40738	66959.86	41.05529
8	7.80	3.74	67185.25	41.18517	72863.14	44.58615	62759.68	38.53998	68437.58	41.94096	67811.41	41.56307
9	7.61	3.32	68859.22	42.18392	76443.00	46.72201	62592.50	38.44024	70176.28	42.97832	69517.75	42.58112
10	7.54	3.16	71248.76	43.61001	81300.16	49.62077	62539.01	38.40832	72590.41	44.41909	71919.59	44.01455

RANGE AT CYCLE Q FOR PATH N = (PATHN RANGE) + (Q-1)*(CYCLE RANGE) FOR A FIXED K
TTIME AT CYCLE Q FOR PATH N = (PATHN TTIME) + (Q-1)*(CYCLE TTIME) FOR A FIXED K

UNCLASSIFIED

PROPAGATION MODE INDEX J = 3

VELOCITY INTERVAL FROM CMIN = 1696.55 TO CMAX = 3345.93 YDS/SEC

NO OF MODES = 237 FROM 81 to 317

UPPER PHASE CHANGE PHI1 = -3.142
LOWER PHASE CHANGE PHI2 = .000

NO. OF CYCLES FROM 0 TO 4

ANGLES (DEG) VS. RANGE (YDS) VS. TRAVEL TIME (SEC) FOR ONE CYCLE:

K	SOURCE ANGLE	RECVR ANGLE	PATH1 RANGE	PATH1 TTIME	PATH2 RANGE	PATH2 TTIME	PATH3 RANGE	PATH3 TTIME	PATH4 RANGE	PATH4 TTIME	CYCLE RANGE	CYCLE TTIME
1	60.24	60.00	6790.48	8.33056	6982.67	8.56079	6674.85	8.1[illegible]263	6867.04	8.42285	6828.76	8.37671
2	47.33	46.95	10916.31	9.80723	11227.09	10.07991	10729.11	9.64366	11039.89	9.91635	10978.10	9.86179
3	36.64	38.09	15855.79	12.02702	16311.94	12.36507	15580.47	11.82383	16036.62	12.16188	15946.20	12.09445
4	27.91	27.12	22118.06	15.22372	22765.93	15.65966	21725.51	14.96066	22373.36	15.39660	22245.72	15.31016
5	21.08	19.98	30165.81	19.64057	31075.21	20.22010	29610.77	19.20830	30520.16	19.86783	30342.99	19.75420
6	10.21	14.73	40033.90	25.27563	41285.17	26.05040	39260.44	24.79861	40511.71	25.57338	40272.80	25.42451
7	13.32	11.45	50730.89	31.50678	52435.67	32.49327	49715.81	30.88902	51330.59	31.87551	51030.74	31.69115
8	12.07	9.97	60269.28	37.11067	62124.32	38.23829	59088.39	36.39552	60943.44	37.52314	60606.36	37.31690
9	11.77	9.59	66687.41	40.89176	68614.63	42.06190	65455.70	40.14666	67382.92	41.31680	67035.17	41.10428
10	11.75	9.57	68411.65	41.90804	70343.98	43.08120	67176.31	41.16082	69108.65	42.33397	68760.15	42.12101

RANGE AT CYCLE Q FOR PATH N = (PATHN RANGE) + (Q-1)*(CYCLE RANGE) FOR A FIXED K
TTIME AT CYCLE Q FOR PATH N = (PATHN TTIME) + (Q-1)*(CYCLE TTIME) FOR A FIXED K

UNCLASSIFIED

PROPAGATION LOSS TABLE:

I	R (KYD)	PL (DB)	PLRMS (DB)
1	1.000	60.244	59.983
2	2.000	67.918	68.355
3	3.000	72.128	71.714
4	4.000	76.883	76.054
5	5.000	79.808	80.267
6	6.000	81.210	81.099
7	7.000	82.445	82.068
8	8.000	84.438	83.788
9	9.000	85.512	84.096
10	10.000	85.479	85.105
11	11.000	96.441	85.937
12	12.000	88.825	86.109
13	13.000	88.308	86.984
14	14.000	85.517	87.376
15	15.000	92.884	87.492
1	16.000	86.688	87.959
17	17.000	84.526	88.066
18	18.000	86.276	88.181
19	19.000	117.348	88.388
20	20.000	93.761	88.272
21	21.000	95.390	88.250
22	22.000	84.059	88.176
23	23.000	82.664	88.039
24	24.000	84.078	88.043
25	25.000	93.427	87.959
26	26.000	96.709	87.859
27	27.000	89.084	87.821
28	28.000	87.510	87.701
29	29.000	88.601	87.605
30	30.000	94.661	87.557
31	31.000	105.940	87.510
32	32.000	91.731	87.546
33	33.000	94.089	87.567
34	34.000	92.545	87.473
35	35.000	95.792	87.610
36	36.000	92.696	87.634
37	37.000	87.521	87.659
38	38.000	84.700	87.707
39	39.000	83.219	87.692
40	40.000	82.269	87.746
41	41.000	82.170	87.848
42	42.000	82.134	87.957
43	43.000	83.262	88.127
44	44.000	86.610	88.225
45	45.000	84.412	88.290
46	46.000	86.917	88.418
47	47.000	96.689	88.420
48	48.000	93.484	88.455
49	49.000	92.893	88.509
50	50.000	96.942	88.445
51	51.000	107.024	88.553
52	52.000	103.411	88.635
53	53.000	100.820	88.664
54	54.000	103.274	88.900
[illegible]	55.000	99.064	88.868
[illegible]	56.000	101.841	88.886
57	57.000	113.750	89.116
58	58.000	108.248	88.849
59	59.000	101.784	88.900
60	60.000	94.658	88.906
61	61.000	92.123	88.252
62	62.000	88.976	87.968
63	63.000	85.948	87.158
64	64.000	85.093	84.931
65	65.000	82.432	83.575
66	66.000	85.930	82.877
67	67.000	88.553	81.989
68	68.000	82.980	82.127
69	69.000	81.356	83.228
70	70.000	84.375	84.430
71	71.000	93.858	86.501
72	72.000	97.242	90.499
73	73.000	93.006	91.785
74	74.000	91.158	91.089
75	75.000	93.436	92.781
76	76.000	91.288	93.336
77	77.000	91.264	93.063
78	78.000	91.759	94.250
79	79.000	90.400	94.187
80	80.000	89.228	94.168
81	81.000	89.279	94.916
82	82.000	88.834	94.624
83	83.000	88.096	94.918
84	84.000	88.364	95.300
85	85.000	91.661	95.004
86	86.000	93.227	95.238
87	87.000	91.506	95.253
88	88.000	90.878	95.038
89	89.000	92.006	95.182
90	90.000	93.822	95.107
91	91.000	93.321	94.934
92	92.000	93.128	95.015
93	93.000	99.177	94.860
94	94.000	97.104	94.900
95	95.000	97.082	94.937
96	96.000	105.515	94.857
97	97.000	100.312	94.967
98	98.000	99.131	94.971
99	99.000	112.632	95.017
100	100.000	99.114	95.098
101	101.000	108.137	95.039
102	102.000	103.610	95.268
103	103.000	104.647	95.448

104	104.000	123.648	95.583	158	158.000	101.657	98.537
105	105.000	107.778	95.754	159	159.000	102.673	98.728
106	106.000	111.518	95.927	160	160.000	100.052	98.862
107	107.000	102.244	95.976	161	161.000	100.792	98.808
108	108.000	103.144	96.064	162	162.000	99.717	99.115
109	109.000	100.907	96.021	163	163.000	98.949	99.198
110	110.000	106.647	95.959	164	164.000	100.245	99.312
111	111.000	108.354	95.897	165	165.000	97.299	99.572
112	112.000	101.726	95.706	166	166.000	100.362	99.665
113	113.000	95.928	95.558	167	167.000	99.853	99.879
114	114.000	95.810	95.408	168	168.000	99.574	100.117
115	115.000	93.756	95.087	169	169.000	90.943	100.142
116	116.000	93.578	94.943	170	170.000	97.458	100.068
117	117.000	93.941	94.708	171	171.000	99.178	100.078
118	118.000	93.303	94.425	172	172.000	99.675	99.967
119	119.000	93.047	94.324	173	173.000	98.800	99.971
120	120.000	91.788	94.051	174	174.000	103.176	99.744
121	121.000	91.137	93.919	175	175.000	100.160	99.438
122	122.000	91.765	93.913	176	176.000	100.464	99.235
123	123.000	91.403	93.650	177	177.000	99.759	98.851
124	124.000	92.538	93.731	178	178.000	99.617	98.546
125	125.000	95.174	93.687	179	179.000	104.098	98.202
126	126.000	103.065	93.209	180	180.000	104.265	97.834
127	127.000	96.566	93.249	181	181.000	98.551	97.612
128	128.000	92.322	92.776	182	192.000	98.863	97.313
129	129.000	93.084	91.306	183	193.000	108.471	97.039
130	130.000	103.267	90.483	184	184.000	101.533	96.924
131	131.000	88.797	89.035	185	185.000	97.310	96.689
132	132.000	86.368	87.550	186	186.000	101.650	96.553
133	133.000	91.614	86.765	187	187.000	108.736	96.502
134	134.000	88.432	86.050	188	188.000	97.378	96.327
135	135.000	91.954	85.652	189	189.000	99.256	96.376
136	136.000	83.578	86.317	190	190.000	106.502	96.299
137	137.000	86.497	87.398	191	191.000	97.499	96.177
138	138.000	87.310	88.565	192	192.000	98.074	96.359
139	139.000	96.461	91.738	193	193.000	99.699	95.913
140	140.000	100.355	95.564	194	194.000	94.793	95.587
141	141.000	93.382	94.315	195	195.000	95.505	95.337
142	142.000	99.106	95.269	196	196.000	93.211	93.735
143	143.000	103.951	97.950	197	197.000	93.134	92.394
144	144.000	96.235	96.814	198	198.000	93.514	91.341
145	145.000	113.648	97.519	199	199.000	93.924	90.041
146	146.000	104.349	98.913	200	200.000	94.823	89.341
147	147.000	103.142	98.008	201	201.000	95.180	88.[illegible]52
148	148.000	108.664	98.652	202	202.000	91.223	88.436
149	149.000	98.808	99.029	203	203.000	88.146	88.655
150	150.000	103.033	98.305	204	204.000	87.268	89.656
151	151.000	99.205	98.833	205	205.000	89.278	90.500
152	152.000	101.101	98.664	206	206.000	99.217	92.159
153	153.000	102.071	98.344	207	207.000	99.769	95.979
154	154.000	104.893	98.743	208	208.000	95.420	96.790
155	155.000	105.136	98.513	209	209.000	101.195	96.147
156	156.000	104.753	98.494	210	210.000	103.467	99.556
157	157.000	104.987	98.729	211	211.000	101.159	100.934

UNCLASSIFIED

212	212.000	103.081	99.228
213	213.000	106.463	101.823
214	214.000	103.160	101.983
215	215.000	108.043	100.948
216	216.000	104.864	102.705
217	217.000	107.892	102.036
218	218.000	105.668	101.667
219	219.000	106.843	102.763
220	220.000	104.524	101.951
221	221.000	108.301	102.184
222	222.000	105.713	102.886
223	223.000	107.090	102.369
224	224.000	106.539	102.921
225	225.000	106.459	103.221
226	226.000	109.314	103.086
227	227.000	107.544	103.879
228	228.000	111.738	103.968
229	229.000	109.340	104.174
230	230.000	113.618	104.925
231	231.000	110.707	104.560
232	232.000	111.330	104.897
233	233.000	113.744	105.416
234	234.000	112.029	104.730
235	235.000	114.781	105.005
236	236.000	108.601	104.921
237	237.000	110.377	104.329
238	238.000	110.052	103.806
239	239.000	110.582	103.354
240	240.000	107.755	102.551
241	241.000	104.278	102.114
242	242.000	105.097	101.435
243	243.000	107.685	101.057
244	244.000	106.503	100.743
245	245.000	106.259	100.278
246	246.000	105.765	99.946
247	247.000	105.657	99.581
248	248.000	105.575	99.305
249	249.000	105.961	99.111
250	250.000	107.746	98.886
251	251.000	106.501	98.794
252	252.000	106.988	98.749
253	253.000	105.224	98.623
254	254.000	106.594	98.706
255	255.000	107.953	98.762
256	256.000	106.379	98.818
257	257.000	108.116	99.062
258	258.000	108.846	99.008
259	259.000	115.082	99.165
260	260.000	109.403	99.144

UNCLASSIFIED

TABLE 7-5. (U) PRINTED OUTPUTS FOR EXAMPLE 2 PROFILE FROM HISTORICAL VELOCITY PROFILE TAPE FOR OCEAN 2, PROFILE 16, SEASON 2

PROFILE UNITS (M, M/S OR DEG C):

VELOCITY PROFILE:

N	2	C OR T
1	.0000	1530.0990
2	30.4801	1528.8798
3	106.6802	1523.3934
4	152.4003	1522.7836
5	304.8006	1523.3934
6	381.0007	1524.0030
7	457.2009	1523.3934
8	533.4010	1522.1742
9	609.6012	1519.4310
10	685.8013	1514.8590
11	762.0015	1509.6774
12	838.2016	1504.8006
13	914.4018	1500.2285
14	990.6019	1496.8757
15	1066.8021	1494.1325
16	1219.2024	1491.0845
17	1371.6027	1490.7797
18	1524.0030	1492.3037
19	1628.8036	1495.9613
20	2133.6042	1499.9237
21	2743.2054	1508.4582
22	3657.6072	1522.4790
23	4572.0090	1537.4142
24	5486.4108	1522.6543
25	6400.8126	1568.5039

SOURCE DEPTH: 20.00

RECEIVER DEPTH: 50.00

BOTTOM DEPTH: 6500.00

UNCLASSIFIED

VELOCITY PROFILE (YD, YD/S):

N	DEPTH	VELOCITY
1	.0000	1673.3333
2	21.8722	1672.4584
3	33.3333	1671.9999
4	54.6806	1670.4629
5	116.6667	1665.9999
6	166.6667	1665.3333
7	333.3333	1665.9999
8	416.6666	1666.6666
9	500.0000	1665.9999
10	583.3333	1664.6666
11	666.6666	1661.6666
12	750.0000	1656.6666
13	833.3333	1650.9999
14	916.6666	1645.6666
15	1000.0000	1640.6666
16	1083.3333	1636.9999
17	1166.6666	1633.9999
18	1333.3333	1630.6666
19	1499.9999	1630.3333
20	1666.6666	1631.9999
21	1999.9999	1635.9999
22	2333.3332	1640.3333
23	2999.9998	1649.6666
24	3999.9998	1664.9999
25	4999.9998	1681.3333
26	5999.9997	1697.9999
27	6999.9997	1715.3333
28	7108.4722	1717.2134

FREQUENCY (HZ): 3500.00

WIND SPEED (KTS): 15.00

SURFACE LOSS TABLE (DEG, DB):

I	ANGLE	LOSS
1	.0000	6.0013
2	2.0000	6.0777
3	4.0000	6.1555
4	6.0000	6.2344
5	8.0000	6.3145
6	10.0000	6.3967
7	12.0000	6.4780
8	14.0000	6.5812
9	16.0000	6.6950
10	18.0000	6.9115
11	20.0000	7.1392
12	22.0000	7.3782
13	24.0000	7.6286
14	26.0000	7.8906
15	28.0000	8.1642
16	30.0000	8.4495
17	32.0000	8.7469
18	34.0000	9.0564
19	36.0000	9.3786
20	38.0000	9.7138
21	40.0000	10.0625
22	42.0000	10.4256
23	44.0000	10.8039
24	46.0000	11.1984
25	48.0000	11.6106
26	50.0000	12.0419
27	52.0000	12.4942
28	54.0000	12.9699
29	56.0000	13.4715
30	58.0000	14.0024
31	60.0000	14.5664

MGS PROVINCE: 2

BOTTOM LOSS TABLE (DEG, DB):

I	ANGLE	LOSS
1	.0000	3.5482
2	2.0000	3.8302
3	4.0000	4.0597
4	6.0000	4.2748
5	8.0000	4.4773
6	10.0000	4.6684
7	12.0000	4.8495
8	14.0000	5.0215
9	16.0000	5.1853
10	18.0000	5.3416
11	20.0000	5.4911
12	22.0000	5.6343
13	24.0000	5.7718
14	26.0000	5.9041
15	28.0000	6.0314
16	30.0000	6.1541
17	32.0000	6.2727
18	34.0000	6.3872
19	36.0000	6.4981
20	38.0000	[illegible]
21	40.0000	6.7096
22	42.0000	6.8107
23	44.0000	6.9088
24	46.0000	7.0043
25	48.0000	7.0971
26	50.0000	7.1875
27	52.0000	7.2756
28	54.0000	7.3615
29	56.0000	7.4453
30	58.0000	7.5271
31	60.0000	7.6070

SOURCE DEVIATION PATTERN (DEG, DB):

I	ANGLE	LOSS
1	-60.0000	30.0000
2	-29.0000	30.0000
3	-28.0000	20.0000
4	-26.0000	15.0000
5	-25.0000	13.0000
6	-23.0000	11.5000
7	-22.0000	11.0000
8	-21.0000	11.0000
9	-20.0000	11.0000
10	-18.5000	13.0000
11	-17.5000	15.0000
12	-16.0000	20.0000
13	-15.0000	30.0000
14	-14.0000	28.0000
15	-13.0000	20.0000
16	-12.0000	14.0000
17	-11.0000	10.0000
18	-10.0000	8.0000
19	-8.0000	5.0000
20	-6.0000	2.7000
21	-5.0000	1.8000
22	-3.0000	.8000
23	-1.0000	.2000
24	.0000	.0000
25	1.0000	.2000
26	3.0000	.8000
27	5.0000	1.8000
28	6.0000	2.7000
29	8.0000	5.0000
30	10.0000	8.0000
31	11.0000	10.0000
32	12.0000	14.0000
33	13.0000	20.0000
34	14.0000	28.0000
35	15.0000	30.0000
36	16.0000	20.0000
37	17.5000	15.0000
38	18.5000	13.0000
39	20.0000	11.5000
40	21.0000	11.0000
41	22.0000	11.0000
42	23.0000	11.5000
43	25.0000	13.0000
44	26.0000	15.0000
45	28.0000	20.0000
46	29.0000	30.0000
47	60.0000	30.0000

SOURCE ANGLES (DEG) FROM .00 TO 60.00

NORMAL MODES FROM 1 TO 10

REFERENCE VELOCITY CO (YD): 1672.4684

UNCLASSIFIED

PROPAGATION MODE INDEX J = 1

VELOCITY INTERVAL FROM CMIN = 1672.47 TO CMAX = 1673.33 YDS/SEC

NO OF MODES = 82 FROM 2859 to 2940

UPPER PHASE CHANGE PHI1 = 1.571
LOWER PHASE CHANGE PHI2 = 1.571

NO. OF CYCLES FROM 0 TO 2

ANGLES (DEG) VS. RANGE (YDS) VS. TRAVEL TIME (SEC) FOR ONE CYCLE:

K	SOURCE ANGLE	RECVR ANGLE	PATH1 RANGE	PATH1 TTIME	PATH2 RANGE	PATH2 TTIME	PATH3 RANGE	PATH3 TTIME	PATH4 RANGE	PATH4 TTIME	CYCLE RANGE	CYCLE TTIME
1	1.85	3.38	76726.94	46.69393	79432.13	48.31114	72521.43	44.17834	75226.62	45.79555	75976.78	46.24474
2	1.85	3.25	76702.28	46.67922	79110.32	48.11884	72689.15	44.24860	75097.19	45.71823	75899.74	46.19872
3	1.45	3.15	76689.80	46.67175	78801.34	47.93416	72855.94	44.37829	74967.48	45.64070	75828.64	46.15622
4	1.24	3.00	76690.39	46.67212	78506.29	47.74780	73020.66	44.47676	74836.57	45.56245	75763.48	46.11728
5	1.04	2.99	76705.44	46.68110	78227.00	47.59082	7312.327	44.57340	74703.88	45.48312	75704.66	46.08211
6	.84	2.92	76736.74	46.69980	77966.24	47.43492	73339.91	44.66760	74569.42	45.40272	75653.08	46.05126
7	.85	2.87	76786.17	46.72936	77727.88	47.29241	73492.33	44.75873	74434.04	45.32178	75610.11	46.02557
8	.45	2.82	76854.23	46.77007	77518.03	47.16697	73636.93	44.84520	74300.73	45.24210	75577.48	46.00608
9	.28	2.81	76934.14	46.81784	77349.75	47.06634	73764.16	44.92127	74179.78	45.16977	75556.96	45.99381
10	.20	2.81	76982.38	46.84668	77271.51	47.01956	73828.40	44.95867	74117.53	45.13255	75549.96	45.98962

RANGE AT CYCLE Q FOR PATH N = (PATHN RANGE) + (Q-1)*(CYCLE RANGE) FOR A FIXED K
TTIME AT CYCLE Q FOR PATH N = (PATHN TTIME) + (Q-1)*(CYCLE TTIME) FOR A FIXED K

UNCLASSIFIED

PROPAGATION MODE INDEX J = 2

VELOCITY INTERVAL FROM CMIN = 1673.34 TO CMAX = 1717.21 YDS/SEC

NO OF MODES = 3922 FROM 2943 to 6864

UPPER PHASE CHANGE PHI1 = 3.142
LOWER PHASE CHANGE PHI2 = 1.571

NO. OF CYCLES FROM 0 TO 2

ANGLES (DEG) VS. RANGE (YDS) VS. TRAVEL TIME (SEC) FOR ONE CYCLE:

K	SOURCE ANGLE	RECVR ANGLE	PATH1 RANGE	PATH1 TTIME	PATH2 RANGE	PATH2 TTIME	PATH3 RANGE	PATH3 TTIME	PATH4 RANGE	PATH4 TTIME	CYCLE RANGE	CYCLE TTIME
1	13.11	13.40	77377.18	47.02556	77565.98	47.14141	76909.44	46.73826	77098.24	46.85413	77237.71	46.93965
2	11.68	12.01	75241.11	45.77830	75454.10	75.90827	74714.65	45.45673	74927.64	45.58671	75004.37	45.68250
3	10.26	10.63	73735.74	44.89489	73979.55	45.04296	73135.05	44.42974	73378.86	44.67701	73557.30	44.78635
4	8.84	9.27	72600.78	44.22547	72885.26	44.39752	71903.33	43.80327	72187.80	43.97531	72304.29	44.10039
5	7.44	7.94	71734.55	43.71290	72075.12	43.91816	70906.00	43.21309	41246.57	43.41835	71480.56	43.55663
6	6.05	6.67	71607.06	43.63730	72029.88	43.89140	70591.88	43.02667	71014.70	43.28077	41310.88	43.45904
7	4.70	5.47	72058.96	43/90634	72613.25	44.23871	70760.53	43.12708	71314.81	43.45944	71686.89	43.68289
8	3.43	4.42	73101.93	44.52843	73895.08	45.00328	71337.26	43.47108	72130.41	43.94592	72616.17	44.23718
9	2.35	3.60	74715.47	45.49200	76031.76	46.27926	72113.10	43.93437	73429.39	44.72163	74072.43	45.10682
10	1.86	3.30	76439.41	46.52214	78870.88	47.87577	72512.14	44.17318	74944.21	45.62602	75961.81	46.07448

RANGE AT CYCLE Q FOR PATH N = (PATHN RANGE) + (Q-1)*(CYCLE RANGE) FOR A FIXED K
TTIME AT CYCLE Q FOR PATH N = (PATHN TTIME) + (Q-1)*(CYCLE TTIME) FOR A FIXED K

UNCLASSIFED

PROPAGATION MODE INDEX J = 5

VELOCITY INTERVAL FROM CMIN = 1717.22 TO CMAX = 3344.94 YDS/SEC

NO OF MODES = 19018 FROM 6867 to 25884

UPPER PHASE CHANGE PHI1 = 3.142
LOWER PHASE CHANGE PHI2 = .000

NO. OF CYCLES FROM 0 TO 2

ANGLES (DEG) VS. RANGE (YDS) VS. TRAVEL TIME (SEC) FOR ONE CYCLE:

K	SOURCE ANGLE	RECVR ANGLE	PATH1 RANGE	PATH1 TTIME	PATH2 RANGE	PATH2 TTIME	PATH3 RANGE	PATH3 TTIME	PATH4 RANGE	PATH4 TTIME	CYCLE RANGE	CYCLE TTIME
1	60.00	60.04	8192.86	9.86181	8218.13	9.89200	8129.74	9.78029	8155.01	9.81649	8173.94	9.83915
2	47.31	47.37	13074.12	11.60206	13114.49	11.63765	12973.27	11.51309	13013.64	11.54868	13043.88	11.57537
3	36.82	36.91	18893.69	14.19600	18952.16	14.23965	16747.71	14.08691	18806.18	14.13056	1884.940	14.16328
4	28.32	28.45	26202.31	17.88887	26283.58	17.94404	25999.56	17.75110	26080.83	17.80627	26141.57	17.84757
5	20.75	21.92	35430.55	22.90124	35548.38	22.97191	35164.90	22.72500	35274.74	22.79567	35356.64	22.84846
6	17.17	17.34	46478.64	29.13183	26620.66	29.22066	46125.51	28.91074	46267.52	28.99957	46373.08	29.06570
7	14.52	14.76	58083.89	34.81145	58253.56	35.91619	57662.86	35.55130	57832.53	35.65603	57958.21	35.73374
8	13.40	13.66	68182.74	41.67338	68367.26	41.78673	67725.43	41.39217	67909.95	41.50553	68046.34	41.58945
9	13.13	13.42	74903.70	45.58520	75092.21	45.70088	74436.69	45.29835	74625.19	45.41402	74764.45	45.49961
10	13.11	13.40	76703.65	46.63333	76892.43	46.74917	76235.97	46.34609	76424.75	46.46193	76564.20	46.54763

RANGE AT CYCLE Q FOR PATH N = (PATHN RANGE) + (Q-1)*(CYCLE RANGE) FOR A FIXED K
TTIME AT CYCLE Q FOR PATH N = (PATHN TTIME) + (Q-1)*(CYCLE TTIME) FOR A FIXED K

UNCLASSIFIED

PROPAGATION LOSS TABLE:

I	R (KM)	PL (DB)	PLRMS (DB)
1	.500	52.841	55.229
2	1.000	63.009	62.752
3	1.500	73.006	68.580
4	2.000	74.887	71.011
5	2.500	70.128	68.653
5	3.000	72.794	74.590
7	3.500	85.434	83.255
8	4.000	85.004	86.094
9	4.500	87.827	87.283
10	5.000	101.888	96.066
11	5.500	91.708	90.423
12	6.000	101.567	98.352
13	6.500	97.664	94.918
14	7.000	97.191	96.102
15	7.500	102.056	100.921
16	8.000	100.142	97.272
17	8.500	110.164	104.085
18	9.000	99.730	99.699
19	9.500	104.845	104.541
20	10.000	104.145	106.435
21	10.500	102.462	102.517
22	11.000	110.321	108.442
23	11.500	101.860	103.137
24	12.000	108.795	107.383
25	12.500	105.945	107.143
26	13.000	105.232	105.279
27	13.500	110.371	112.430
28	14.000	105.686	106.782
29	14.500	112.938	112.286
30	15.000	110.250	110.829
31	15.500	111.229	109.823
32	16.000	116.011	116.760
33	16.500	111.723	109.683
34	17.000	114.851	116.109
35	17.500	113.620	112.793
36	18.000	111.719	113.594
37	18.500	120.169	117.009
38	19.000	114.348	112.407
39	19.500	123.613	118.251
40	20.000	116.536	113.614
41	20.500	114.146	115.550
42	21.000	117.157	117.145
43	21.500	114.332	114.562
44	22.000	126.468	122.144
45	22.500	112.762	115.419
46	23.000	121.415	119.807
47	23.500	116.285	119.947
48	24.000	117.828	115.483
49	24.500	120.603	117.924
50	25.000	111.844	114.901
51	25.500	122.873	116.442
52	26.000	109.696	115.804
53	26.500	118.599	114.617
54	27.000	114.568	115.392
55	27.500	118.749	113.958
56	28.000	114.270	114.338
57	28.500	108.959	113.492
58	29.000	125.304	113.536
59	29.500	113.781	113.882
60	30.000	119.102	113.225
61	30.500	110.758	113.827
62	31.000	122.775	113.299
63	31.500	111.781	113.586
64	32.000	115.048	113.633
65	32.500	112.214	113.517
66	33.000	114.589	114.159
67	33.500	114.984	113.521
68	34.000	114.244	114.318
69	34.500	121.091	114.554
70	35.000	111.959	114.356
71	35.500	112.534	114.934
72	36.000	118.674	114.608
73	36.500	113.298	115.722
74	37.000	117.770	115.736
75	37.500	119.044	115.742
76	38.000	118.961	117.344
77	38.500	117.816	116.529
78	39.000	121.531	117.820
79	39.500	119.142	118.066
80	40.000	122.882	118.230
81	40.500	123.228	119.603
82	41.000	118.004	113.605
83	41.500	120.472	119.700
84	42.000	118.533	119.179
85	42.500	134.545	120.333
86	43.000	119.870	121.001
87	43.500	125.900	119.936
88	44.000	121.789	121.581
89	44.500	124.359	120.088
90	45.000	120.244	121.298
91	45.500	138.441	123.451
92	46.000	128.852	120.240
93	46.500	135.968	124.608
94	47.000	134.532	120.139
95	47.500	129.309	121.231
96	48.000	123.314	124.850
97	48.500	126.568	120.130
98	49.000	126.312	125.968
99	49.500	130.204	119.566
100	50.000	132.021	123.110
101	50.500	130.861	123.806
102	51.000	135.111	122.119
103	51.500	126.667	125.113

104	52.000	134.017	121.011
105	52.500	132.663	124.651
106	53.000	126.344	120.131
107	53.500	131.504	124.102
108	54.000	122.092	123.054
109	54.500	120.132	120.645
110	55.000	122.447	123.095
111	55.500	118.976	119.723
112	56.000	127.042	123.062
113	56.500	122.117	124.767
114	57.000	130.615	119.450
115	57.500	121.166	122.193
116	58.000	121.154	119.160
117	58.500	129.443	119.362
118	59.000	122.415	121.924
119	59.500	133.837	117.097
120	60.000	119.731	117.819
121	60.500	124.396	116.742
122	61.000	122.668	116.958
123	61.500	121.266	118.509
124	62.000	123.509	114.689
125	62.500	124.831	119.424
126	63.000	129.829	114.189
127	63.500	131.429	115.048
128	64.000	112.539	114.331
129	64.500	97.271	97.142
130	65.000	107.940	97.674
131	65.500	104.047	97.757
132	66.000	99.498	99.245
133	66.500	101.608	96.485
134	67.000	103.440	97.128
135	67.500	108.530	100.878
136	68.000	112.609	100.455
137	68.500	102.900	97.650
138	69.000	102.400	104.268
139	69.500	103.843	105.803

UNCLASSIFIED

Appendices A and B of Yarger (1976) has been undertaken to obtain the meaning of each specific RAYMODE product. The inclusion of the printed outputs, therefore, is intended to minimize the conversion process required to adapt the model at other installations. References to the IGS plotting system may be removed by deleting the code specifically marked for this purpose form the listing of the model's main element RAMODX and deleting the four plotting subroutines.

1. (U) Print Option: IPRINT

(U) Optional prints of ray information are available for each propagation model index J referring to the separate propagation types sustained by the selected SVP in order of increasing source ray angle, where typically

J = 1 refers to surface duct,
J = 2 refers to convergence zone,
and J = 3 refers to bottom bounce.

(U) The printout shows the velocity interval from CMIN $\geq C_0$ to CMAX used for the propagation type and the number of trapped normal modes of that type. The next information reveals phase changes where PHI1 is the phase change undergone when propagation direction reverses from an upward to a downward direction (ray apex or surface reflection), and PHI2 is the corresponding phase change from a downward to an upward direction (ray nadir or bottom reflection). The ray path cycle limits used by the program for that J index are also printed. A table of source and receiver angle in degrees versus range in yards and travel time in seconds for one cycle (Q = 1) and all propagation paths n from 1 to 4 at each entry k in the ray table is output along with cycle range and cycle travel time. The four paths between source S and receiver R may be illustrated using first BB(Q = 1) as follows:

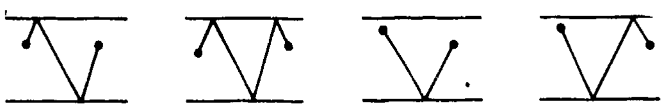

Path 1 Path 2 Path 3 Path 4

Higher order paths (Q>1) are identified by generalizing the above scheme. Short range direct paths (Q=0) consist of only Path 2 with Path 1 if ZS>ZR or Path 4 if ZS<ZR. To compute horizontal range and travel time at cycle Q=0 (direct path) or Q>1 for a particular path n

$$\text{Range}_k = (\text{path n range for Q=1})_k + (Q-1) * (\text{cycle range})_k$$

$$\text{Time}_k = (\text{path n time for Q=1})_k + (Q-1) * (\text{cycle time})_k$$

for each entry k in table ignoring negative ranges for Q=0, which restricts the terms to the appropriate direct paths. The number of points printed in the table will be equal to NL or a value selected by the program. Similar expressions to the above will be printed after the table as a user aid to hand calculations of range and/or travel time at particular source and/or receiver angles. This information is plotted for each cycle in the angle versus range plots and travel time plots discussed below. To suppress or include the ray tracing outputs the user must input IPRINT as follows:

IPRINT<0 to cancel ray information print
$\geq$0 to include ray information print (default 1)

2. (U) Plot Options: PLOTCZ, PLOTOP, PLOTT, PLOTPL and Scale Term: PLO

(U) The following plotting options are available from the RAYMODE computer program with the NUSC/NL IGS system.

(1) SVP plot and a plot of bottom loss, surface loss, and deviation loss (beam) data.

(2) Source and/or receiver angle versus horizontal range from each ray path n from 1 to 4 and cycle Q included in propagation loss computations.

(3) Travel time versus horizontal range for the same ray paths.

(4) Propagation loss versus horizontal range for coherent or random phase combination of multipaths.

(U) The coherent phase (PL) curve is drawn with a normal line (if not deleted) and the random phase (PLRMS) curve is drawn with a heavier line L(if not deleted). The key containing frequency, source depth, and receiver depth again appears to identify the case inputs.

(U) The various user controls for the plots follow:

PLOTCZ = integer plot option for velocity profile and input loss table plots, where

- ≤ 0 cancels SVP and input loss table plots.
- > 0 plot SVP and input loss tables (default 1).

PLOTOP = integer plot option for ray angle versus range plots

- ≤ 0 cancels ray angle versus range plots.
- = 1 plot only source angle vs. range.
- = 2 plot only receiver angle vs. range.
- ≥ 3 plot both source and receiver angle vs. range on separate graphs (default 3).

PLOTT = integer plot option for travel time versus range plot

- ≤ 0 cancels travel time plot.
- > 0 plot travel time vs. range (default 1).

PLOTPL = integer plot option for random/coherent propagation loss versus range

- = 1 plot only coherent phase propagation loss.
- = 2 plot only random phase propagation loss.
- = 1,2 plot both coherent and random propagation loss on same graph (default 3).

PLO = smallest dB value of propagation plot loss scale, PLO≥0. (default 40.).

8.0 (U) Organization Responsibility for RAYMODE X

(U) Responsibility for the RAYMODE X model resides at the Naval Underwater Systems Center, New London Laboratory, New London, Connecticut 06320.

(U) For theory upon which the model is based:

- Dr. Gustave A. Leibiger, Code 327, 447-4221.
- Mr. Roy Deavenport, Code 321, 447-4779.

(U) For model development:

- Dr. Gustave A. Leibiger, Code 327, 447-4221.
- Ms. Donna F. Yarger, Code 327, 447-5198.
- Mr. Eugene M. Smith, Code 327, 447-5347.

(U) For computer implementation:

- Ms. Donna F. Yarger, Code 327, 447-5198, for UNIVAC.
- Mr. Eugene M. Smith, Code 327, 447-5347, for UNIVAC.
- Mr. Thomas Cannan, Code 3351, 447-4738, for Tektronix.
- Mr. George Brown, Code 3351, 447-4680, for PDP 11/70.
- Mr. James Bairstow, Code 3351, 447-5514, for HP9845.

For model maintenance: all individuals listed above.

9.0 (U) Test Cases for Implementation on a New Computer

(U) The only test cases which can be used to check out RAYMODE X on a new computer are given in Appendices A and B of the User's Guide (Yarger, 1976) and also in Tables 7-2 and 7-3 (inputs) and Tables 7-4 and 7-5 (printed outputs). The graphical outputs would be of interest to only those users with an IGS system. The second test case utilizes a historical velocity profile (from a

tape) which is also given in the output. A word of caution in using these test cases: the test cases should be used only for the version of RAYMODE given in Appendix C of the user's guide. Many versions of RAYMODE exist which, due to changes in physics, program language, and method of calculation, will not give answers to the test problems identical to those of the users's guide.

9.1 (U) Computer Systems on Which RAYMODE Versions are Running

(U) Versions of RAYMODE exist on the following computers at NUSC/NL:

UNIVAC 1108
PDP 11/70
HP 9825
HP 9845
Tektronix 4051

(U) Outside NUSC/NL, many decks of RAYMODE have been supplied to Navy contractors and military laboratories upon request, as listed in Table 9-1. Upon what machines these decks have been implemented is not readily available. A potential new user of RAYMODE may, however, recognize one of the organizations of Table 9-1 as processing an identical computer to the one of intended RAYMODE implementation and, hence, gain from the experience of that organization. RAYMODE is known to exist on IBM computers and on the UYK-20.

(U) The RAYMODE Univac, IBM, and PDP 11/70 models are written in FORTRAN V; the UYK-20 version is in CMS-2; the HP 9845 and Tektronix 4051 versions are in BASIC.

(U) The UNIVAC versions of the RAYMODE model use single precision arithmetic on a 36-bit machine. In converting to a computer system of less precision (i.e., a 32-bit IBM 360), revised versions of subroutine THREEH, which computes a sensitive range derivative, and subroutine SQUD, which computes a term based on a large machine dependent integer to reduce the arguments of trigonometric functions, may be necessary. All UNIVAC versions use NAMELIST inputs which are not available in PDP, HP, or Tektronix machines; these machines use a conversational mode of input and output parameter selection keyed in at the terminal by the user, guided by the software.

10.0 (U) RAYMODE Versions

(U) The following information was supplied by NUSC/NL on 8 August 1980.

(U) On the UNIVAC 1108 at NUSC/NL there are several current versions of RAYMODE, all in FORTRAN:

- The RAYMODE Standard model, as described in enclosure (1); all previous versions of the model before 1976 (i.e., RAYMODE IV or RAYMODE IX) are no longer in use.

- The SUBSEA RAYMODE version, as described by Weitzner and Pearson (1980); this version allows convenient multiple inputs (up to 125) of frequency for broadband computations and up to ten source/receiver depth combinations for a given environment and writes random phase propagation loss vs. range outputs to magnetic tape or disc files.

- The RAYMODE Upgrade version being implemented at System Consultants, Inc., Arlington, Virginia, currently being tested and debugged, contains a more sophisticated surface duct calculation and a revised "RAYMODE method" or an FFT calculation as well as more efficient mode summation and bottom bounce code; this model shows promise of significantly reducing RAYMODE run time for some cases while improving accuracy.

- A multi-path version of RAYMODE prints a large matrix of source angle, receiver angle, travel time, and propagation loss for each discrete range, path cycle, and angular grouping and optionally writes this data to magnetic tape for further processing; this model is not checked out at this time.

Table 9-1. (U) List of activities using RAYMODE from 1976 to June 1980

N	Date	Individual	Organization	Address
1	Feb 9, 1976	Ed Chaika	NUC (POSSM Comm.)	San Diego, CA 92132
2	Jun 10, 1976	David Michel	Magnavox Co.	1700 Magnavox Way Dept. 529, Plant 3 Ft. Wayne, IN
3	Jun 24, 1976	Jerry Lobdill	Tracor	Austin, TX
4	Jul 12, 1976	Dr. Grant Gartrell	Weapons Research Estab.	Box 2151 GPO, Adelaide, 5A 5001 Australia
5	Jul 1976	Steven Schuster	Rockwell International	Anaheim, CA
6	Jun 1, 1977	Dr. Richard Johnson	Oregon State Univ. School of Oceanography	Corvallis, OR 97331
7	Jul 1, 1977	John Salsbury	NUSC/NPT Code 444	Newport, RI
8	Oct 14, 1977	Raymond R. Guenther	Automation Indus. VITRO	Silver Springs, MD 20910
9	Dec , 1978	Bert Loomis	NAVOCEANO	
10	Jan , 1979	Jerry Bardin	RADIAN	Austin, TX
11	Mar 21, 1979	Raya Stern	Bolt, Berenak, & Newman	Cambridge, MA
12	Mar 29, 1979	R.J. Urick	TRACOR, Inc.	1601 Research Blvd, Rockville, MD 20850
13	May 2, 1979	Dr. Charles E. Schmidt	Honeywell, Inc. Marine Systems	5303 Shilshole Ave, NW Seattle, Wash. 98107
14	May 10, 1979	Bob Zeskind	BBN	1701 Fort Myer Drive Arlington, VA 22209
15	May 15, 1979	via Dr. VonWinkle	SACLANT ASW Research Center	
16	Jul 12, 1979	Hy Greenbaum	A&T	
17	Jun 1979	Ron Maeur	Rockwell International	Anaheim, CA
18	Aug 15, 1979	Mike Turner	TRW	7600 Colshire Drive McLean, VA 22102
19	Aug 28, 1979	Ed Burledge	TRACOR, Inc.	6500 Tracor Lane Austin, TX 78721
20		Robert McGirr	Naval Ocean Systems Center	San Diego, CA 92153 (Code 724)

UNCLASSIFIED

Table 9-1 (cont.). (U) List of activities using RAYMODE from 1976 to June 1980

N	Date	Individual	Organization	Address
21	Oct 19, 1979	Stewart Lingley	System Planning Corp.	1500 Wilson Blvd Arlingotn, VA 22209
22	Nov 29, 1979	D. Paquette	Code 38211, NUSC	NUSC/NPT
23	Feb 12, 1980	Michael Libby	IBM, Manassas	Bldg 400/041, 9500 Goodwin Drive Manassas, VA 22110
24	Feb 12, 1980	W.H. Lunceford	Naval Training Equip. Center	Code N233 Orlando, FL 32813
25	Mar 5, 1980	LCdr Frank Hiestand	COMOPTEVFOR Naval Base	Norfolk, VA 23511
26	Mar 1980	ASA Davis	NUSC	NUSC/NPT
27	Apr 5, 1980	George E. Miller	RCA Automated Systems	PO Box 588 MS 1-1 Burlington, MA 01803
28	Mar 28, 1980	Joe Fenier	McDonald Dougas Aeronautics	PO Box 516 St. Louis, MO 63166
29	Apr 2, 1980	Bob Woodham	Naval Surface Weapons Center	Code 031 Silver Spring, MD 20910
30	May 10, 1980	Paul Scherer	Naval Air Development Center	Warminster, PA 18974
31	Jun 19, 1980	Stephen P. Koch	B-K Dynamics, Inc.	15825 Shady Grove Road Rockville, MD 20850

UNCLASSIFIED

(U) On other computers within NUSC/NL, there exists:

- An HP 9845 version of RAYMODE written in BASIC language. Bairstow and Medieras (1980) describe this version and give a test case.

- An HP 9825 version also in BASIC used by developer Dr. G. A. Leibiger for testing new concepts and techniques; this version has inputs keyed in by user and has limited graphical output.

- A Tektronix 4051 version also in BASIC, again used by Dr. Leibiger, as an experimental model.

- A PDP 11/70 version used by the Surface Ship Department written in FORTRAN.

- A Tektronix 4051 version as implemented from the propagation loss tape of the Fleet Mission Library using conversational input guidance and selectable varied output graphics used in the fleet.

(U) A ROM version of RAYMODE for the Tektronix is nearly ready, which is estimated to improve RAYMODE run time by a factor of ten.

11.0 (U) Test Cases Used in the Evaluation of RAYMODE X

(U) Test cases were chosen from experimental data sets. The experimental data sets are described in detail by Martin (1982) and constitute a Portable Test Package for model evaluation. A subset of these cases were selected for the RAYMODE X evaluation based on time and cost constraints and availability of the data during this evaluation. The experimental sets selected were SUDS, HAYS-MURPHY, PARKA II, BEARING STAKE, JOAST, LORAD, FASOR, and GULF OF ALASKA. Some general information on these data sets is given in Table 11.1. As can be read from this table, the data sets were selected to provide broad geographic and frequency coverage and coverage with redundancy of the various propagation models. Specific characteristics of the subsets selected for the RAYMODE X evaluation are given in Table 11.2a-h which include source and receiver depths, mixed layer depth and depths of sound channel axis and bottom, frequency, and maximum range of data. Sound speed profiles, bottom loss versus grazing angle curves, and the measured acoustic data are found in Appendices IIA - IIH, respectively, for the experimental sets mentioned above. The bottom loss versus grazing data is that associated with the RAYMODE X model with bottom loss determined from geographic area designator charts with the following exceptions: (1) for PARKA II and HAYS-MURPHY, FNOC/NOO bottom loss versus grazing angle curves used by the FACT PL9D model (evaluated by AMEC as reported in Volume II of this series) with bottom loss being determined from NAVOCEANO area designator charts was used for RAYMODE X in addition to the standard RAYMODE inputs; (2) a constant bottom loss of 50 dB was used for all SUDS cases, effectively eliminating bottom interacting paths, since the experiment resulted from pulsed transmission and bottom reflected paths were time-gated out; and (3) bottom loss measurements from the experiment site were used for BEARING experiment site were used for BEARING STAKE since they differed so greatly (i.e., show much less loss) than would be obtained from either MGS or NAVOCEANO (used for FACT) area designator charts and their associated curves.

11.1 (U) Results of Test Cases Used in the AMEC Evaluation of RAYMODE X

(U) <u>SUDS:</u> (1) In terms of decibel differences between SUDS and RAYMODE data, only Cases II, IV, and VI show fair agreement. Cases II and IV are cases of cross-layer source/receiver geometry at 200 and 1000 Hz, respectively. Cases of cross-layer geometry at higher frequencies shows basic qualitative and quantitative disagreement between SUDS data and RAYMODE X results. All cases of both

TABLE 11.1. (U) EXPERIMENTAL DATA USED IN RAYMODE X EVALUATION

DATA SETS	LOCATION	PROPAGATION MODE	Z_S/Z_R	FREQUENCY $\leq$ 1KHZ	FREQUENCY $1 \leq F \leq 5$KHZ	NO. OF AMEC CASES
HAYES-MURPHY	MED	BB	S/S	✓		6
PARKA	PAC	BB, CZ	S/S	✓		2
SUDS	PAC	SD	S/S	✓	✓	12
GULF OF ALASKA	GULF OF ALASKA	BB MULTI CZ	D, S/S		✓	14
BEARING STAKE	IND	BB	S/S	✓		12
LORAD	PAC	MULTI CZ	S/S	✓	✓	14
FASOR	PAC & IND	CZ, SD BBM SHAL	S/S		✓	6
JOAST	MED	CZ	S/S		✓	12

BB = BOTTOM BOUNCE
SD = SURFACE DUCT
CZ = CONVERGENCE ZONE

S: $\leq$ 1 KFT
D: > 1 KFT

CONFIDENTIAL

TABLE 11.2A. (U) SUDS: TEST CASE CHARACTERISTICS

CASE	SOURCE DEPTH(m)	RECEIVER DEPTH(m)	FREQUENCY (kHz)	MIN RANGE (km)	MAX RANGE (km)	NO. OF POINTS	LAYER DEPTH (m)	MAX SOUND SPEED DEPTH (m)	DEEP SOUND CHANNEL AXIS DEPTH (m)
I	45	17	0.4	2.0	24.5	925	68	68	900
II	45	112	0.4	2.0	17.4	625	68	68	900
III	42	43	1.0	2.0	24.4	959	68	68	900
IV	42	112	1.0	2.0	24.8	818	68	68	900
V	41	6	1.5	0.4	24.6	796	20	250	900
VI	41	59	1.5	0.4	24.8	811	20	250	900
VII	41	6	2.5	0.4	24.8	868	20	250	900
VIII	41	59	2.5	0.4	24.8	866	20	250	900
IX	45	17	3.5	0.1	35.3	1311	79	79	900
X	45	112	3.5	0.1	35.8	918	79	79	900
XI	42	17	5.0	0.1	35.5	1421	79	79	900
XII	42	112	5.0	0.1	33.8	959	79	79	900

CONFIDENTIAL

TABLE 11.2B. HAYS-MURPHY: TEST CASE CHARACTERISTICS (U)

CASE	SOURCE DEPTH (m)	RECEIVER DEPTH (m)	FREQUENCY (Hz)	SOUND AXIS DEPTH (m)	BOTTOM DEPTH (m)
I	24.4	137.2	35.0	61	2750
II	24.4	137.2	67.5	61	2750
III	24.4	137.2	100.0	61	2750
IV	24.4	137.2	200.0	61	2750
V	24.4	106.7	35.0	61	2750
VI	24.4	106.7	100.0	61	2750

CONFIDENTIAL

TABLE 11.2C. PARKA: TEST CASE CHARACTERISTICS (U)

CASE	FREQUENCY (#2)	SOURCE DEPTH (m)	RECEIVER DEPTH (m)	LAYER DEPTH (m)	SOUND AXIS DEPTH (m)	BOTTOM DEPTH (m)
I	50	152.4	91.4	80	1000	5500
II	400	152.4	91.4	80	1000	5500

CONFIDENTIAL

TABLE 11.2D. BEARING STAKE: TEST CASE CHARACTERISTICS (U)

CASE	SOURCE DEPTH(m)	RECEIVER DEPTH(m)	FREQUENCY (Hz)	MIN RANGE (km)	MAX RANGE (km)	LAYER DEPTH (m)	SOUND AXIS DEPTH (m)	BOTTOM DEPTH (m)
I	91	496	25	6	288	75	1676	3353
II	91	1685	25	6	288	75	1676	3353
III	91	3320	25	6	288	75	1676	3353
IV	91	3350	25	6	288	75	1676	3353
V	18	496	140	6	288	75	1676	3353
VI	18	1685	140	6	288	75	1676	3353
VII	18	3350	140	6	288	75	1676	3353
VIII	18	3350	140	6	288	75	1676	3353
IX	18	496	290	6	288	75	1676	3353
X	18	1685	290	6	288	75	1676	3353
XI	18	3320	290	6	288	75	1676	3353
XII	18	3350	290	6	288	75	1676	3353

CONFIDENTIAL

TABLE 11.2E. JOAST: TEST CASE CHARACTERISTICS (U)

CASE	STATION	RUN	SOURCE DEPTH(m)	RECEIVER DEPTH(m)	FREQUENCY (KHz)	LAYER DEPTH(m)	SOUND AXIS DEPTH(m)	BOTTOM DEPTH(m)
I	1	43	6.1	18.3	3.5	-	137	2816
II	1	43	6.1	79.2	3.5	-	137	2816
III	2	43	6.1	163.1	3.5	-	137	2816
IV	2	63	6.1	18.3	3.5	-	61	2725
V	2	63	6.1	79.2	3.5	-	61	2725
VI	2	63	6.1	163.1	3.5	-	61	2725
VII	3	43	6.1	18.3	3.5	-	70	3471
VIII	3	43	6.1	79.2	3.5	-	70	3471
IX	3	43	6.1	163.1	3.5	-	70	3471
X	3	103	6.1	18.3	3.5	-	70	3471
XI	3	93	6.1	163.1	3.5	-	70	3471
XII	5	43	6.1	18.3	3.5	65.5	442	2743
XIII	5	43	6.1	79.2	3.5	65.5	442	2743
XIV	5	43	6.1	304.8	3.5	65.5	442	2743

CONFIDENTIAL

TABLE 11.2F LORAD: TEST CASE CHARACTERISTICS (U)

Case	Run Number	Frequency (Hz)	Source Depth(m)	Receiver Region	Bottom Bounce Zone	Convergence Zone	Min Range (km)	Max Range (km)	Sound Axis Depth(m)	Bottom Depth (m)	Layer Depth (m)
IA	3S	530	15.2	30.5	First	First	2	79	750	5670	33
IB	6S	530	15.2	30.5	Second	Second	45	143	750	5670	33
IC	8S	530	15.2	30.5		Third	182	216	750	5670	33
ID	10S	530	15.2	30.5		Fourth	250	274	750	5670	33
IE	12S	530	15.2	30.5		Fifth	313	350	750	5670	33
IF	14S	530	15.2	30.5		Sixth	376	416	750	5670	33
IG	16S	530	15.2	30.5		Seventh	440	478	750	5670	33
IIA	3D	530	15.2	304.8	First	First	3	76	750	5670	33
IIB	6D	530	15.2	304.8	Second	Second	45	143	750	5670	33
IIC	8D	530	15.2	304.8		Third	182	216	750	5670	33
IID	10D	530	15.2	304.8		fourth	250	274	750	5670	33
IIE	12D	530	15.2	304.8		Fifth	313	350	750	5670	33
IIF	14D	530	15.2	304.8		Sixth	376	416	750	5670	33
IIG	16D	530	15.2	304.8		Seventh	440	478	850	5670	33

UNCLASSIFIED

TABLE 11.2g. FASOR: TEST CASE CHARACTERISTICS (U)

CASE	STATION	RUN	SOURCE DEPTH(m)	RECEIVER DEPTH(m)	FREQUENCY (KHz)	MIN RANGE(km)	MAX RANGE(km)	LAYER DEPTH(m)	AXIS DEPTH(m)	BOTTOM DEPTH(m)
I	FIG	3	6.1	37.0	1.5	6.0	54.0	0	NA	7648
IIa	OAK	1	23.0	37.0	1.5	26.0	44.0	30	NA	120
IIb	OAK	2	23.0	37.0	1.5	12.0	24.5	30	NA	120
IIIa	THORN	1	23.0	37.0	1.5	19.5	33.5	55	NA	104
IIIb	THORN	2	23.0	37.0	1.5	12.0	25.5	55	NA	104
IV	REDWOOD	3	6.1	37.0	1.5	1.0	36.0	19	1200	3282

UNCLASSIFIED

TABLE 11.2H. GULF OF ALASKA: TEST CASE CHARACTERISTICS (U)

CASE	RUN NO.	SOURCE DEPTH(m)	RECEIVER DEPTH(m)	FREQUENCY (KHz)	MIN RANGE(km)	MAX RANGE(km)	LAYER DEPTH(m)	SOUND SPEED MIN. DEPTH(m)	BOTTOM DEPTH(m)
I	140	30.5	30.5	1.5	37.0	63.0	10	75	4078
II	140	30.5	304.8	1.5	37.0	63.0	10	75	4078
III	143	30.5	30.5	1.5	8.5	53.0	10	90	4042
IV	143	30.5	304.8	1.5	8.5	53.0	10	90	4042
V	124	30.5	30.5	1.5	2.5	11.0	10	75	4042
VI	124	30.5	304.8	1.5	2.5	11.0	10	75	4042
VII	108	1067.0	30.5	2.5	2.5	28.0	0	85	4060
VIII	108	1067.0	304.8	2.5	2.5	28.0	0	85	4060
IX	107	1067.0	30.5	2.5	30.0	67.0	10	85	4060
X	107	1067.0	304.8	2.5	30.0	67.0	10	85	4060
XI	112B	304.8	30.5	2.5	2.0	19.5	10	75	4042
XII	112B	304.8	304.8	2.5	2.0	19.5	10	75	4042
XIII	112A	304.8	30.5	2.5	15.0	58.0	10	75	4060
XIV	112A	304.8	304.8	2.5	15.0	58.0	10	75	4060

CONFIDENTIAL

source and receiver in the layer show lack of agreement between SUDS and RAYMODE. Of the two below-layer cases, VI showed good agreement between SUDS and RAYMODE, but VIII did not. (2) The figure of merit analysis shows RAYMODE predictions of detection range to be strongly pessimistic compared to SUDS results in Cases I, II, III, IV, V, IX and X (not uncommonly by a factor of two). Only in Case VIII were RAYMODE detection ranges much longer (by a factor of two) than those of SUDS. No clear trend emerges with regard to source/receiver geometry. (3) It would appear from comparison with SUDS data that the surface duct module of RAYMODE X is deficient. This is further borne out in Section 3.0, The Physics of the RAYMODE X Model, by R. Deavenport.

(U) HAYS-MURPHY: (1) Significant differences in mean levels were primarily responsible for pessimistic detection range predictions by the RAYMODE. These differences appear to be attributable to the bottom loss inputs for the first bottom bounce region (i.e., to 25 km). Beyond this range, differences are as great and unexplained, but bottom loss is not a factor. It is to be noted that for this scenario, RAYMODE and FACT bottom loss inputs led to essentially the same results. (2) Mean differences between the Hays-Murphy data and the RAYMODE model were smaller by about 2 dB for incoherent results as compared to coherent results. This is reversed for standard deviations of differences between the model and Hays-Murphy data, for which RAYMODE coherent generally showed about 2 dB greater standard deviation than did RAYMODE incoherent. The net effect is that the RAYMODE incoherent curve is in better agreement with the experimental data than is the RAYMODE coherent curve with regard to general characteristics (i.e., shape), but the RAYMODE coherent results are more in agreement with the experimental data with regard to detection range coverage (although the agreement is far from satisfactory). This is understandable since detections, particularly of a zonal nature, are determined more by fluctuations than by mean levels (particularly for average signal-to-noise ratios which are negative or near zero).

(U) PARKA: (1) The FNOC bottom loss used in RAYMODE leads to better agreement with PARKA data than does use of the MGS bottom loss. (2) At 50 Hz, the three convergence zones as predicted by RAYMODE are successively more severely retarded in range compared to the PARKA data. The peak levels of the RAYMODE first and second zones are 2 and 1 dB less than PARKA's peak levels, respectively. The third zone RAYMODE peak is 4 dB less than PARKA's. (3) At 50 Hz, the PARKA data shows substantially less loss than does RAYMODE in all bottom bounce regions (using RAYMODE's MGS values); at 400 Hz the trend is the same, but agreement is somewhat closer. (4) At 50 Hz the PARKA data and RAYMODE predictions agree well (near the RAYMODE coherent peaks) in the first bottom bounce region and agree well in the middle of the second bottom bounce region. In the third bottom bounce region, the RAYMODE prediction shows less loss than the PARKA data. This is in contrast to the 400 Hz results for which PARKA showed significantly less loss in all bottom bounce regions compared to RAYMODE. (5) At 50 Hz the first convergence zone as predicted by RAYMODE is in very good agreement with that of PARKA, but is slightly wider. The second RAYMODE CZ is found at shorter range than is PARKA's by about 5 km. This situation is exaggerated in the case of the third convergence zone. At 400 Hz the results for the first and second CZ starts are basically the same. The RAYMODE first CZ is wider than PARKA's, and the second is narrower.

(U) BEARING STAKE: (1) RAYMODE X coherent predictions are in better agreement with BEARING STAKE data than are RAYMODE X incoherent predictions. (2) Agreement between RAYMODE and BEARING STAKE results are often in reasonable agreement to ranges from as far as 60 to 150 km. (3) In the difference curves, there is

an underlying trend causing the difference between BEARING STAKE and RAYMODE results to become increasingly negative with range. This suggests that a higher critical angle in the bottom loss versus grazing angle curve would lead to better agreement, offsetting this trend. (4) BEARING STAKE data for the receiver on and 30 m off the bottom show strong interference patterns. RAYMODE X predictions show patterns which are generally out of phase with those of BEARING STAKE at short ranges (<30 km) and are dissimilar at longer ranges. The RAYMODE interference patterns are generally stronger (i.e., greater peak-to-peak excursion) than are those of BEARING STAKE data. (5) Detection coverage results are usually in rough agreement for figures of merit of 75 and 80 dB between RAYMODE X predictions and BEARING STAKE data. This agreement often extended to 85 and 90 dB and in one case to 95 dB. (6) For FOM $\geq$ 95 dB, BEARING STAKE detection coverage was to much longer range and was more complete (i.e., better percentage coverage) than were RAYMODE's.

(U) LORAD: For Cases IA-IG for which the source in the surface duct and the receiver at the duct limit of 100 feet (30.5 m): (1) LORAD shows somewhat better detection coverage than RAYMODE X in the bottom bounce regions. Changing the bottom class in the model should not provide significant improvement, since the shapes of the propagation loss versus range curves for LORAD and RAYMODE are different in the bottom bounce regions. (2) The LORAD first convergence zone has one lobe whereas RAYMODE X's has two. (3) The LORAD CZ start precedes RAYMODE's in the first, third, and fifth CZs and the converse is true for the second, fourth, and seventh CZs. (4) The ends of the LORAD CZs occur at equal or greater ranges than do RAYMODE's. (5) Fluctuations in the convergence zones are greater for LORAD data than for RAYMODE predictions. (6) The RAYMODE X coherent results are in better agreement with LORAD data than are RAYMODE X incoherent results.

(U) For Cases IIA-IIG for which the source is in the surface duct and the receiver is below the duct at 1000 feet (305 m): (1) LORAD data and RAYMODE predictions differ by about 10 dB in bottom bounce regions, with LORAD showing less propagation loss. The use of lower bottom loss as model input would lead to better agreement. (2) The start and end ranges for LORAD and RAYMODE agree for the first and second convergence zones (averaging over all figures of merit). The first CZ is double-lobed for both model and experimental data. (3) From the third CZ on, the start of the LORAD CZ precedes that of RAYMODE and the model's CZ start is steeper than that indicated by the experimental data. Range disparities as great as 10 km are found in CZ start range between LORAD and RAYMODE. (4) The range at which the convergence zone ends for LORAD data is equal to or greater than that for RAYMODE by as much as 6 km. (6) Fluctuations in the LORAD data are of roughly the same magnitude as the unsmoothed RAYMODE coherent output. (7) The RAYMODE X coherent prediction is generally in better agreement with the LORAD data than is the RAYMODE X incoherent prediction.

(U) JOAST: RAYMODE X predictions and JOAST experimental data were in basically good agreement with regard to convergence zone shape, peak level, start range, and zone duration. Exceptions are (1) in Cases II and III the RAYMODE CZ end was broader by about 2-3 km than that of JOAST, and (2) the RAYMODE and JOAST CZs were displaced in level by 10 dB (JOAST exhibiting greater loss) in Cases XII-XIV. The use of FNOC bottom loss may have been responsible for the greater evidence of bottom loss contamination of the convergence zone (particularly at its end) for the RAYMODE predictions as compared to JOAST data. This is true for station 3 where relatively less loss was predicted from the FNOC bottom loss charts (FNOC Type 3 for station 3). This compares to MGS Type 6 for station 3. This is not true for stations 1 and 2 where both are characterized by

FNOC Type 2 and MGS Type 2 (Note: The MGS and FNOC bottom loss vs. grazing angle curves differ, but by less than 1 dB over the full angular extent).

(U) FASOR: Aside from Case IIa, agreement between FASOR data and RAYMODE X predictions is qualitatively good. For Case IIa, the model is utilizing a low loss bottom and a significant reduction of levels is probably unachievable with available bottom loss curves. Overall, there is a slight tendency for the FASOR results to show less loss and give slightly better detection coverage, although this varies from case to case and also depends upon the RAYMODE coherence option chosen.

(U) GULF OF ALASKA: (1) Fluctuations were not as rapid for RAYMODE coherent as for Gulf of Alaska (GOA) data and were larger for GOA by factors as great as two, with the exceptions of Case I where fluctuations were 10-15 dB for each, Case XI with 3 dB fluctuations, Cases XII and XIII with 5-15 dB fluctuations and Case XIV where GOA fluctuations were 12 dB and RAYMODE's varied between 5 and 20 dB. Note: the final four cases are in the sound channel with the source below the axis; frequency of 2.5 kHz. (2) The 1.5 kHz results (Cases I-VI) show basic similarity between GOA and RAYMODE coherent results. The RAYMODE incoherent curve usually provided a low propagation loss envelope for the unsmoothed GOA data. (3) There is good agreement in start and end ranges between GOA and RAYMODE convergence zones except that in Case VII, a CZ was predicted by RAYMODE incoherent but not by RAYMODE coherent, nor was it evident in GOA data. (4) Results for the 1067 m source were inconsistent. More often than not, however, RAYMODE results corresponded to low-loss envelopes of GOA data (Case VII showed severe unexplained disagreement). (5) For the last four cases (305 m source) the RAYMODE curves were generally low-loss envelopes for GOA data or were parallel to the low-loss envelope but with 3 dB less loss. (6) For the 1.5 kHz data, figure of merit analysis shows the extent of range coverage of GOA data to be greater than or equal to that of RAYMODE output. This trend is reversed for the 2.5 kHz data for which RAYMODE had consistently better range coverage than did GOA data. (7) Over range increments where both RAYMODE and GOA data had detection coverage, the zonal detection coverage (detections per opportunity in percent) was greatest for RAYMODE incoherent (usually 100%) and least for GOA data due to fluctuations. Two exceptions were Case II for which the ZDCs were about equal and Case IV for which the GOA data had better ZDC than either RAYMODE option.

12.0 (U) Summary and Recommendations

(U) The RAYMODE model produces propagation loss as a function of range and frequency in an environment characterized by a single sound speed profile and a horizontal ocean floor. The evaluation herein reported has been for a specific version of the RAYMODE model, which is known as RAYMODE X, and all test cases were run on the UNIVAC 1108 computer (with EXEC VIII compiler) at the New London Laboratory of the Naval Underwater Systems Center. Although RAYMODE has been primarily developed for tactical sonar applications, it has been used over the span of frequencies implied by surveillance through torpedo applications. RAYMODE can produce both coherent and incoherent transmission loss results; however, when used for fleet applications (as opposed to research usage), the incoherent phase addition option is selected. The fleet user is not given the option of selecting values for various program controls. These are minimum and maximum number of ray cycles for all propgation modes, maximum number of ray cycles for bottom bounce, positive and negative minimum sonar angle (default 0°), positive and negative maximum sonar angle (default 60°), the first relative normal mode processed by mode summation (default 1), the last relative normal mode processed by mode

summation (default 0), the maximum number of modes processed by mode summation (default 10), and the number of points in ray tables (default 10). A detailed description of these program controls is given in section 7.0. The choice of these parameters can have a large effect on running time. In all cases used in this evaluation, default values were assigned for these parameters with one exception (in one FASOR case, the maximum sonar angle default of 60° led to unrealistically high values of propagation loss over a short range extent; changing the maximum sonar angle to 85° eliminated the problem). Under default conditions, run times on the UNIVAC 1108 varied from extremes of 5.1 to 54.1 seconds (usually between 6 and 30 seconds) and were strongly scenario dependent. The number of range points at which propagation loss was calculated in these runs varied from 200 to 400. It should be noted that by altering the default values of the program controls, increased accuracy can be achieved at the expense of running time.

(U) The computer core required by RAYMODE X (when dimensioned for 400 ranges and 50 modes and ray points) without plots in 17319 decimal words. When dimensioned for 200 ranges and 25 modes and ray points, the core required (without plots) is 15894 decimal words. We recall that the defaults for numbers of modes and ray points is 10.

(U) At NUSC/NLL, versions of RAYMODE exist on the following computers: UNIVAC 108, PDP 11/70, HP 9825, HP 9845, and Tektronix 4051. Of these, the UNIVAC and PDP versions are written in FORTRAN V, and the HP and Tektronix versions in BASIC. A version also exists on a UYK-20 computer written in CMS-2 language. RAYMODE versions support the following fleet systems and applications: TRIDENT Optimum Mode Selection (OMS), BQQ-5 sonar OMS, BQQ-6 sonar OMS, Improved Sonar Processing Equipment (ISPE), Submarine Active Detection System (SADS), Submarine System Effectiveness and Assessment (SUBSEA), Sonar In-Situ Mode Assessment System (SIMAS), and Fleet Mission Library.

(U) The physics of the RAYMODE X model was examined by Roy Deavenport of NUSC/NLL, New London, Conn. The resultant description (c.f., section 3.0) represents the most detailed description of RAYMODE's known physics. Indeed, a primary deficiency of RAYMODE is its lack of documentation both in the form of reports describing the physics of the model and its implementation on a subroutine-by-subroutine basis and in the form of comment cards within the RAYMODE computer code. Deavenport selected two test cases for RAYMODE. The first case tested surface duct propagation with the result that RAYMODE can yield poor surface duct results at the lower frequencies (≤200 Hz). The second case was concerned with low-frequency propagation in an environment where the sound speed profile has a depressed channel above a deep sound channel. It was concluded that RAYMODE does not properly account for depressed channel propagation at the lower frequencies (<300 Hz). This appears to be related to the fact that in RAYMODE there is no consideration of partial trapping of energy within the depressed channel.

(U) Two test cases for RAYMODE X exist in the RAYMODE User's Guide (Yarger, 1971) but are not necessarily applicable to other versions of RAYMODE. In fact, it appears that RAYMODE is not under configuration management. It is acknowledged that different versions have slightly different physics in some subroutines (this includes the surface duct treatment), are programmed in different languages, and are run on different computers with different word lengths. There do not appear to be test cases for which all versions have been run to assure uniformity of results.

(U) Responsibility for the RAYMODE X model resides at the Naval Underwater Systems Center, New London Laboratory, New London, CT 06320, for the model's

theory, development, computer implementation and model maintenance as detailed in section 8.0.

(U) Results of test cases (see sections 11.0 and 11.1) indicate (a) basic disagreement between SUDS data and RAYMODE X output for surface duct propagation, (b) basic agreement of convergence zone levels and range for PARKA and JOAST data with somewhat less agreement with LORAD data, (c) variable agreement in bottom bounce regions with best agreement between RAYMODE and experimental data found in the first bottom bounce region with successive deterioration of agreement as successively distant bottom bounce regions are encountered.

(U) Useful features present in RAYMODE X are:

- user specification of source and receiver beam patterns,

- availability of eigenray information including travel times,

- independent specification of initial range of range increment, and

- user specification of bottom loss versus grazing angle table.

(U) The variety of RAYMODE versions available implies that different results are obtainable from all models carrying the name RAYMODE for the same environmental inputs and the same program control selections.

(U) In light of the above, the following recommendations are given:

- Improve RAYMODE documentation, specifically describing the physics and its implementation on a subroutine-by-subroutine basis, defining all physical variables and giving their FORTRAN (also Basic and CMS-2) names, providing flow charts and internal to the program, providing adequate comment cards to allow the user to trace the program logic.

- Initiate a "fault-finding" evaluation of RAYMODE physics whereby test cases may be designed to evaluate specific aspects of RAYMODE physics including approximations and assumptions.

- Test the effect of word length on the RAYMODE X output. Determine if and where the use of double precision arithmetic is indicated.

- Provide a variety of test cases to assure that transfer of RAYMODE X to a new computer is accomplished with RAYMODE providing consistent answers on both computers.

- Assure concordance of all RAYMODE versions with regard to the physics used.

- Bring RAYMODE under configuration management, keeping track of and documenting all upgrades, cataloging RAYMODE distribution, and providing a feedback mechanism for identification of problems encountered, errors and missing but needed features. This also implies a plan for upgrading RAYMODE or otherwise altering the program. It is particularly important to document the aspects of RAYMODE versions which differ from the basic model due to constraints such as achieving a given run time or core storage requirement. It is also required that any change to RAYMODE undergo test and evaluation before being distributed.

(U) No model evaluation can claim to be complete and such is the case here. There are some particular omissions of test case scenarios which require identification:

- Propagation in an environment characterized by a sound speed profile with a double deep sound channel such as found in the eastern Atlantic Ocean,

- No analysis was performed for frequencies above 5 kilohertz due to a lack of experimental propagation loss data with supporting environmental data,

• No analysis for shallow water scenarios, once again due to a lack of experimental data (and possibly lack of knowledge of the physics of the boundary interactions where their effect overwhelms the effect of propagation within the water medium),

• Under-ice propagation was not examined, and

• The deterioration of the range independent RAYMODE X as the environment becomes increasingly range dependent was not addressed due to its complexity.

(U) To properly evaluate a model such as RAYMODE X it is necessary to catalogue problem runs (i.e., those that produce clearly invalid answers), the frequency with which they occur, and the environmental and acoustic conditions which accompany their occurrence. Information of this type is most valuable for problem identification and diagnosis and can mainly be obtained from user feedback. The importance of user feedback and its solicitation by those responsible for configuration management of the RAYMODE model cannot be overemphasized.

(U) Future acoustic experiments should be performed with model evaluation support as one of the primary objectives; this has implications for frequency coverage, source/receiver geometries, data density and supporting environmental measurements. Attention to modes of propagation (e.g., surface duct, bottom bounce, convergence zone) is most important to model evaluation to fill many scenario holidays.

13.0 (U) References

Yarger, D. F. (1976). The User's Guide for the RAYMODE Propagation Loss Program. Naval Underwater Systems Center Tech. Memo. No. 222-10-76, 9 August.

Leibiger, G. A. (1971). A Combined Ray Theory-Normal Mode Approach to Long Range Low Frequency Propagation Loss Prediction (U). Naval Underwater Systems Center Tech. Memo. No. PA3-0109-71. (CONFIDENTIAL)

Podezwa, E.M. and J.W. Prentice (1975). Percentage Distribution of Acoustic Provinces Based on Marine Geophysical Survey Bottom Loss Data (U). Naval Underwater Systems Center Tech. Report 4903. (CONFIDENTIAL)

Weitzner, E. and R. Pearson (1980). Submarine System Effectiveness and Assessment (SUBSEA) Model User's Guide. Analysis and Technology, Inc., Report No. P-733-4-80,

DiNapoli, F. and R. Deavenport (1980). Computer Models of Underwater Acoustic Propagation. Naval Underwater Systems Center Report No. 5867.

Martin, R. L., et al. (1982). Summary of Range Independent Environment Acoustic Propagation Data Sets (U). Vol. IA, The AMEC Reports, Naval Ocean Research and Development Activity, NSTL Station, Miss., NORDA Report 34. (CONFIDENTIAL)

Bairstow, J.B. and R.C. Medeiros (1980). RAYMODE Propagation Loss User's Manual. Naval Underwater Systems Center Technical Document No. 6923.

Beckman, P. and A. Spizzichino (1963). The Scattering of Electromagnetic Waves from Rough Surfaces. MacMillan Co., N.Y.

DISTRIBUTION LIST

Department of the Navy
Asst Secretary of the Navy
(Research Engineering & System)
Washington DC 20350

Department of the Navy
Chief of Naval Research
800 N. Quincy St.
ATTN: Code 102C
Arlington VA 22217

Chief of Naval Research
800 N. Quincy St.
ATTN: Code 420
Arlington VA 22217

Department of the Navy
Chief of Naval Operations
ATTN: OP 981F
Washington DC 20350

Department of the Navy
Chief of Naval Operations
ATTN: OP 952D
Washington DC 20350

Department of the Navy
Chief of Naval Operations
ATTN: OP 224
Washington DC 20350

Department of the Navy
Chief of Naval Operations
ATTN: OP 353C
Washington DC 20350

Department of the Navy
Chief of Naval Operations
ATTN: OP 551E
Washington DC 20350

Department of the Navy
Chief of Naval Operations
ATTN: OP 981F
Washington DC 20350

Department of the Navy
Chief of Naval Operations
ATTN: OP 986G
Washington DC 20350

Department of the Navy
Chief of Naval Operations
ATTN: OP 951F
Washington DC 20350

Department of the Navy
Chief of Naval Operations
ATTN: OP 095T
Washington DC 20350

Department of the Navy
Chief of Naval Material
ATTN: MAT 0724
Washington DC 20360

Commander
Naval Air Development Center
Warminster PA 18974

Commander
Naval Air Development Center
ATTN: C. L. Bartberger
Warminster PA 18974

Commander
Naval Air Systems Command
Headquarters
Washington DC 20361

Commander
Naval Air Systems Command
Headquarters
ATTN: Code 370
Washington DC 20361

Commanding Officer
Naval Coastal Systems Center
ATTN: G. McLeroy
Panama City FL 32407

Commanding Officer
Naval Coastal Systems Center
ATTN: D. P. Vasholz
Panama City FL 32407

Commander
Naval Electronic Sys Com
Headquarters
ATTN: PME 124
Washington DC 20360

Commanding Officer
Naval Environmental Prediction
Research Facility
Monterey CA 93940

Commanding Officer
Naval Research Laboratory
Washington DC 20375

Commander
Naval Oceanography Command
NSTL Station, MS 39522

Commander
Naval Ocean Systems Center
San Diego CA 92152

Commander
Naval Ocean Systems Center
ATTN: M. A. Pederson
San Diego CA 92152

Commanding Officer
Fleet Numerical Ocean Cen
Monterey CA 93940

Commanding Officer
Naval Oceanographic Office
NSTL Station MS 39522

Commander
Naval Sea System Command
Headquarters
Washington DC 20362

Commander
Naval Sea System Command
Headquarters
ATTN: Code 63D3
Washington DC 20362

Superintendent
Naval Postgraduate School
Monterey CA 93940

Project Manager
ASW Systems Project (PM-4)
Department of the Navy
Washington DC 20360

Officer in Charge
Naval Underwater Sys Cen Det
New London Laboratory
ATTN: F. R. DiNapoli
New London CT 06320

Commander
Operational Test & Eval Force
Naval Base
Norfolk VA 23511

Director, Liaison Office
Naval Ocean R&D Activity
800 N. Quincy Street
502 Ballston Tower #1
Arlington VA 22217

Commander
Submarine Dev Sqdn TWELVE
Box 70 NAVSUBASE NLNDN
Groton CT 06349

Commander
Surface Warfare Dev Group
Naval Amphibious Base,
Little Creek
Norfolk VA 23521

Director
Naval Tactical Support Activity
P. O. Box 1042
Silver Springs MD 20910

Director
Woods Hole Oceanographic Inst
ATTN: E. Hays
Woods Hole MA 02543

Director
Marine Physical Lab
Scripps Institute of Oceanography
ATTN: V. L. Anderson
P.O. Box 6049
San Diego CA 92106

Director
University of Texas
Applied Research Lab
ATTN: K. Hawker
P. O. Box 8029
Austin TX 78712

Director
University of Washington
Applied Physics Laboratory
ATTN: C. Sienkiewicz
1013 NE 40th ST
Seattle WA 98105

Director
University of Washington
Applied Physics Laboratory
ATTN: J. B. Lilly
1013 NE 40th ST
Seattle WA 98105

Director
Pennsylvania State University
Applied Research Laboratory
ATTN: C. P. Janota
P.O. Box 30
State College PA 16801

Director
Pennsylvania State University
Applied Research Laboratory
ATTN: S. T. McDaniel
P.O. Box 30
State College PA 16801

Commanding Officer
Naval Underwater Systems Center
Newport RI 02840

THIS
PAGE
INTENTIONALLY
LEFT
BLANK

CONFIDENTIAL
(This page is unclassified)

UNCLASSIFIED

SECURITY CLASSIFICATION OF THIS PAGE (When Data Entered)

REPORT DOCUMENTATION PAGE

READ INSTRUCTIONS BEFORE COMPLETING FORM

1. REPORT NUMBER: NORDA Report 36	2. GOVT ACCESSION NO.: AD-C034 021L
3. RECIPIENT'S CATALOG NUMBER	
4. TITLE (and Subtitle): The Acoustic Model Evaluation Committee Reports Volume III: Evaluation of the RAYMODE X Propagation Loss Model (U)	5. TYPE OF REPORT & PERIOD COVERED: Final
	6. PERFORMING ORG. REPORT NUMBER
7. AUTHOR(s): Richard B. Lauer	8. CONTRACT OR GRANT NUMBER(s)
9. PERFORMING ORGANIZATION NAME AND ADDRESS: Naval Ocean Research and Development Activity, Ocean Science and Technology Laboratory, NSTL Station, MS 39529	10. PROGRAM ELEMENT, PROJECT, TASK AREA & WORK UNIT NUMBERS: PE63708N, PE63795N
11. CONTROLLING OFFICE NAME AND ADDRESS: Naval Ocean Research and Development Activity, Ocean Science and Technology Laboratory, NSTL Station, MS 39529	12. REPORT DATE: September 1982
	13. NUMBER OF PAGES: 122
14. MONITORING AGENCY NAME & ADDRESS (if different from Controlling Office)	15. SECURITY CLASS. (of this report): CONFIDENTIAL
	15a. DECLASSIFICATION/DOWNGRADING SCHEDULE: Declassify ~~31 December 1990~~ OADR

16. DISTRIBUTION STATEMENT (of this Report)

T&E 12 APR 1984

Distribution limited to U.S. Government agencies only. Other requests for this document must be referred to the Commanding Officer, Naval Ocean Research and Development Activity, NSTL Station, MS 39529

17. DISTRIBUTION STATEMENT (of the abstract entered in Block 20, if different from Report)

18. SUPPLEMENTARY NOTES

19. KEY WORDS (Continue on reverse side if necessary and identify by block number)

Acoustic Model Evaluation Committee
RAYMODE X model
Underwater acoustics
Propagation loss
AMEC

20. ABSTRACT (Continue on reverse side if necessary and identify by block number)

(U) The Acoustic Model Evaluation Committee (AMEC) has applied the methodology described in Volume I of this series of reports to evaluated the RAYMODE X propagation loss model. The accuracy of RAYMODE X has been assessed by quantitative comparisons with eight sets of experimental data covering a broad spectrum of environmental acoustic senarios. The physics of RAYMODE X has been examined by R. Davenport of the Naval Underwater Systems Center, New London, Laboratory. RAYMODE X typically has run times between 5 and 30 seconds on the UNIVAC 1108 computer. The model is poorly documented with the exception

DD FORM 1 JAN 73 1473 EDITION OF 1 NOV 65 IS OBSOLETE S/N

CONFIDENTIAL

UNCLASSIFIED

SECURITY CLASSIFICATION OF THIS PAGE (When Data Entered)

(This page is unclassified)

of a well-written user's guide; this extends to a severe lack of comment cards within the computer code. The program could clearly benefit from an improved surface duct module; no other serious deficiencies in the physics of RAYMODE X been noted. Various versions of RAYMODE exist in fleet operations. These versions do not contain identical physics, are written in different computer languages, and are run on hardware utilizing different word lengths. Consistency of results from these versions has not been demonstrated. It is recommended that a program of configuration management be applied to all RAYMODE versions. RAYMODE X has many useful features including eigenray information, independence of initial range and range increment for propagation loss calculations, provision for vertical beampatterns, and the ability to input an external bottom loss table. This evaluation was completed in September 1980.

DEPARTMENT OF THE NAVY
OFFICE OF NAVAL RESEARCH
800 NORTH QUINCY STREET
ARLINGTON, VA 22217-5660

IN REPLY REFER TO
5510/1
Ser 93/160
10 Mar 99

From: Chief of Naval Research
To: Commander, Naval Meteorology and Oceanography Command
1020 Balch Boulevard
Stennis Space Center MS 39529-5005

Subj: DECLASSIFICATION OF PARKA I AND PARKA II REPORTS

Ref: (a) CNMOC ltr 3140 Ser 5/110 of 12 Aug 97

Encl: (1) Listing of Known Classified PARKA Reports

1. In response to reference (a), the Chief of Naval Operations (N874) has reviewed a number of Pacific Acoustic Research Kaneohe-Alaska (PARKA) Experiment documents and has determined that all PARKA I and PARKA II reports may be declassified and marked as follows:

   Classification changed to UNCLASSIFIED by authority of Chief of Naval Research letter Ser 93/160, 10 Mar 99.

   DISTRIBUTION STATEMENT A: Approved for public release. Distribution is unlimited.

2. Enclosure (1) is a listing of known classified PARKA reports. The marking on those documents should be changed as noted in paragraph 1 above. When other PARKA I and PARKA II reports are identified, their markings should be changed and a copy of the title page and a notation of how many pages the document contained should be provided to Chief of Naval Research (ONR 93), 800 N. Quincy Street, Arlington, VA 22217-5660. This will enable me to maintain a master list of downgraded PARKA reports.

3. Questions may be directed to the undersigned on (703) 696-4619, DSN 426-4619.

Peggy Lambert

PEGGY LAMBERT
By direction

Copy to:
NUWC Newport Technical Library (Code 5441)
NRL Washington (Mary Templeman, Code 5227)
NRL SSC (Roger Swanton, Code 7031)
✓DTIC (Bill Bush, DTIC-OCQ)

The Acoustic Model Evaluation Committee (AMEC) Reports, Volume 2, The Evaluation of the Fact PL9D Transmission Loss Model, Book 3, Appendices E-H, September 1982, NORDA-35-VOL-2-BK-3, 428 pages
(DTIC # C034 020)

The Acoustic Model Evaluation Committee (AMEC) Reports, Volume 3, The Evaluation of the RAYMODE X Propagation Loss Model, Book 1, September 1982, NORDA-36-VOL-3-BK-1, 127 pages
(DTIC # C034 021)

The Acoustic Model Evaluation Committee (AMEC) Reports, Volume 3, TheEvaluation of the RAYMODE X Propagation Loss Model, Book 2, Appendices A-D, September 1982, NORDA-36-VOL-3-BK-2, 324 pages
(DTIC # C034 022)

The Acoustic Model Evaluation Committee (AMEC) Reports, Volume 3, The Evaluation of the RAYMODE X Propagation Loss Model, Book 3, Appendices E-H, September 1982, NORDA-36-VOL-3-BK-3, 388 pages
(DTIC # C034 023)